공학박사학위논문

고정식 태양 집광기의 굴절을 기반으로 한 광학 설계

Refraction-Based Optical Design for Static Solar Concentrator

2014 년 8 월

서울대학교 대학원

기계항공공학부

하 성 문

Refraction-Based Optical Design for Static Solar Concentrator

Seong Moon Ha
School of Mechanical and Aerospace Engineering
Seoul National University

Abstract

The concentrated photovoltaic system (CPV) had advantage over the non-concentrated one in that they can generate more electricity per cell and thus reduce the overall energy price. However, the system was not suitable for the installments in individual house, small building, or remote places because it normally needed an active tracking component that requires frequent maintenance. Therefore, static concentrated photovoltaic system (SCPV) had been demonstrated as solution for maintenance problems of tracking system in CPV. Most static concentrators had been mainly designed by reflection mechanism. Thus, their low concentration ratio and manufacturing issues were obstacles for application in industry.

In present study, more flexible and cheaper static concentrator for higher concentration ratio and seasonal variation was developed by non-imaging lens as the primary method of concentration. And a design optimization procedure was suggested.

Two lenses system which consisted conventional concave lens and design convex lens having a lot of optimized prisms for non-imaging was a basic design element. The convex lens was designed by simple refraction and total internal reflection theory. Its width and angle of prisms in lens were optimized by ray-

tracing method which was in-house code and system performance was evaluated by optimization approach how rays of all distributed angles enter systems simultaneously. Simulation method was validated by comparing simulation results and experimental data. Simple two lenses which were commercial convex lenses having different size and focal length was set in experiment. Simulation results are reasonably close to experiment one and mean absolute percentage error between simulation and experiment is less than 5%.

Designed non-imaging lens help lights concentrate onto photovoltaic. It consists of many prisms whose shape is different. Concentration ratio varies seasonally and yearly average concentration ratio is 1.82. The maximum concentration ratio is 3.745 at vernal and autumnal equinox because sunlight perpendicularly enters system at these times. The maximum concentration ratio is quiet higher than yearly average concentration ratio. And the yearly average concentration ratio is higher than the previous SCPV. Therefore designed non-imaging lens has potential for effective concentration for peak power demand.

Array system where several small-sized single systems are combined is considered. It can be applicable in practical situations. Array system is more benefit able than bulky single system in cost-wise and installment-wise. The yearly average concentration ratio of array system sharply increases. Its value is 2.33. Especially concentration ratio at the summer and winter solstices remarkably improve because a lot of sunlight reaches photovoltaic in the adjacent system. The yearly average concentration ratio of array system is within about 10% of the available maximum concentration ratio defining as thermodynamic.

Semi-SCPV system whose meaning is that passively changing angle facing the a few times a year without dynamic tacking system is suggested for another practical model system. Two models for bi-yearly semi-SCPV are considered. In

first model, system position change to maximize average concentration ratio. At the middle of between vernal equinox and summer solstices, position of SCPV change to receive sunlight perpendicularly and after about 6 month, position of SCPV change. At this time sunlight normally enter the system. The yearly average concentration ratio of first model is 3.6 and the maximum concentration ratio is 5.92. The concentration ratio is remarkably increased. And periodic variation for seasons of concentration ratio reduces. As a result, more energy provides during each season. A motivation of second model is to maximize concentration ratio for peak seasons like summer and winter. System is located at angles where sunlight perpendicularly enters system at summer and winter solstices. Its concentration ratio is the same as array system one. However, the maximum concentration ratio generates at summer and winter solstices as planned. Therefore second model can flexible concentrates sunlight for replying to peak power demand.

Keywords: Photovoltaic, Static concentration, Concentration ratio, Non-image, Lens, Semi-SCPV.

Student Number: 2007 – 20867

Contents

List of Tables

List of Figures

Nomenclature

Roman symbols

c	light of velocity [m/s]
E	gained energy [W]
f	focal length of lens [cm]
H	ratio of enterd the number of rays to the number of toal rays
l	location [cm]
n	refractive index
r	rays, light and sunlight
S	angle variacne
t	amplutide tranmission coefficient
T	tranmission
W	total width [cm]
w	width [cm]
X	ratio of distance
Y	ratio of location

Greek symbols

λ	wavelength [m]
θ	angle [°]

Subscripts

$( )_{1st}$	1st lens
$( )_{2nd}$	2nd lens
$( )_{3rd}$	3rd lens
$( )_{accep}$	acceptance angle
$( )_{cri}$	critical
$( )_{in}$	incidence
$( )_{prism}$	prism
$( )_{PV}$	photovoltaic
$( )_{re}$	refraction
$( )_{t}$	transmittance

Abbreviation

CPC	compound parabola concentrator
CPV	concentrated photovoltaic
CR	concentration ratio; ratio concentrated energy to general solar energy
PV	photovoltaic
SCPV	static concentrated photovoltaic
TIR	total internal reflection

Chapter 1.

Introduction

1.1 Background

The photovoltaic(PV) system which is called solar cell are the most promising alternative energy sources for replacing fossil fuel and solving CO_2 emission. It is very attractive because it gives zero emission and depends on very reliable energy source of virtually infinite resources. Therefore, many researchers are interested in development of PV system. Figure 1.1 summarize tendency of efficiency about various types of PV systems. However, PV system has difficulty in commercialization largely, because it is yet to be competitive in price and efficiency. Thus, many researches realize the importance of concentration and pay attention to the concentrated PV systems, because concentration generating by optical devices can improve PV in cost and efficiency. In other words, concentration can help to reduce system price, because lens is quite cheaper than PV module in case of PV system. Concentrated PV system (CPV) which includes optical devices such as lenses and reflectors was emerged. Several novel concentrators and systems for improving *CR* are developed.

E. Lorenzo et al. (1982) compared performance about curved lens, reflector and flat or roof lens as PV concentrator. They concluded a curved lens (Fresnel lens)

was useful for concentrating light. Akiba Segal et al. (2004) provided a detailed assessment and analysis of the tower reflector optics as a basis for a large-scale concentrating PV system with beam splitting, and various geometries and configurations were analyzed and optimized in order to solar power plant developments. K.K. Chong et al. (2009) suggested a novel configuration of solar concentrator, which was the non-imaging planar concentrator, capable of producing much more uniform sunlight and reasonably high concentration ratio. And some researches focused on prototype of PV for the concentrated photovoltaic (CPV) .Vikrant A.et al (2009) suggested the optimizations values such as variation of metal grid, metal resistance, and junction depth for crystalline silicon PV by changing *CR* from 1 sun to 10 suns. Some projects for the concentrated photovoltaic (CPV) were held. These projects performed the concentrated photovoltaic (CPV) installment in real states and checked system performance (Garboushian et al. (1994), Brunotte et al. (1996), O'Neill et al. (1994), and so on).

The Concentrated Photovoltaic (CPV) is greatly profitable for triple-junction PV system. Although multi-junction PV called tandem solar cell has the best efficiency among PV, it spends so much cost for manufacture. Thus, manufacturing large-sized modules is difficult. In industry for multi-junction, concentrator should be essential component. Kenji Araki1 et al (2005) experimented the concentrated system with multi-junction PV. They reported that the temperature-corrected efficiency of the 550X module under optimal solar irradiation condition was

31.5±1.7%. Most studies about CPV system focus on concentrator providing high concentration ratio. Solar tracking system (Figure 1.2) which moves to follow solar altitude is CPV`s indispensable requisites in order to maintain maximum *CR* for variations of sunlight during days and seasons. Table 1.1 shows the tracking requirements for categorizing CPV system by *CR*. The solar tracking system which helps high *CR* has the limitation. Major limitation of solar tracking system is should need maintenance problem for moving parts. This may not be a problem for solar power plant with a full-time maintenance staff. However, it will be a real nuisance for house and remote locations. Therefore, static concentrated system (SCPV) becomes very important in these cases.

1.2 Overview of the static concentrated photovoltaic systems

The Static Concentrated Photovoltaic (SCPV) systems were developed for remedy the CPV shortcomings. The SCPV can concentrate sunlight onto a PV without any moving parts such as solar tracking system despite variations of sun altitude about seasons or days.

The Compound Parabolic Concentrator (CPC) is typical SCPV system. Figure 1.3 (a) indicates the configuration of CPC. It has two different parabola reflectors which have a different focal point respectively. In CPC, while incident angles of rays are lower than acceptance angle, all sunlight can be collected on a PV.

Acceptance angle means the maximum available angle of inclined sunlight for concentration. In general, acceptance angle is set by designer`s preferences and application. The *CR* of CPC (2-dimension) is defined as

$$CR_{CPC_{2-D}} = \frac{1}{\sin\theta_{accep}}$$

where, θ_{accep} is acceptance angle of CPC. This relation is the same the max *CR* approaching thermodynamics. The any well-designed static system cannot exceed the *CR* of CPC. Therefore, CPC is called the ideal static concentrator. When acceptance angle is ±23.5° which is azimuth angle, the *CR* becomes 2.51. Figure 1.4 illustrates the max *CR* approaching thermodynamics. Although CPC is static concentrator, CPC has some drawbacks for commercialization and application. CPC can`t flexibly reply to peak power demand because of constant concentration ratio throughout all seasons. Secondly, its size becomes steep and narrow for high concentration ratio. It is difficult to manufacture this shape. Third drawback is related to manufacturing issue. Manufacturing of perfect parabolic is difficult and reflector cost cannot be reduced well in mass production. Thus, novel concentrator models are demonstrated for application.

Minano et al. (1995) suggested RXI system. Huge dielectric material whose refractive index is higher than air put on the PV for concentration based on total

internal reflection (TIR). Another approach to static concentrators is the dielectric prism, which relies on total internal reflection. Wenham et al. (1997) introduced static concentration to put on the roof of house. (Figure 1.5(a)) This system could also concentrate inclined sunlight by TIR, because dielectric material was filled in the groove. Yoshioka et al. (1994) proposed a new static concentrator with a refractive lens for wider acceptance angles. The arc lens was designed and some sunlight directly entered to a PV, others collected by reflector on side of system. The V-groove rear reflectors were devolved by K.J. Weber et al. (2006) and their group (2001) suggested reflector having similar to shape of prism. However, earlier studies for static concentrator had low concentration ratio for commercialization and application. (Table 1.2)

1.3 Scope of the present study

In present study, the major objective is to develop more flexible and cheaper static concentrator for higher *CR* and seasonal variation and to present an optical design for small & medium–range concentrator for the usage in house and remote areas. Proposing a design optimization procedure using the non-imaging lens as the primary method of concentration is minor objective.

Chapter 2 introduces the basic design elements such as non-imaging optics,

roles of two lenses existing in system, optimization approach for 2nd lens design, and algorithm of setting parameters for 2nd lens design. Concentration performance of 2nd lens is evaluated and compared with static concentrator models in previous study.

Chapter 3 deals with the experimental setup for validating proposed simulation method. Explanation of the optical experimental setup process and characterization of optical components using for experiment is presented. Power distribution is measured. Simulation is conducted to compare experimental results with its result for verification of ray tracing method. Optics and method for lens design in simulation is introduced. And the results of experiment and simulation are compared.

Chapter 4 shows optimization process of designed lens. There lenses system is suggested to collect more rays. And algorithm for 3rd lens is introduced. Some parameters are fixed by qualitative evaluation during 2nd lens design, because these parameters don't manly affect system performance. For robust system, estimating collection efficiency by variation of minor parameters is necessary. The variation of concentration ratio about various parameter changes is shown. And reliability of system for diffusive radiation is shown

Chapter 5 presents the practical system for application. Two practical models are introduced and explanation of systems and feasibility of models is shown. And simulation algorithm for design and estimation is covered. Results of these systems

are shown.

Chapter 6 summarizes and concludes present study.

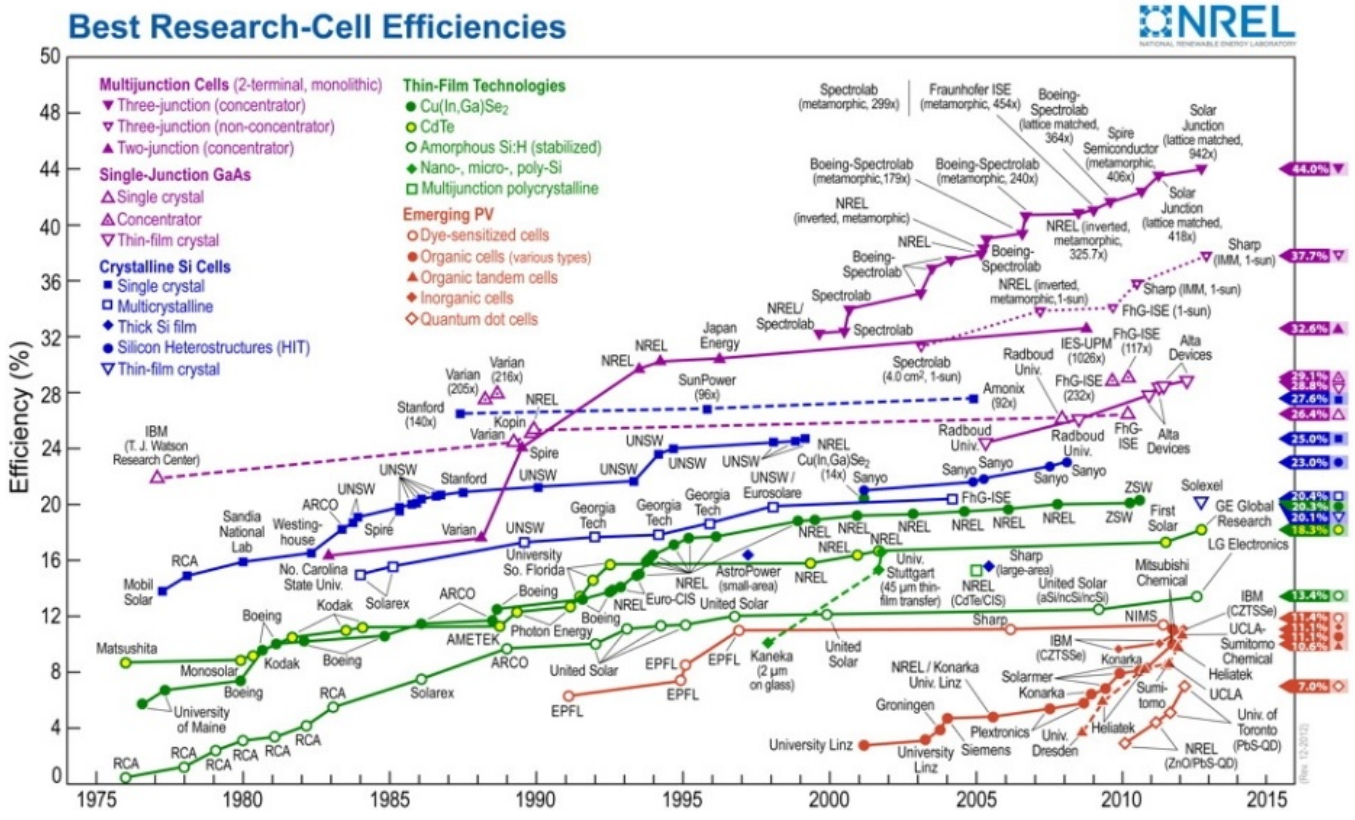

Figure 1.1 Prospect for photovoltaic (PV) efficiencies from National Renewable Energy Laboratory (NREL)

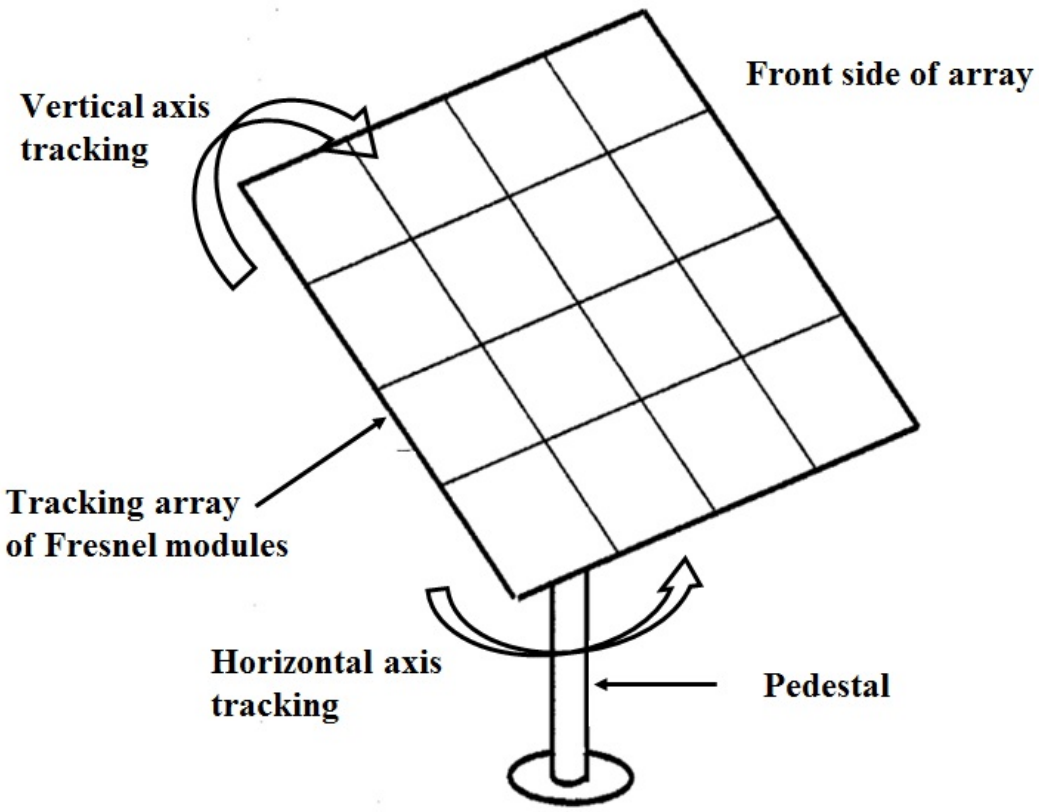

Figure 1.2 Configuration of solar tracking system.

Table 1.1 Suitability of non-imaging concentrator concepts for different concentration ratio and tracking requirements. (Ralf Leutx, 2001)

	CR **≈ 2 (Static)**	***CR*** **≈ 20 (1-axis tacking)**	***CR*** **>> 20 (2-axis polar tacking)**
Compound parabolic concentrator (CPC)	++	+	-
Nonimaging Fresnel lens	+	++	+
Lens / mirror integrated concentrator & parabolic mirror	-	+	++

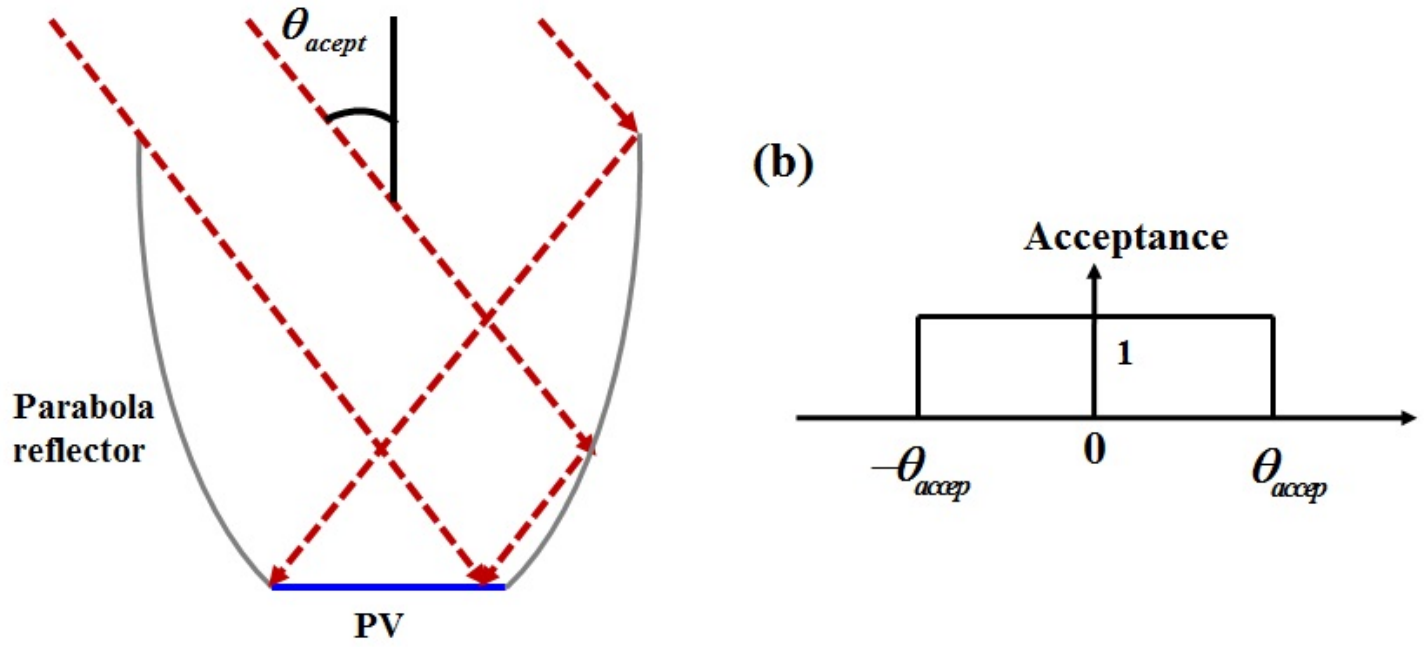

Figure1.3 Compound Parabola Concentrator: (a) Configuration of compound parabolic concentrator (CPC), and (b) Performance

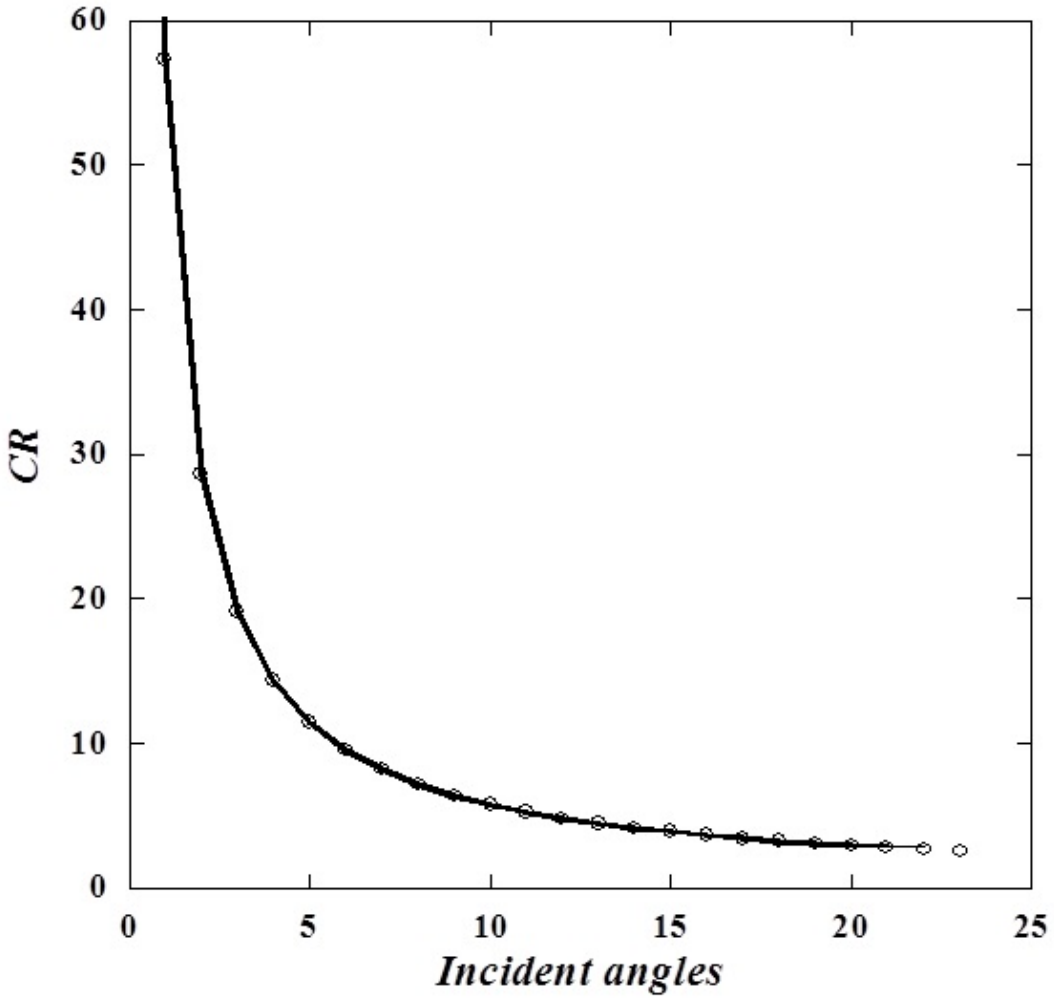

Figure 1.4 Available maximum *CR* approaching thermodynamics

Table 1.2 Comparison of system performance in previous study results: (a) S. Bowden et al. (1993), (b) K. Yoshioka et al. (1994), (c) K.J. Weber et al. (2001) (d) K.J. Weber et al. (2006)

Schematic	Mechanism	CR
CPC 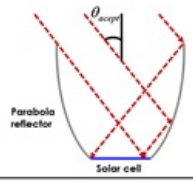	Non-imaging -Reflective mirror	2.51
(a) 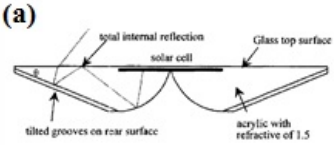	Total internal reflection	~ 1.8
(b) 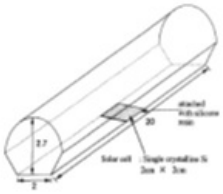	Reflection & Refraction	~1.6
(c) 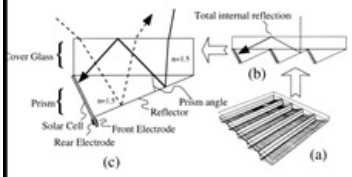	Total internal reflection	~1.8
(d) 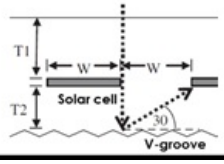	Reflection (V-groove)	~1.6

Chapter 2.

Design of static concentrator

2.1 Introduction

Most static concentrator had been mainly designed by reflection mechanism. Their concentration ratio is less than ‘2’. This value is an obstacle for application in practical situation. The reason for low concentration ratio is reflector characteristic. The performance of reflector is good during particular incident angles. However, it rapidly drops at different incident angles. Therefore, in present study, more flexible and cheaper static concentrator for higher concentration ratio and seasonal variation were developed by non-imaging lens as the primary method of concentration.

2.2 Fundamental optics

2.2.1 Non-imaging optics

The objective of the present study is to suggest novel static concentrator using refractive mechanism unlike previous studies. Understanding fundamental optics is necessary for carrying out objective. There are two approaches for design of optical devices such as general optics and non-imaging optics.

In general optics system (Figure 2.1 (a)), a main role of optical device is to make clear images about objects. The components of general optics system are object, optical device and image. Unlike general optics, the non-imaging optics does not make an image of the light source. Instead, optical device is designed to concentrate radiation at a density as high as theoretically possible. In other words, non-imaging optics focus on how much light of source can collect to receiver instead of clear image for objects. Thus, in Figure 2.1(b), non-imaging optics system usually consists of components source of light, optical device and receiver. Therefore, based on non-imaging optics, static concentrator would be designed because the major purpose of study is concentration of sunlight. The application of non-imaging optics is design of concentrator for PV industries like CPC and parabolic reflector. (Table.1.1)

2.2.2 Prism characteristic

The static concentrator for this thesis included a lot of prisms. Prism characteristic was the major idea for concentrator design. The comprehension of prism characteristic is surely required before design. Light behaviors in a prism shows in Figure 2.2 (a).

In general, refraction angle can be expressed by the Snell`s law; rays translate from air to glass,

$$\theta_{re} = \sin^{-1}\left(\frac{n_1 \sin\theta_{in}}{n_2}\right)$$

where, n_1 *and* n_2 are refractive index of air and prism respectively.

In a prism, since light passes a prism after two refractions occurred at front and inclined surfaces so, refraction angle is complexly defined as

$$\theta_{re} = \sin^{-1}\left[n_2 \sin\left(\sin^{-1}\left[\frac{n_1 \sin\theta_{in}}{n_2}\right] + \theta_{prism}\right)\right] - \theta_{prism}$$

Where, n_1 and n_2 are respectively refractive index of air and prism. The refractive angle is a function of two angles like incident and prism angles. Refraction angles are nearly proportional to incident angles at the same prism angle. And refraction angles proportionally increase with prism angles while incident angles are constant. (Figure 2.2 (b)) A linear relation between incident angles and refraction angles clearly appears at small prism angles. Figure 2.2 (c) illustrates interesting phenomenon about relation between incident angles and refraction angles. The differences of incident angles in a prism are small, and the differences of refraction angles are also small. Therefore, although lights which have each different angle enter to a prism, lights can reach receiver by controlling prism

angles.

When light escapes from medium having larger refractive index to smaller refractive index, if refraction angle is larger than critical angle the total internal reflection occurs. As a result, light can`t pass dense medium which has larger refractive index than air and light reminds in dense medium after reflection. (Figure 2.3 (a))

The critical angle for total internal reflection can be expressed by

$$\theta_{cri} = \sin^{-1}\left(\frac{1}{n_2}\right)$$

Where, n_2 is refractive index of dielectric material.

Figure 2.3(b) illustrates the critical angles for various refractive index. The prisms are generally made of PMMA which is kinds of plastics. Its refractive index is 1.5. The critical angle is about 42°. Total internal reflection also is useful mechanism for static concentrator.

2.3 Basic optimization approach for simulation

Ray tracing method made by in-house code was used in order to design static concentrator and evaluate lens performance. In ray tracing method, velocity, position and energy of rays were given as initial value. The behaviors of rays were

changed by refraction and total internal reflection. Energy and position of rays on a PV were estimated as final value and collection efficiency was calculated. In simulation, light firstly passing through the lens was named the 1st lens and lens below the 1st lens was called the 2nd lens whose design based on non-imagine optics was purpose of this thesis. (Figure 2.4)

2.3.1 Simultaneous evaluation

In present study, some different incident angle along variation of seasons was considered. Thus, designed static concentrator about all rays having different incident angles must be respectively concentrated onto a PV. As evaluation method for performance of designed static concentrator, sequential estimation is the one of way. This way is that designing concentrator and checking collection performance about each different incident angle step by step. Figure 2.5(a) shows the way of sequential evaluation. Sequential evaluation is inefficient method. Since modifications about concentrator shapes for maintaining collection performance are surely required and a lot of times spend calculating total concentration ratio.

In present study, simultaneous evaluation was selected in order to estimate concentration performance of 2nd lens. In other words, all ray having incident angles within variation of season (-23.5° ~ 23.5°) entered simultaneously the system and design and evaluation for performance was conducted about all incident

rays. (Figure 2.5(b)) Therefore performance could be evaluated once a time.

2.3.2 Convergence test

The number of real sunlight is infinite. However, it is difficult to reproduce the infinite lights as initial ray in ray tracing method. Thus reasonable finite the number of initial rays was determined. The number of initial rays as well as initial value such as velocity, position and energy of rays in ray tracing method is important value for exact design, because the performance of concentration may be changed by the number of initial rays.

Figure 2.6 shows ray distribution after passing 1st lens with different the number of initial rays. While the number of initial rays was increased, void space among rays was disappeared. On the same position, angle distribution or variance was eventually changed by the number of initial rays. And then, the 2nd lens shape was changed by variation of angle variance. Thus, convergence tests about initial rays were conducted in order to find ray-number-independent condition.

The number of initial rays was set by initial positions (distance of between each ray) and the number of rays having different angles. (Figure 2.7) The number of initial rays was increased by reducing the space of between each ray for convergence tests. As a result, when the number of initial rays was higher than 42,000, simulation results were converged (Figure 2.8). Therefore 42,000 rays were

set as the number of incident rays in ray tracing method.

2.3.3 Transmittance of lens

Energy of rays on a PV was one of the results in ray tracing method. Calculating concentration ratio based on ray`s energy on a PV and comparing it and collection efficiency of previous models were ultimate objective of 2nd lens design. In general, energy losses are generated by passing lens, because reflection is occurred on the surface and lights are absorbed in lens. Transmittance is useful for estimating energy of light after passing lens.

Transmittance is generally defined as ratio of the intensity of the incident radiation to intensity of the radiation coming out of the lens. This transmittance is a function of incident angle of incident. In present study, various incident angle distributions existed on the lenses because of designing 2nd lens about variation of angles. Amplitude transmission coefficient dependent on incident angle can by expressed by the Fresnel equations.

$$t_{\perp} = \frac{2\sin\theta_t \cos\theta_{in}}{\sin(\theta_{in} + \theta_t)}$$

$$t_{//} = \frac{2\sin\theta_t \cos\theta_{in}}{\sin(\theta_{in}+\theta_t)\cos(\theta_{in}-\theta_t)}$$

where, $t_{\perp}$ is amplitude transmission coefficient of electric field, $t_{//}$ is amplitude transmission coefficient of magnetic field, θ_{in} is incident angle, and θ_t is transmission angle.

Transmittance which depends on incident angles is defined as

$$T_{\perp} = \left(\frac{n_2 \cos\theta_t}{n_1 \cos\theta_{in}}\right) t_{\perp}^2$$

$$T_{//} = \left(\frac{n_2 \cos\theta_t}{n_1 \cos\theta_{in}}\right) t_{//}^2$$

where, $T_{\perp}$ is transmittance of electric field, $T_{//}$ is transmittance of magnetic field, n_1 is refractive index of air, and n_2 is refractive index of lens.

Sunlight is unpolar waves, so total transmittance dependent on incident angle was calculated by the arithmetical mean.

$$T = \frac{\left(\frac{n_2 \cos\theta_t}{n_1 \cos\theta_{in}}\right) t_{\perp}^2 + \left(\frac{n_2 \cos\theta_t}{n_1 \cos\theta_{in}}\right) t_{//}^2}{2}$$

Figure 2.9 indicates transmittance of lens about incident angle. Significant change of transmittance was not caused within 60°. However, transmittance is rapidly dropped by passing 60°. In ray tracing method, the range of incident angle before entering to 1st and 2nd lens was 0° ~ 50.5°. In this range, typical value (=0.95) of transmittance is almost consistent variation of it about incident angles. The difference of each value is about 1 %. (Figure 2.9) Therefore, typical value (=0.95) for transmittance to calculate energy of ray after passing lenses was applied for all incident angles.

2.4. Determination for effective design parameters

In present system, several parameters exist because system consists of two lenses and a PV. (Figure 2.4) Determining effective parameters for concentrator is required for design. Variation of parameters may directly or indirectly affect system performance. Thus, parameters affecting efficiency weakly were set as fixed parameters. The f_{1st}, w_{1st} which were related to 1st lens shape and l_{1st} were qualitative evaluated as input value for 2nd lens design. The θ_{prism}, w_{prism} and $l_{2nd\ lens}$

were set by computational evaluation because these variables directly affected static concentrator performance. All parameters are reduced by $W_{1st,total}$.

2.4.1 Focal length of 1st lens (f_{1st})

In general case of CPV, focal length of the lens is set by system size or designer`s preference since only perpendicular rays to system are considered. However setting focal length of 1st lens by general way may cause the problems in current thesis. Because inclined incident rays should be considered for static concentrator.

f_{1st} is typical parameter determining characteristic of lens. Lens thickness is actually changed where focal point of lens. In other words, if the lens has short focal length, rays should take big refraction angles in order to focus on a point quickly. As mentioned before, prism angles must become high to make high refraction angles. After all, thickness of lens having short focal length becomes thicker. A, refraction angles in a prism are proportionally changed by prism angles while incident angles are the constant. And total internal reflection is generated when prism angles are higher than critical angle and then, a lot of rays escape a system.(Figure 2.10) This phenomenon deemed the losses in present study. Therefore focal length of 1st lens was set by the minimum value at which whole incident sunlight passed the 1st lens without total internal reflection. Therefore f_{1st} is 1.9 in this study.

2.4.2 The width of prism in 1st lens (w_{1st})

The w_{1st} weakly affects the collection efficiency. This value was arbitrarily set by basing on calculation time in simulation and manufacture limitation. The w_{1st} was consequently set as 0.1.

2.4.3 Position of PV (l_{PV})

In typical CPV system, a PV is located near focal point of lens in order to get concentered whole sunlight, so a PV was set at focal point of 1st lens in this study. Therefore, the l_{PV} was 1.9 like f_{1st}

2.5 Algorithm for 2nd lens design

As seen Figure 2.4, this system consists of two lenses to make SCPV system. The 1st lens was a concave lens and characteristic of 2nd lens was similar to a convex lens. The reason for why two lens having different characteristic used was that spread rays should require for effective design of 2nd lens. Directly designing 2nd lens without the concave lens was so difficult to achieve high concentration ratio. Without 1st lens, difference between the maximum angle of incident sunlight and the minimum value of those is always 47° everywhere. In other words, angle variances in every space are the same and these values are higher than effective value for concentration. However in with 1st lens case, because of disturbance of ray angle by lens, difference between the maximum angle of incident sunlight and

the minimum value of those is smaller than 47° in some segments. Because sunlight is spread concave lens, its angle distribution became somewhat regular. As a result, angle variance became smaller. Therefore role of 1st lens was to reduce variance in ray angles. (Figure 2.11)

2.5.1 Prism width of the 2nd lens (w_{2nd})

Prism width of the 2nd lens (w_{2nd}) was set by dividing some zones in which light having similar angles existed. The key idea of algorithm for prism width of the 2nd lens (w_{2nd}) was comparison variance of angle among zones. In general, the meaning of small variance is that many values are distributed near its average value and differences between each value are small. As mentioned before, lights getting similar incident angles can have similar refraction angles by passing a prism. Thus, rays in space having small angle variance were effectively collected.

Procedure for evaluating prism width of the 2nd lens follows; (Figure 2.12)

1st step; divide zones ($\triangle x$) whose size was the same.

2nd step: calculate the ray angle variance (S_i) in each zone.

$$S_i = \sum_{j=1}^{m} \left[\left(r_j - r_{av} \right)^2 \right]$$

Where m is the number of rays in divided zones ($\triangle x$), r_j is j th ray`s angle in

divided zones (△x) and r_{av} is average ray`s angle in divided zones (Δx).

3rd step; calculate average angle variance ($\overline{S}$) about whole zones.

$$\overline{S} = \frac{\sum_{j=1}^{m} S_j}{m}$$

where, m is the number of divided zones (△x).

4th step; compare average angel variance with individual angle variance in each zone. If individual angle variances (S_i) are higher than average angle variance ($\overline{S}$), zones are split. And if individual angle variances are lower than average value, zones combine with adjacent zone.

5th step; finally, adjust zone by repeatedly compare average angel variance with individual angle variance in each zone until individual angle variances in each zones is almost the same as average angle variance.

2.5.2 Prism angle of the 2nd lens (θ_{prism})

The computational design procedure for prism angle of the 2nd lens (θ_{prism}) was

(Figure 2.13); firstly calculate average angles (r_{av}) in each zone. Secondly find target rays (r_T) whose angles were close to average angle. Lastly prism angle was set when these rays (r_T) entered to PV center.

In algorithm, prism angle of the 2nd lens (θ_{prism}) was set by only target rays (r_T). Other lights can also reach a PV by considering only target ray because of prism characteristic. Figure 2.2(c) illustrates that small difference of among incident angles can make similar refraction angles and lights passing a prism can be collected onto a receiver (PV). Before setting prism angle of 2nd lens (θ_{prism}), light was divided by comparing angle variances. In other words, difference of angle in each zone was small. If target rays entered to the center of PV, others having similar refraction angles reached near the center of PV. Therefore, lights in each prism can concentrate onto a PV.

While prism angle of the 2nd lens (θ_{prism}) was calculated, two different mechanisms were respectively applied by following regions of lens. The angle of prisms in edge of 2nd lens was fixed by applying total internal reflection phenomenon. Since large refraction angle was necessary in order that rays in edge part of 2nd lens reach to a PV. As mentioned before, total internal reflection occurs by increasing prism angle, so lights can`t pass a prism. However, when prism angle exceed any critical angle range (Figure 2.14(c)), lights after total internal reflection pass a prism without trapping and these have larger refraction angles. Therefore,

edge prisms in 2nd lens were designed by using total internal reflection. (Figure 2.14(d)) Prisms except edge regions were designed by simple refraction. (Figure 2.14(a))

2.5.3 2nd lens location

2nd lens location was set where concentration ratio is the maximum values between 1st lens and photovoltaic.

2.6 Simulation results

2.6.1 2nd lens location

In this study, 2nd lens set location at which concentration ratio is the maximum between 1st lens and a PV. Figure 2.15 shows the results of *CR* by changing 2nd lens locations. In a result, when *Y* (defined as ratio of distance between 1st lens and 2nd lens to distance 1st lens and PV) was 0.868, the maximum *CR* became 1.82. As can be seen, *CR* markedly increased while 2nd lens was close to a PV. Causing better angle variance by reducing distance between 2nd lens and a PV was the reason for increasing *CR*. Since sunlight after passing 1st lens spread more and more as 2nd lens became closer to a PV. As a result, angle variance became smaller. and light`s average angle variances which is important for setting prism width in 2nd lens become also small with distance between 2nd lens location and a PV. As mentioned in previous section, light can be effectively concentrated at low average angle

variance, because effective dividing zones where lights had similar incident angles could be easily conducts.

On the other hand, although average angle variance become smaller, *CR* dramatically drops when 2nd lens location was over *Y*=0.85. While 2nd lens was located near a PV, light in edge of 2nd lens should have so large refraction angles in order to reach a PV. Large prism angles required getting large refraction angles. In general prism, critical angle for total internal reflection can be defined by

$$\theta_{cri} = \sin^{-1}\left(\frac{1}{n}\right)$$

where, *n* is refractive index of dielectric materials such as glass or plastic. When prism angles become higher than critical angle, total internal reflection occurred. (Figure 2.3(b)) These reflected lights in edge part of 2nd lens were used to send it a PV. If prism angles become much larger by reducing distance between 2nd lens and a PV, total internal reflection was no longer valid for concentration. In other words, when 2nd lens became quite close to a PV, lights can never enter to a PV and go out target region.(Figure 2.16) Therefore, the reason of *CR* drop was that a lot of lights escaped from a target region by extreme total internal reflection.

2.6.2 Basic characteristics of final 2nd lens design

In this work, novel concentrator was suggested for static concentrated PV system whose acceptance angle is ±23.5° that is sun altitude range by seasons. Light distribution (concentration effect) and designed 2nd lens based on non-imaging optics can be seen Figure 2. 15. Rays were concentrated onto a PV after passing 2nd lens. Lights in edge part of 2nd lens were collected by total internal reflection, and others were simply refracted by individually designed prisms. The information of 2nd lens is summarized in Table 2.2. The designed 2nd lens consists of many different prism shapes. Prism size became the smaller toward center of lens, because ray distribution was denser toward center of lens. Smaller prisms for getting small angel variance were required in denser distribution of lights**.** Figure 2.18 illustrates change of the concentration ratio by seasons. As can be seen, concentration ratio varies seasonally. At vernal and autumnal equinox, concentration ratio was the maximum, because light perpendicularly enter system. The maximum concentration ratio was far higher than average concentration ratio.

The maximum value is about two times higher than average value. And average concentration ratio was higher than most of the previous studies except CPC that has the ideal thermodynamic concentration ratio. (Table 2.3) From simple comparison of average concentration ratio between 2nd lens and CPC, the collection performance of this study reached about just 70% of CPC. However different result was estimated by comparing gained energy in systems during a year. The gained energy in system during a year was defined as

$$E_T = \int_{\theta} E \cos\theta_{in} d\theta_{in}$$

where, E_T is the total gained energy during a year, and θ_{in} is the incident angle of sunlight entering to system.

After comparing gained energy in system during a year between concentrator of this thesis and CPC, energy collection ability of 2nd lens approached about 85% of CPC, because of quite higher concentration ratio at small incident angle in 2nd lens system. In general, the available radiative energy is decreased by increasing incident angles. In other words, the available radiative energy becomes the maximum when incident angle is 0°. In Figure 2.17, when sunlight entered a system perpendicularly, that is, at vernal and autumnal equinox, concentration ratio of 2nd lens was higher that of CPC. These values could compensate the lower gained energy than CPC at high incident angles. Thus, static concentrator in present study was useful in energy collection ability –wise.

The 2nd lens was beneficial for replying electrical power consumption for season. Power demands in summer and winter dramatically increase due to cooling and heating facilities. As mentioned in previous section, one of the CPC`s drawbacks is the constant concentration ratio for season, so CPC cannot flexibly handle the peak power periodic. However, concentration ratio of designed concentrator based on non-imaging optics was seasonally varied. Therefore, an

installment position of system with 2nd lens was changed in order to face the sun at summer and winter, the phenomenon about electric power shortage can be solved. The new system that can change installment position of system with 2nd lens for season was designed.

2.7 Summary

The major objective of present study is to develop cheaper static concentrator for higher concentration ratio and more flexible concentration about seasonal variation. Deigning lens based on refraction differs with pervious study. The non-imagine optics is one of the basic elements.

To achieve objective, two lenses system is considered where role of each lens is different; a role of 1st lens is to reduce variance in ray angles and 2nd lens is convex lens and help to direct rays into a designated position.

Ray tracing method which is in-house code utilized for optic design. In simulation, simultaneous analysis method is applied and converged value is used for initial condition. And typical transmittance is applied, because variance of transmittance about incident angles is quite small. Major design parameter is determined by estimating importance about performance. Design parameters are computationally calculated.

As a result, designed lens based on non-imaging help many light concentrate onto a PV. It is composed by a lot of prism having different size. Concentration

ratio varies seasonally. Then maximum concentration ratio is far higher than average concentration ratio and yearly average concentration ratio (1.82) is higher than most of the previous studies. Therefore this system has potential for effective concentration for peak power demand.

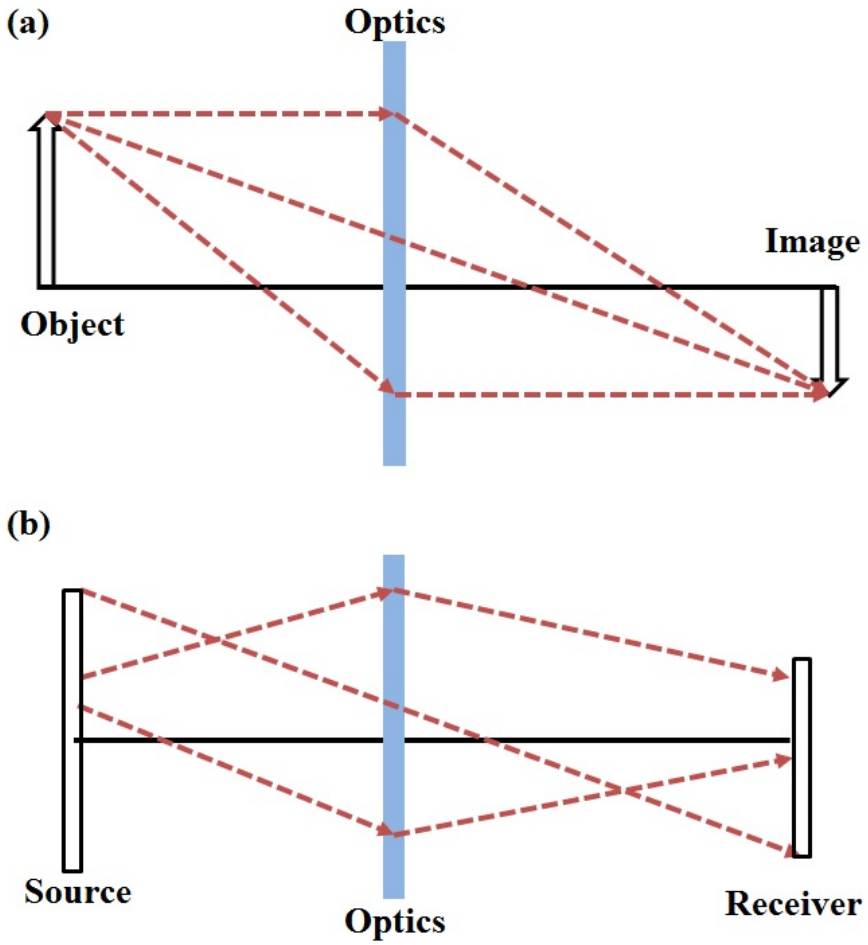

Figure 2.1 Schematic for comparison between imaging and non-imaging optics: (a) Imaging optics, and (b) Non-imaging optics

Table 2.1 Optical principles and classes of solar concentrator. (Ralf Leutz, Akio Suzuki, 2001)

Principle	Imaging optics	Nonimaging optics
Reflection	· Parabolic through · Paraboloidal dish · Fresnel reflector · Spherical reflector with tracking receiver · Cassegrain optics · Heliostat	· Compound parabolic concentrator (CPC) · Hyperboloid (flow line concentrator) ·Derived and other shape ·Higher order concentrator
Refraction	·Fresnel lens	·Nonimaging Fresnel lens ·Compound elliptic rod lens
Dispersion diffraction	·Prism, hologram ·Diffraction grating	
Fluorescence (luminescence)		·Fluorescent planar concentrators

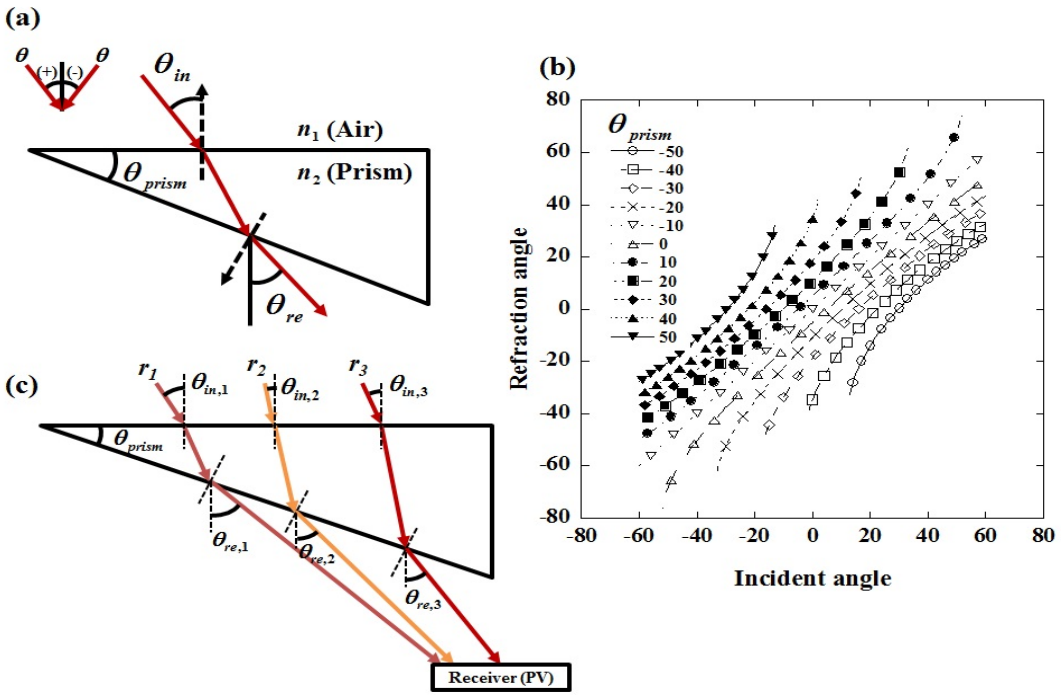

Figure 2.2 Relationship between incident angle and refraction angle in a prism: (a) The schematic of a ray path in a prism, (b) Refraction angles for the given incident and prism angle is proportional to incident angle. (c) Some light's behavior in a prism.

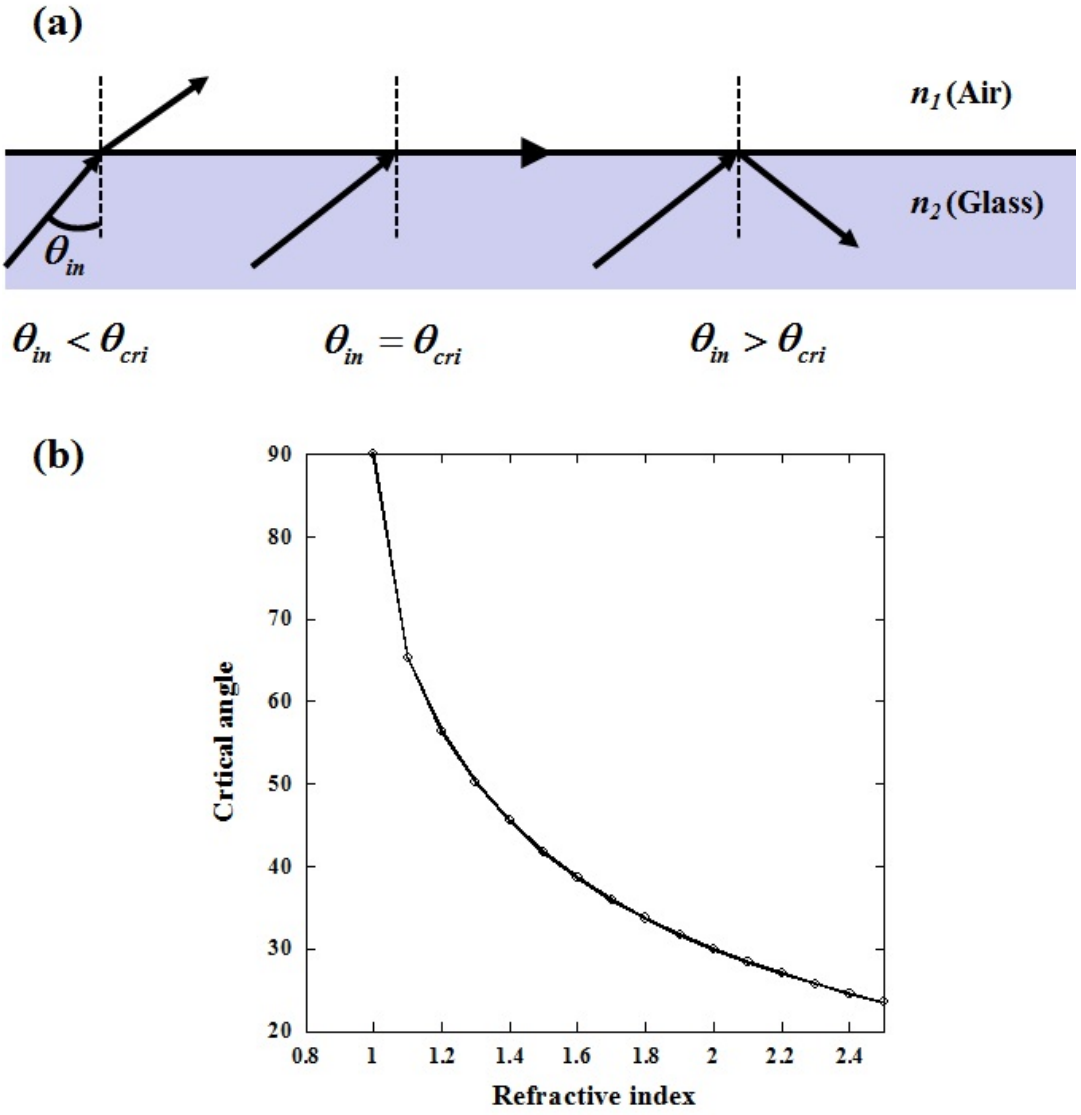

Figure 2.3 Total internal reflection: (a) Schematic of phenomenon, and (b) Critical angles for total internal reflection about different material.

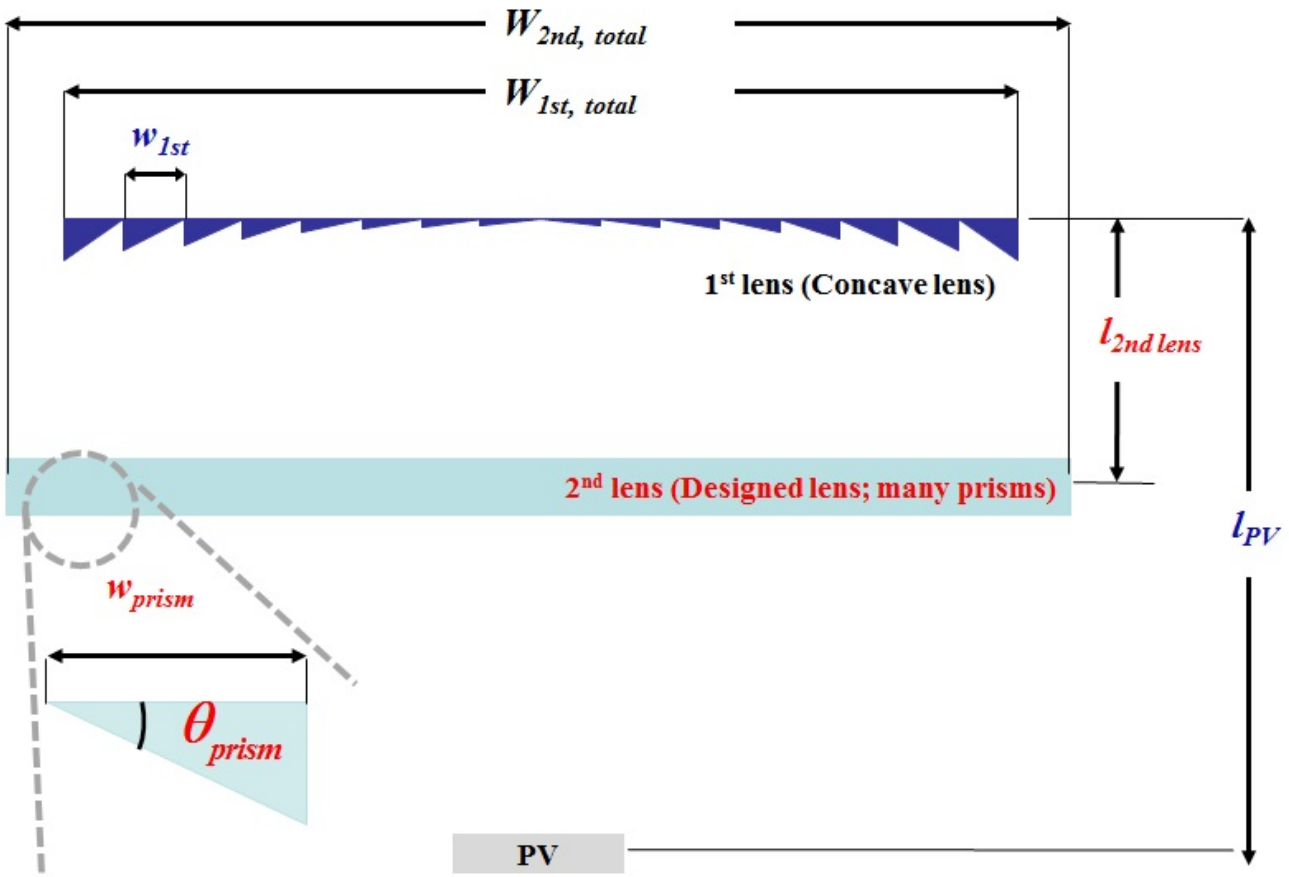

Figure 2.4 Configuration and parameters in present study (two lenses system)

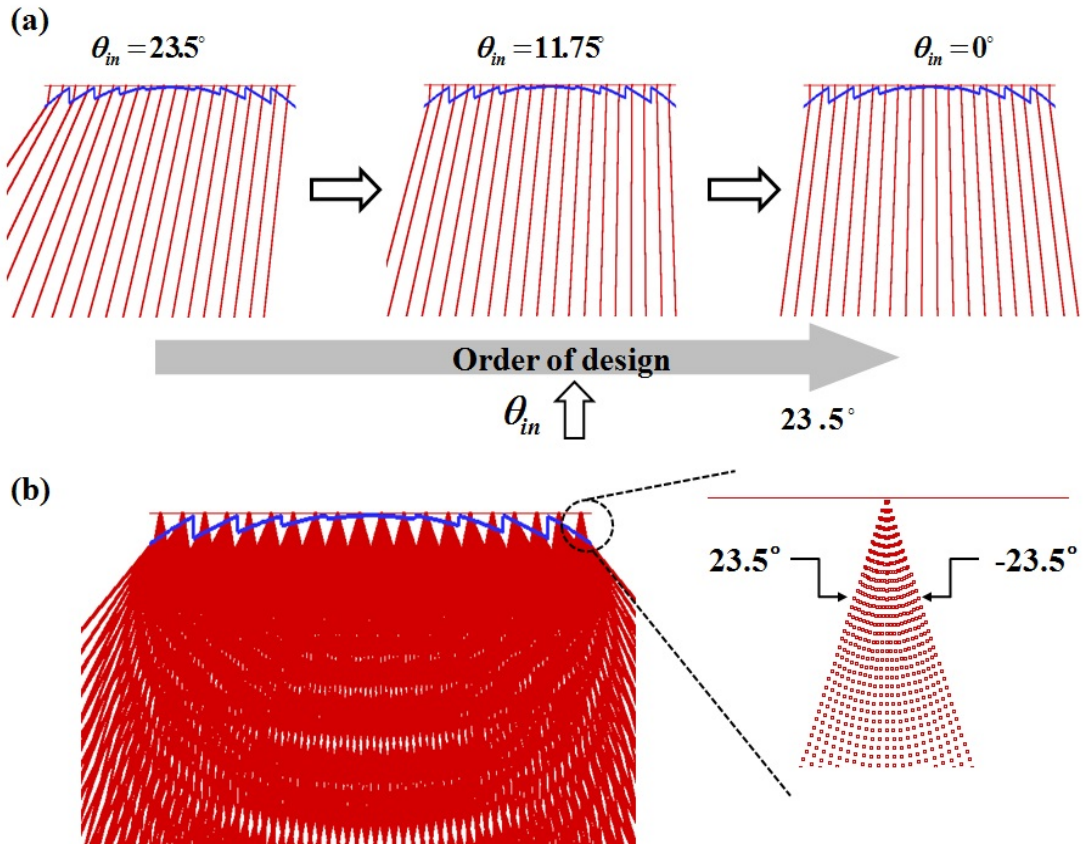

Figure 2.5 Basic optimization approaches for ray tracing method: (a) Sequential evaluation for 2nd lens design, (b) Simultaneous evaluation for 2nd lens design

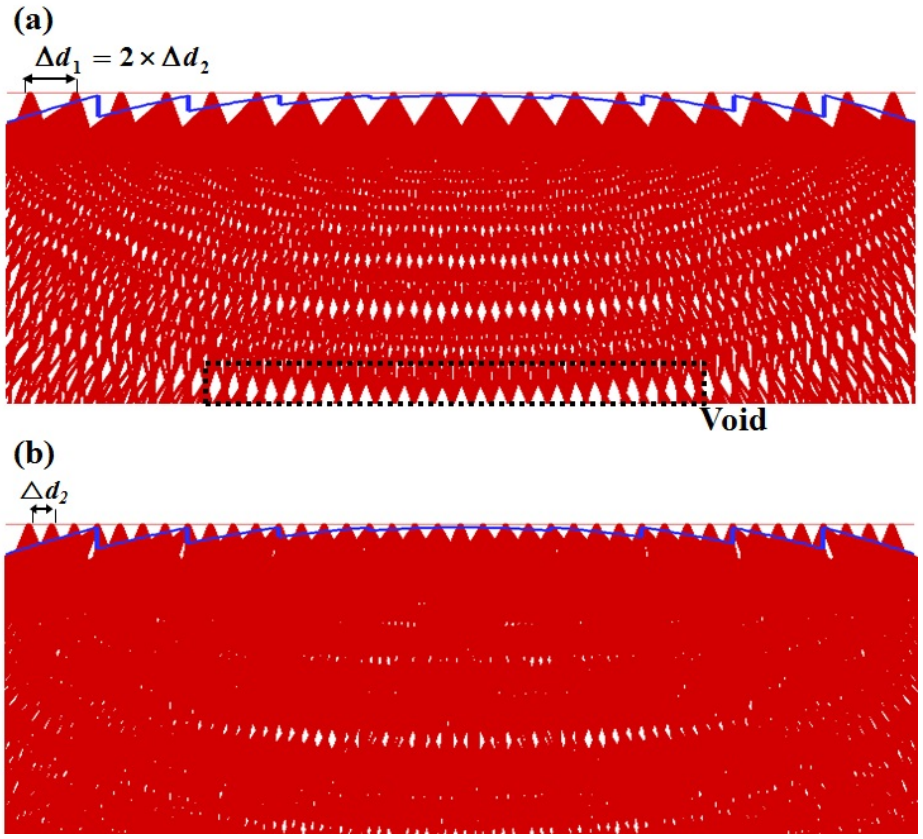

Figure 2.6 Light distribution by different the number of initial rays in simulation : (a) Distance of each initial ray = 1, (b) Distance of each initial ray = 0.5

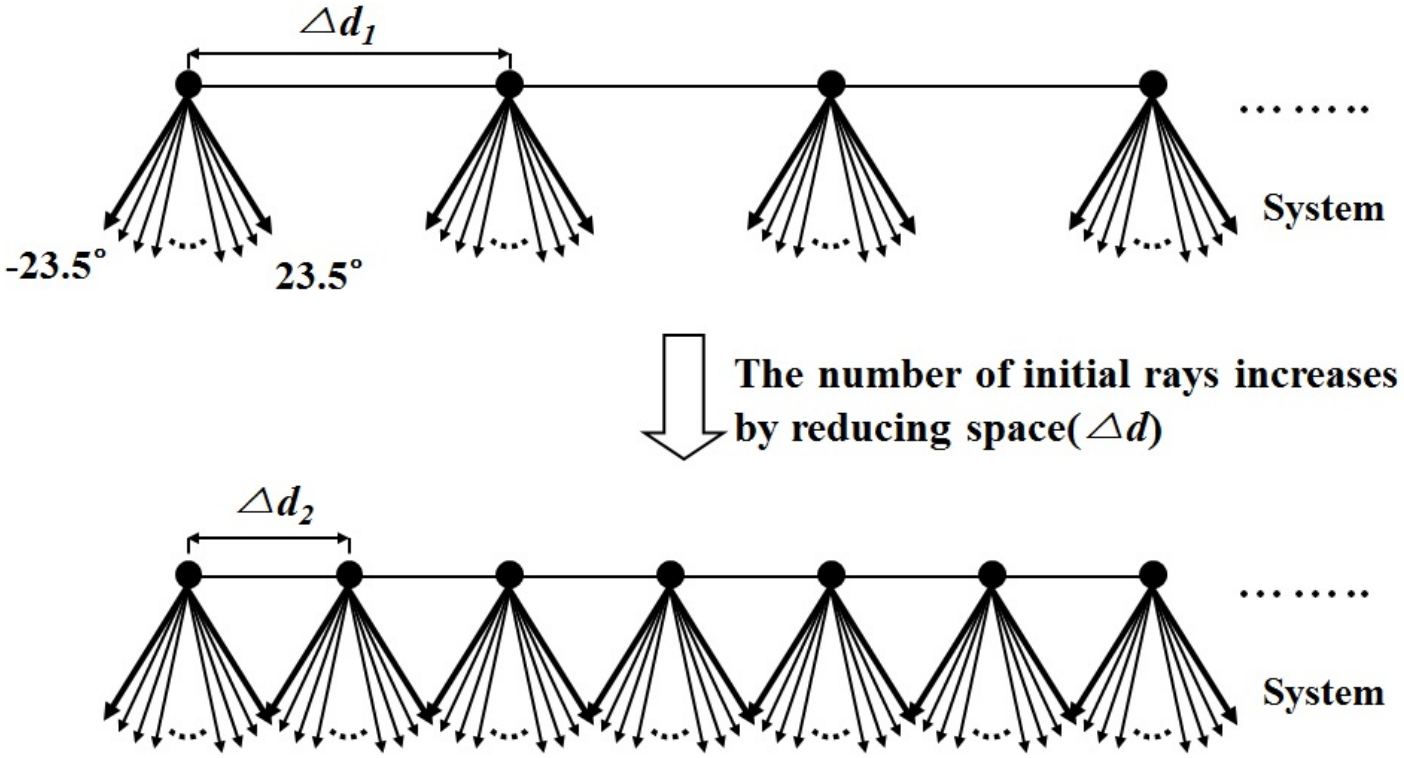

Figure 2.7 Method of increasing the number of initial rays in simulation for convergence tests

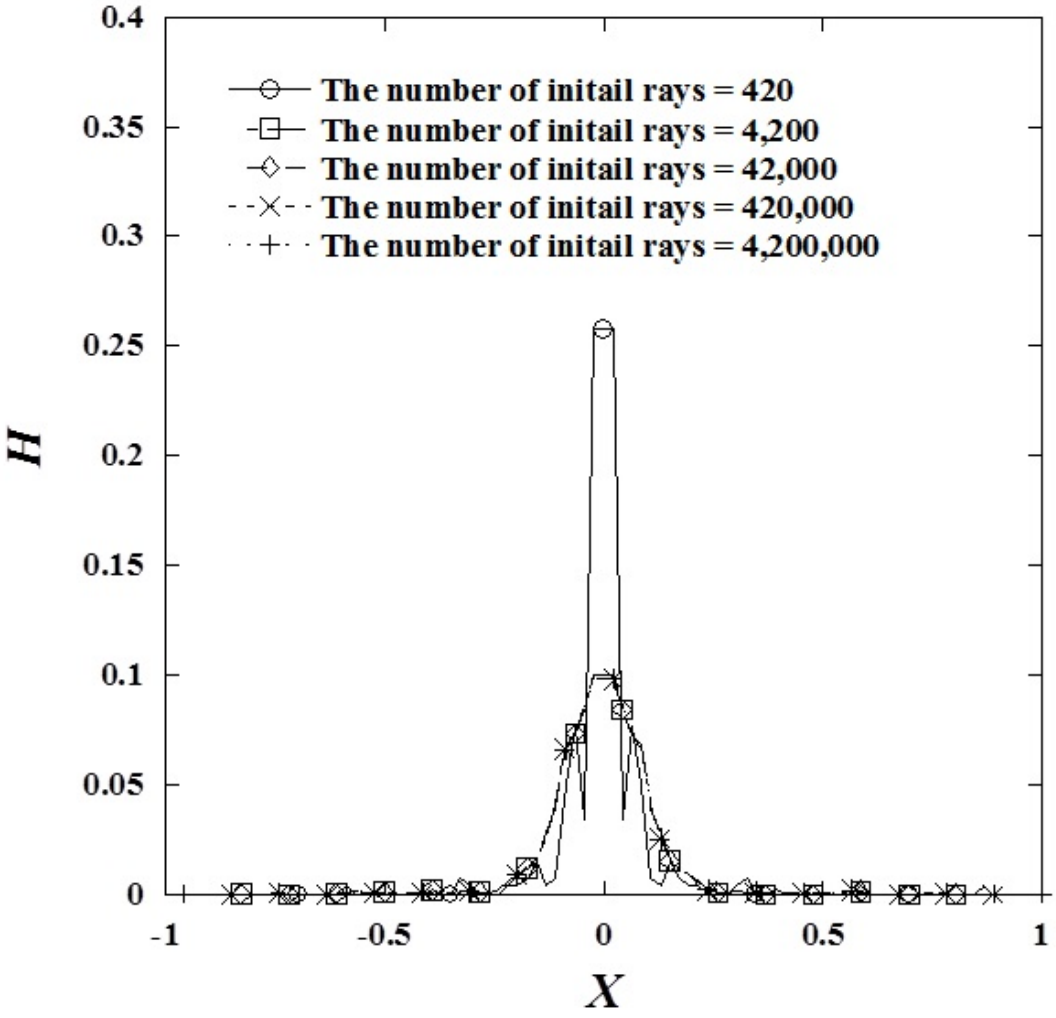

Figure 2.8 Result of convergence tests about the number of initial rays in simulation.

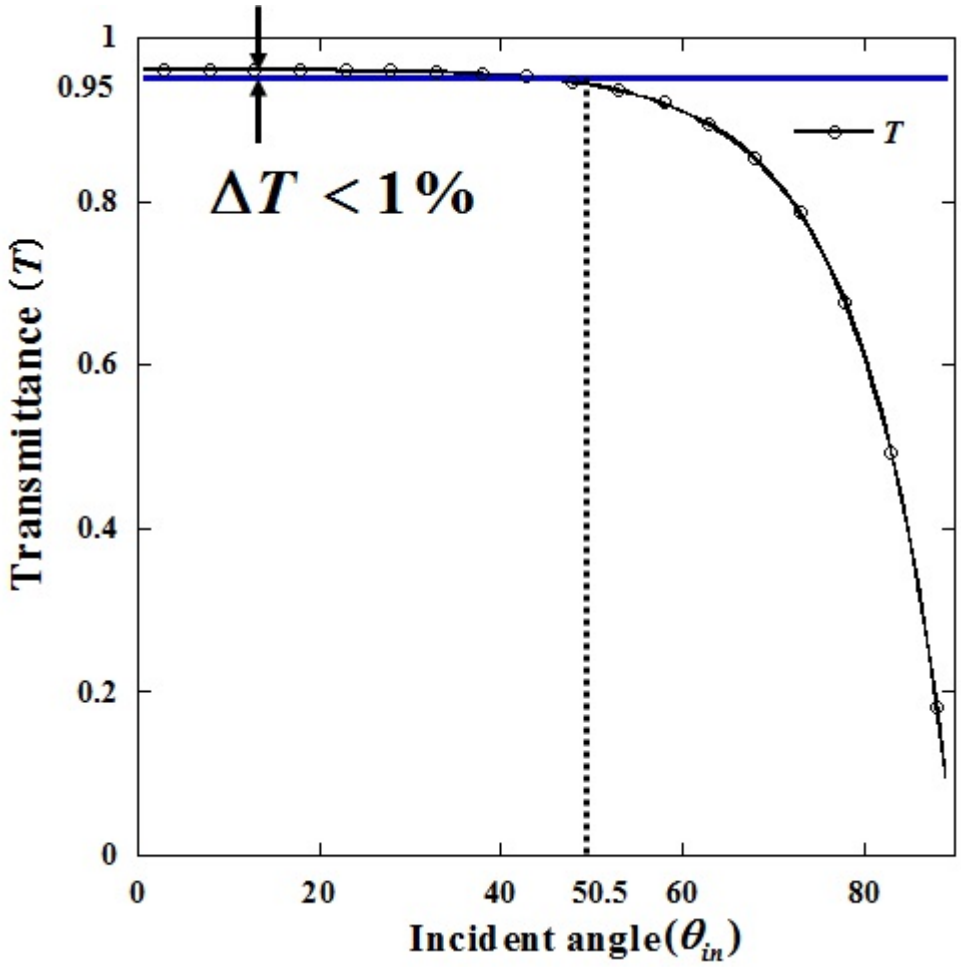

Figure 2.9 Transmittance of lens versus incident angle.

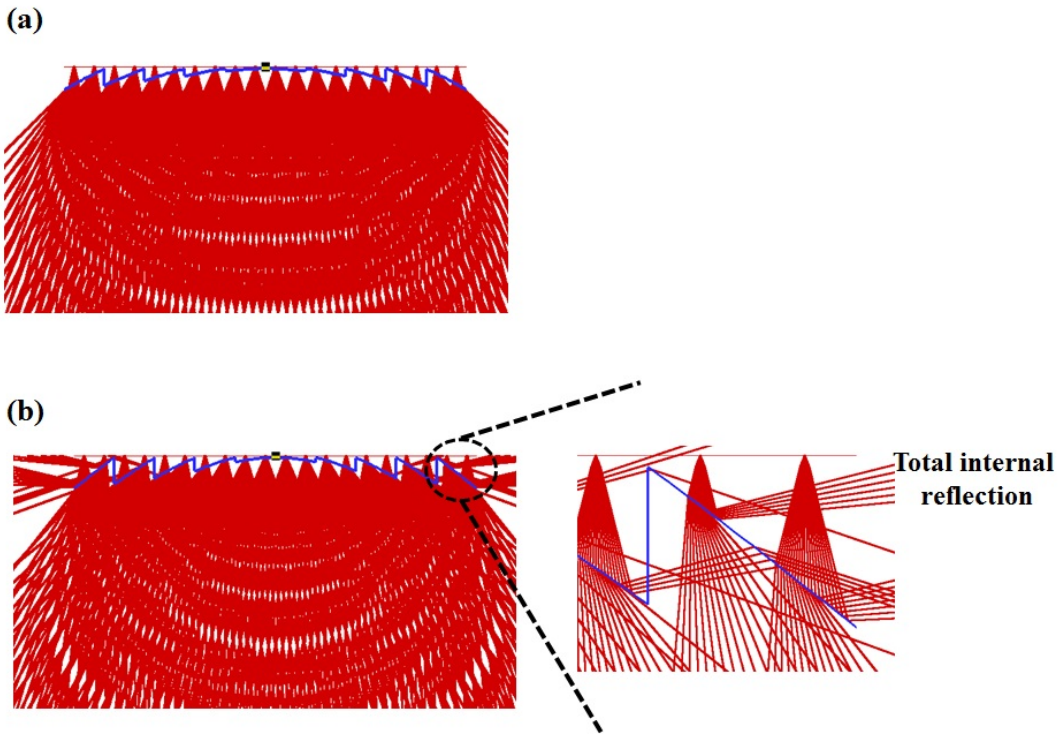

Figure 2.10 Total internal reflection in lens where incident angle is the same, but different focal length of lens: Ray distribution when focal length of lens = 38 and (b) Ray distribution when focal length of lens = 19

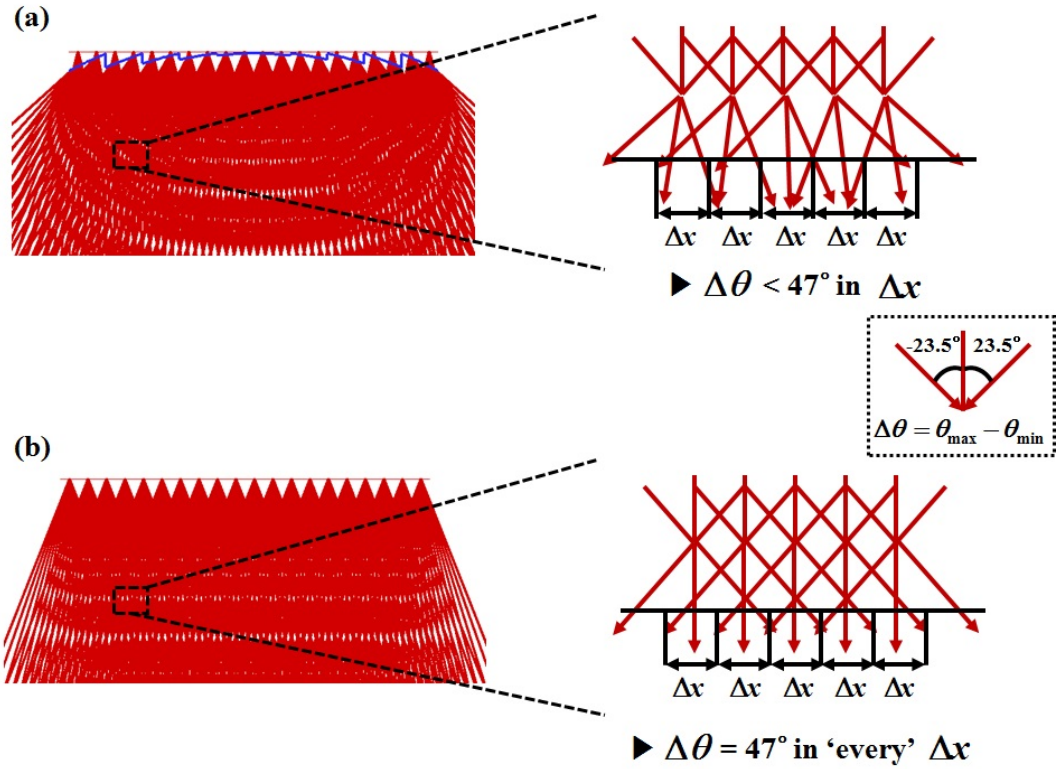

Figure 2.11 Importance of 1st lens roles for 2nd lens design: (a) Ray distribution after passing 1st lens; difference of ray`s angle in some segment became small, (b) Ray distribution without 1st lens; differences of ray`s angle in anywhere were the same.

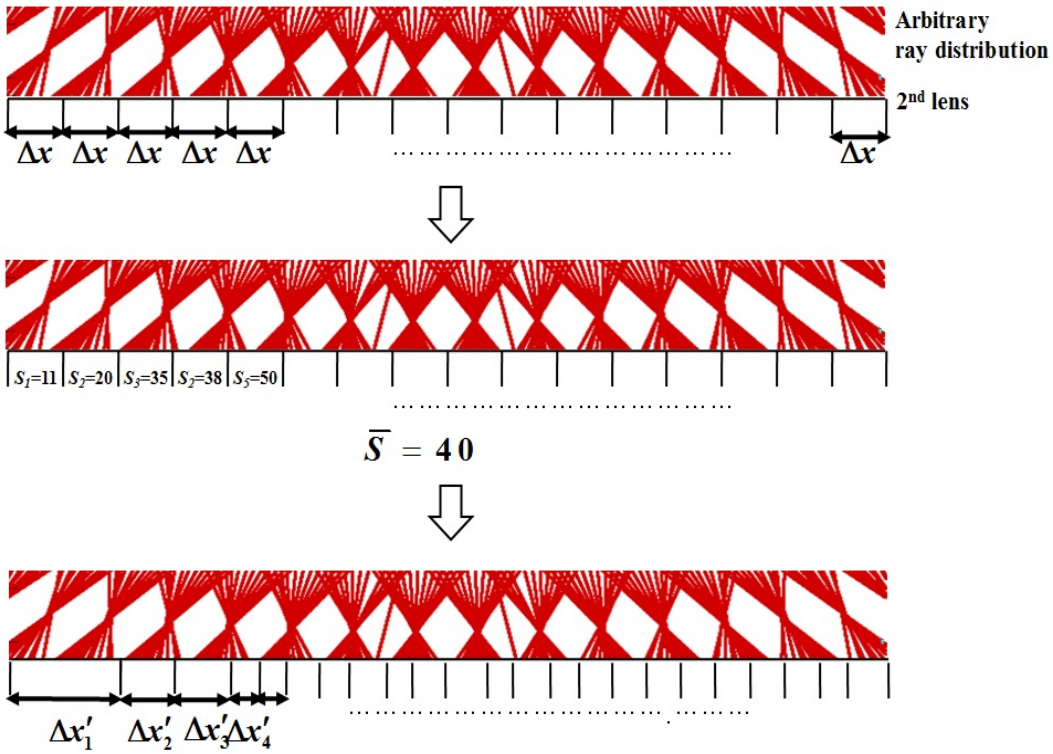

Figure 2.12 Procedure for setting prism width in 2nd lens (w_{2nd}).

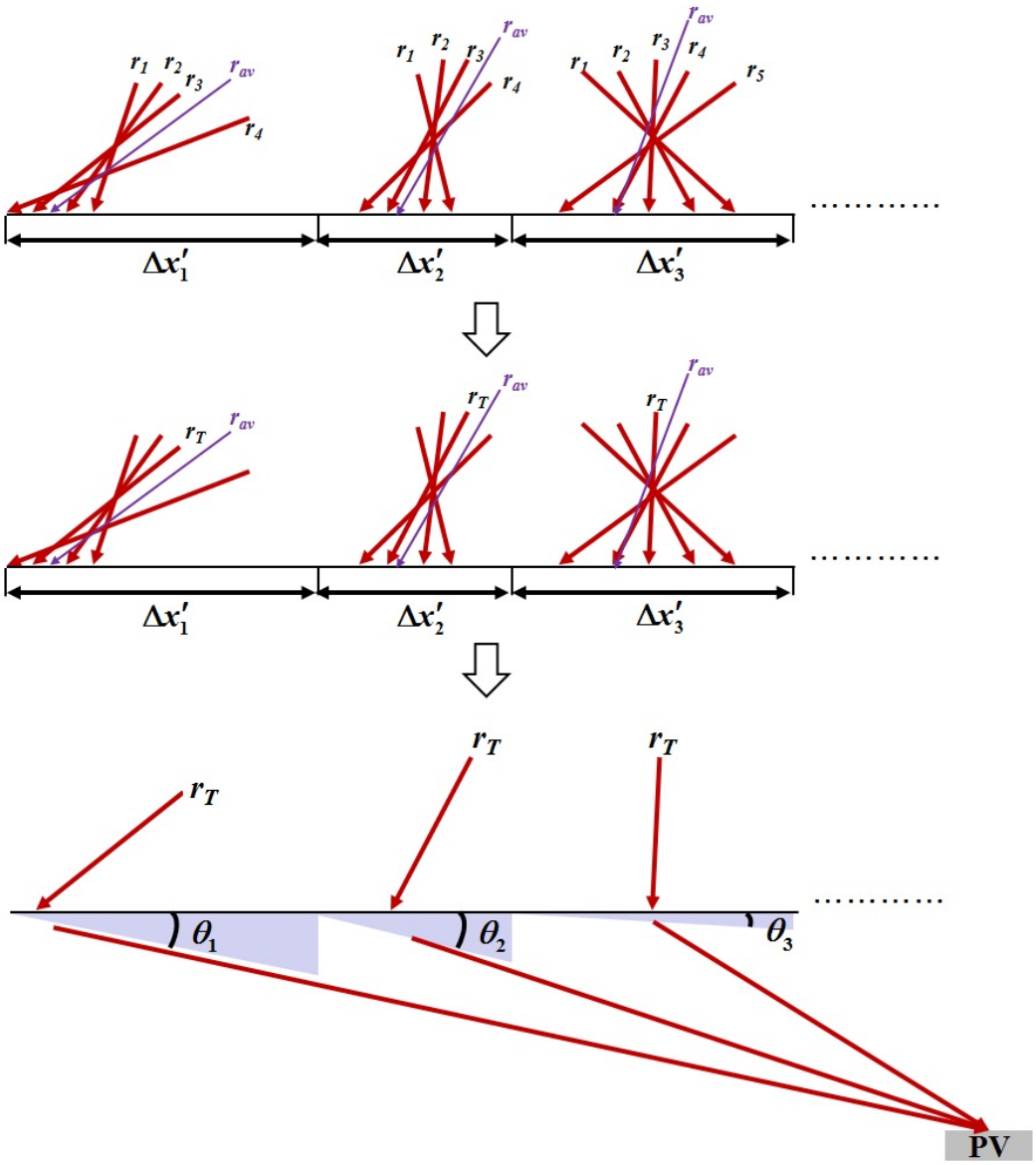

Figure 2.13 Procedure for setting prism angles in 2nd lens (θ_{prism}).

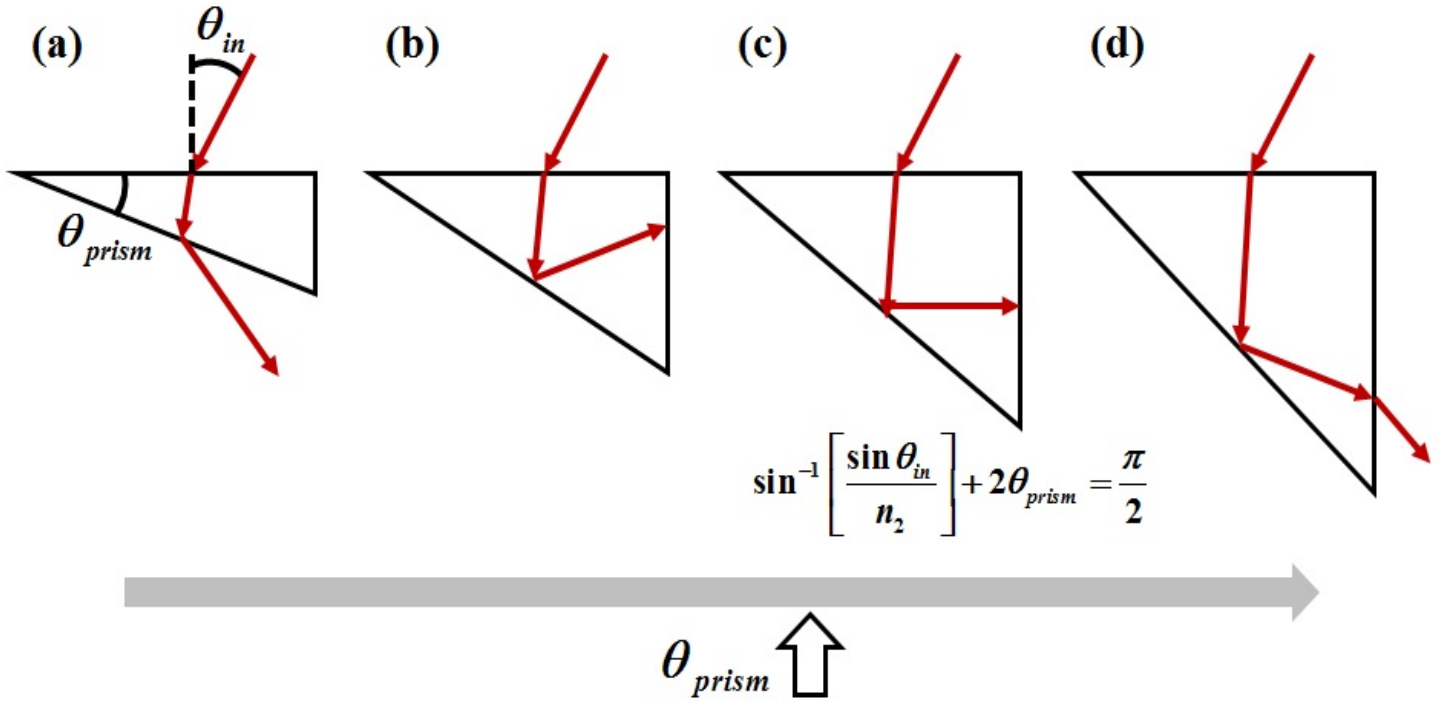

Figure 2.14 Progress of total internal reflection; (a) General refraction in a prism, (b) Total internal reflection , (c) Critical situation for escaping light from a prism, (d) Escaped light from a prism after total internal reflection.

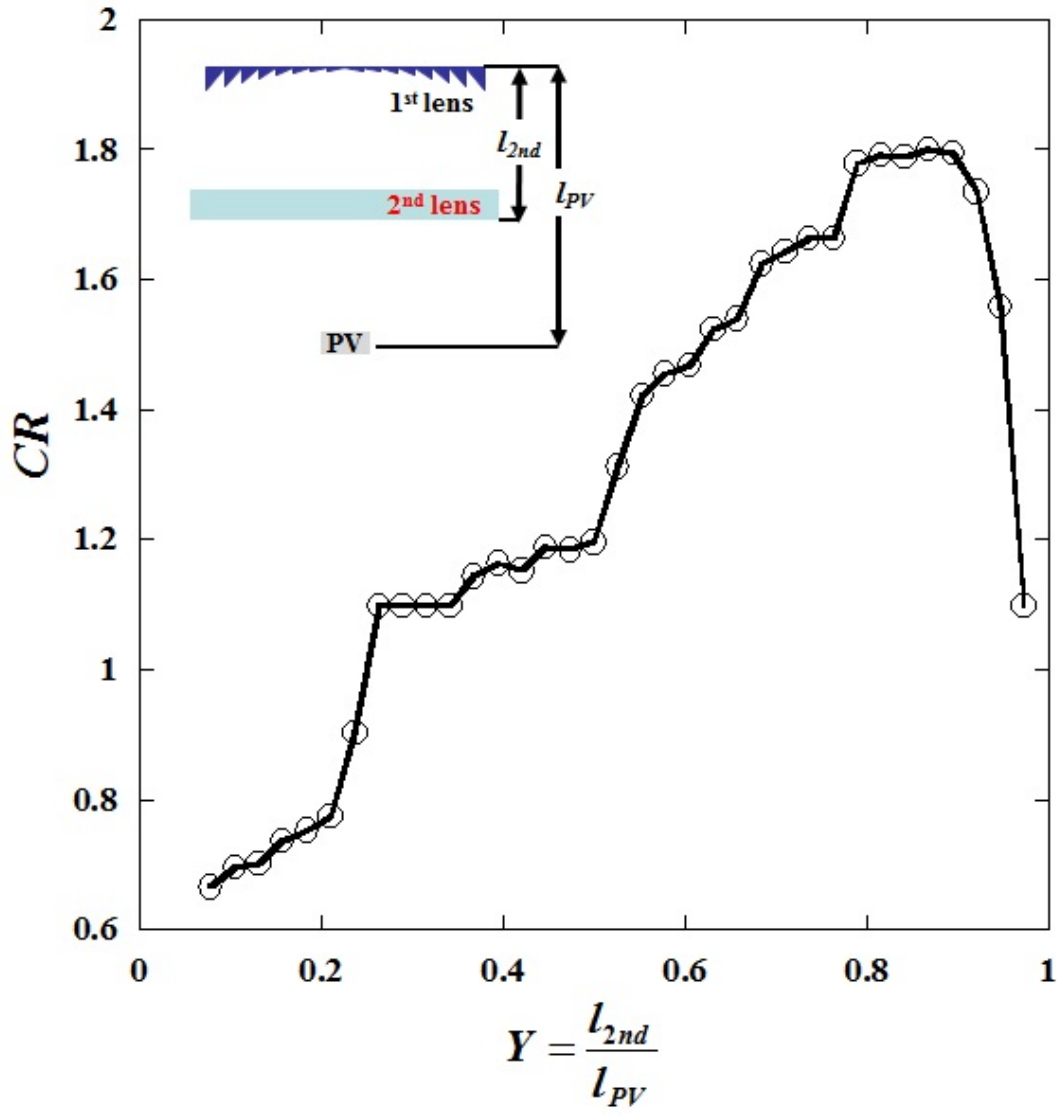

Figure 2.15 Simulation result of optimum 2nd lens location.

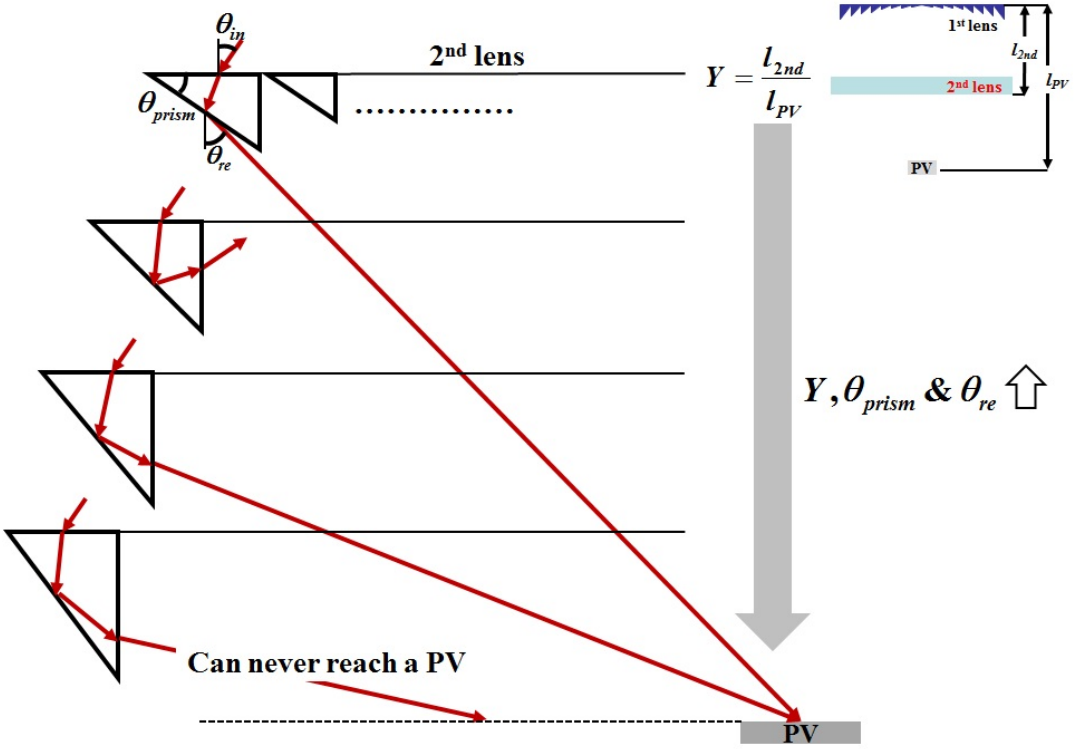

Figure 2.16 Path of light in the edge prism while 2nd lens location becomes closer to a PV

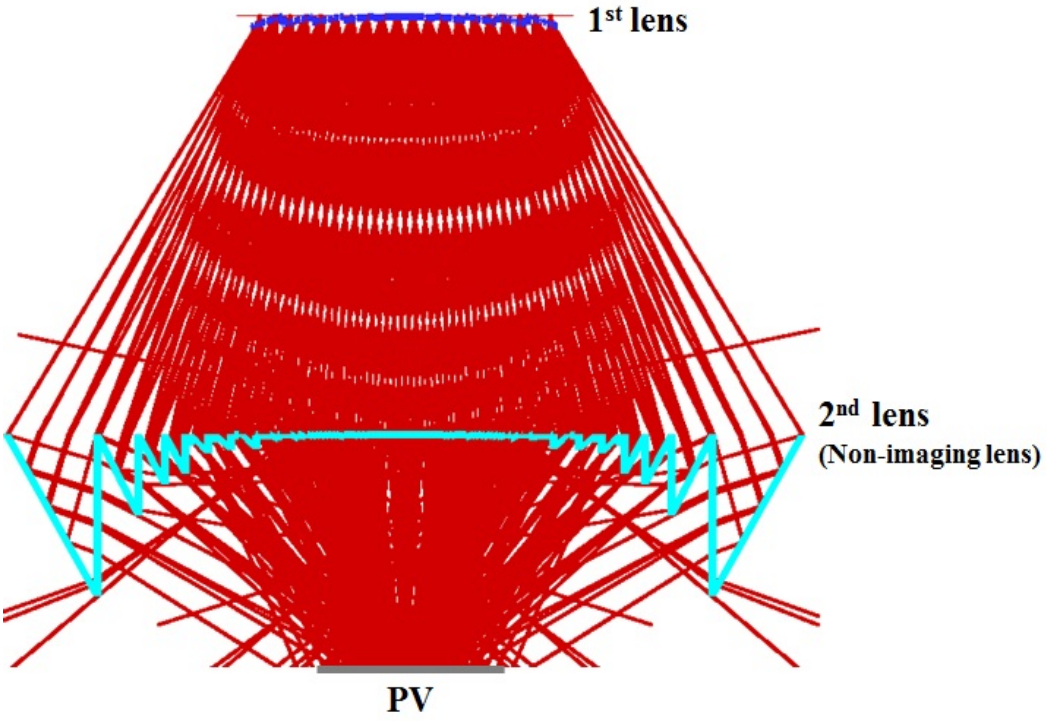

Figure 2.17 Ray distribution about designed system which includes 2nd lens

Table 2.2 Information of designed non-imaging lens.

Parameter	Value
The number of prism	4094
Width of prism (w_{2nd})	0.0005 ~ 0.1015
Prism angle (θ_{prism})	0.17° ~ 71.62°
Location (Y)	0.868

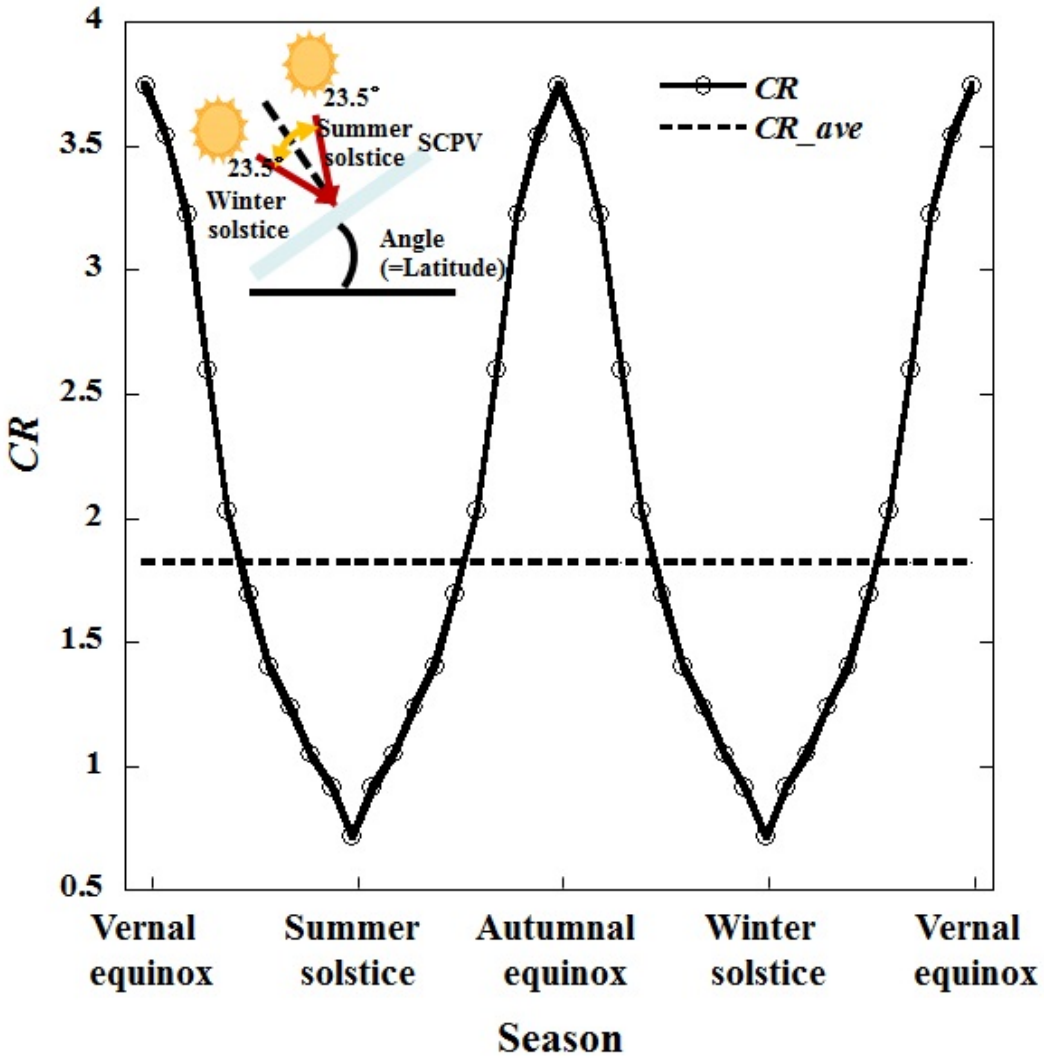

Figure 2.18 Yearly variation of concentration ratio about 2nd lens.

Table 2.3 Comparison of system performance in previous study results: (a) S. Bowden et al. (1993), (b) K. Yoshioka et al. (1994), (c) K.J. Weber et al. (2001) (d) K.J. Weber et al. (2006)

Schematic	Mechanism	CR
CPC 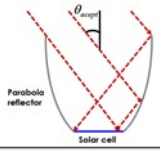	Non-imaging -Reflective mirror	2.51
(a) 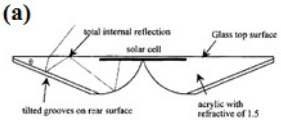	Total internal reflection	~ 1.8
(b) 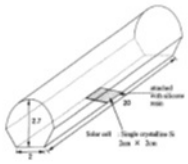	Reflection & Refraction	~1.6
(c) 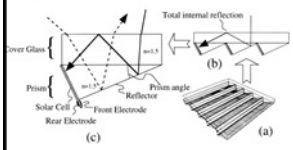	Total internal reflection	~1.8
(d) 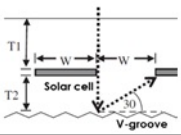	Reflection (V-groove)	~1.6
My model 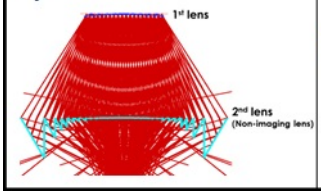	Non-imaging – Designed Lens (refraction)	1.82

Chapter 3.

Experiment

3.1 Introduction

The objective of experiment was to validate simulation method which used for concentrator design in present study. In other words, purpose of experiment was just to check reliability of ray tracking method instead of verifying concentration performance of designed static concentrator. Conducting experiment with lens which was designed by non-imaging optics and comparing results of experiment and those of simulation are the best way to verify performance of designed static concentrator. Cost-effectiveness for experiment with new non-imagining lens should be considered. In general, lens is made by metallic mold method. When new lens produces, high initial cost for manufacturing new mold fame is taken. Manufacturing new lens was inefficient for a few experiments. Thus, it is also meaningful to conduct experiment about simple system which consists of conventional lenses in order to estimate ray tracing method and algorithm of lens design. Therefore, in experiment two lenses that can easily and cheaply be purchased in real were set as experiment components, power distribution after passing two lenses was measure. (Figure 3.1) And measured power distribution in experiment was compared to simulated power distribution in equivalent experiment

condition.

3.2 Experimental setup

Figure 3.2 shows experimental setup A solar simulator (Model; K3000 lab 55, Mcscience) were used to reproduce real sunlight. Its source is xenon and effective source size is 5 x 5 cm. Lenses for experiment were linear Fresnel lens, because liner Fresnel lens is 2-dimensional lens; linear prism is connected. (Figure 3. 4) Design of 2-dimensional static concentrator was the objective of present study. And algorithm of ray tracing method was also just considered in 2-dimension. Therefore, Linear Fresnel lens is suitable to set up 2-dimensional experiment. The sizes of two lenses were different. Table 3.1 summarizes specification of the two lenses. A lens whose width was similar to width of solar simulator was selected as 1^{st} lens in experiment, and 2^{nd} lens having wider width than 1^{st} lens was set in order to receive all lights passing by 1^{st} lens. The distance between 1^{st} lens and 2^{nd} lens was 5cm by considering focal length of 1^{st} lens. Black paper was attached on side of 1^{st} lens in order to block out other lights passing 2^{nd} lens directly. (Figure 3.5)

Powermeter (Model; OP-2 UV, Coherent) was used to measure power distribution. It can measure up to 50 mW. This maximum available measurement range of powermeter sufficiently covers generating power ranges during present experiment. Active area diameter for detection is 7.9 cm. (Figure 3.5(b)) As mentioned before, experiment and simulation were considered in 2-dimension. Thus, 1-dimesional distribution was useful data in this experiment. In general,

powermeter measures sum of power in detection area. Circle active area for measurement causes uncertainty by sum of power including unnecessary power for 1-dimesional distribution. Therefore, detection area changed from circle to rectangle by attaching paper having small rectangle on detector. The active area for measuring power distribution was 0.7 x 0.1 cm. (Figure 3.5(c)) Powermter was put at 7.52 cm below 2^{nd} lens. Measurement points for power distribution passing by two lenses were 21points and distance each point was 0.7 cm.

Translation stage was required for measuring 1-dimensional power distribution. An alignment of the optical devices is important, because light behavior may be sharply changed by installment angle or position of optical devices, Installment angles of experimental components such as two lenses, and power meter were adjusted by digital protector .(Figure 3.6(a))

Experiment was repeatedly conducted 10 times.

3.3 Simulation condition

Results of simulation should be necessary for comparing those of experiment. Surely, simulation condition corresponded with experimental condition.

3.3.1 Transmittance of lens

As mentioned earlier, transmittance of lens is a function of incident angles. Thus, variation of transmittance about incident angles should be considered for

estimating exact power distribution after passing lens. In experimental condition, incident angles before entering 1^{st} lens and 2^{nd} lens were smaller than 50°. Applying typical value (=0.95) for transmittance was not problem. Therefore, transmittances of lenses were set by 0.95.

3.3.1 Determination of lens shape

Two linear Fresnel lenses having different sizes were set as experimental component. These lenses consist of a lot of small prisms. An optics company never generally provides exact lens shape like the number of prisms, prism size, and so on; hence shape of lens was reproduced by Fermat's principle in present study. The Fermat`s principle is that a ray of light passes from one point to another in such a way that the time taken is a minimum. Fermat's principle leads to refraction phenomenon. Aspherical lens whose curvature is not parabola instead of circle is easily expressed by Fermat`s principle. And Fresnel is made by rearranging divided small parts by keeping curvature of aspherical lens. As a result, Fresnel lens shape or curvature is naturally taken by aspherical lens.

In Figure 3.8, light-travel time for reaching a focal point can expressed by Fermat`s principle

$$t = \frac{n_2 \overline{AP}}{c} + \frac{n_1 \overline{PF}}{c} \quad \text{---------- for 1st ray}$$

$$t = \frac{n_2 \overline{BC}}{c} + \frac{n_1 \overline{CF}}{c} \quad \text{----------for 2nd ray}$$

where, t is light-travel time, n_2 is refractive index of lens, n_1 is refractive index of air, and c is velocity of light.

After arranging two equations, the trace of ashperical lens can be expressed by

$$(1-n_2)y_c + n_2 y = \sqrt{(y-y_f)^2 - (x-y_f)^2}$$

Fresnel lens shapes can be gotten by controlling some variables. Two different shapes which have the same focal point can be generated by kinds of controlling variables. If x is controlled, Fresnel lens having constant prism width can be shown. And if y_c is controlled, Fresnel lens having constant thickness can be gotten. In experiment, lenses were type of constant thickness. (Figure 3.9) These lenses were also utilized by simulation.

3.4 Results and discussion

The results of experiment were compared with those of simulation. Figure 3.10 shows the result of both experiment and simulation. The simulation data was

reasonably close to experiment results. The MAPE (Mean Absolute Percentage Error) is defined as

$$MAPE = \frac{1}{m}\sum_{t=1}^{m}\frac{\left|E_t - S_t\right|}{E_t} \times 100[\%]$$

where, m is the number of fitted points, E_t means the experiment values and S_t is simulation values. In result, MAPE about this experiment was 4.371 %. Therefore, simulation method for static concentrator was reliable.

There was some uncertainty of measurement which causes errors in experiment. First of all, uncertainty was caused by ignoring variations of optical properties by wavelength. As mentioned before, refractive index is a function of wavelength. In simulation, typical value was applied for simple calculation. But light source of solar simulator includes various wavelengths in order to reproduce real sunlight. This different condition between experiment and simulation somewhat caused uncertainty. Secondly, inaccurate center align for optics devices may generate error. The aligning center of optical device was conducted by hand. Last uncertainty was related with devices themselves. In other words tolerance for manufacture, cleanness of lenses and light condition of solar simulator may be affected uncertainty of measurement.

3.5 Summary

In this chapter, experiment is discussed. The objective of experiment is to validate simulation method. Simple system which consists of two linear convex Fresnel lenses having different sizes is set for experiment. Power distribution is measured and compared with simulation results.

Based on comparison of both results, reliability of simulation method is verified because the error (MAPE) is less than 5%.

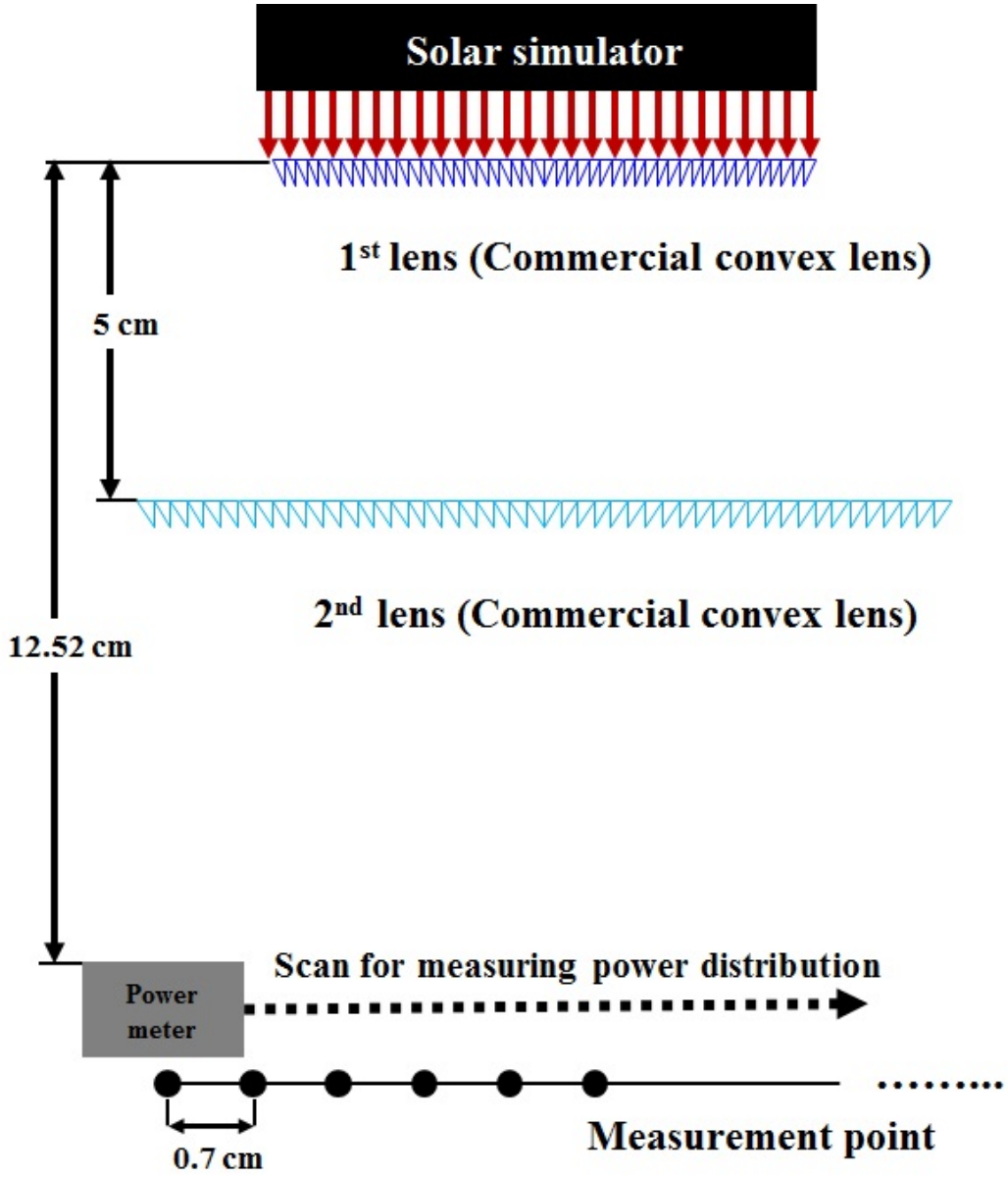

Figure 3.1 Schematic of experiment and simulation condition.

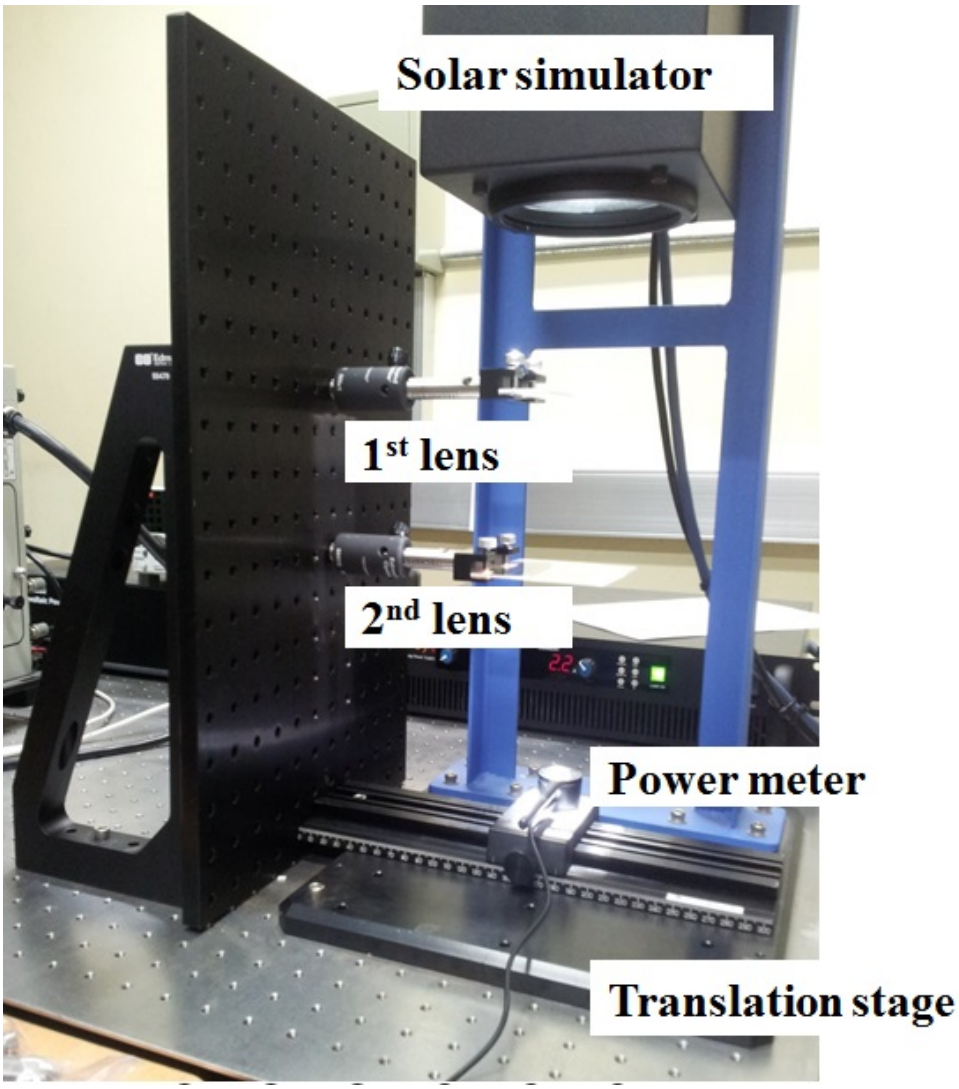

Figure 3.2 Experimental setup including Solar simulator (Model; K3000 lab 55, Mcscience), 1st and 2nd lens (Linear convex Fresnel lens), Powermeter (Model; OP-2 UV, Coherent) , and Translation stage.

Table 3.1 Specification of linear Fresnel convex lenses

Parameter	1st lens	2nd lens
width (cm)	5.715	8.225
length (cm)	6.858	10.16
Focal length (cm)	5.08	15.24

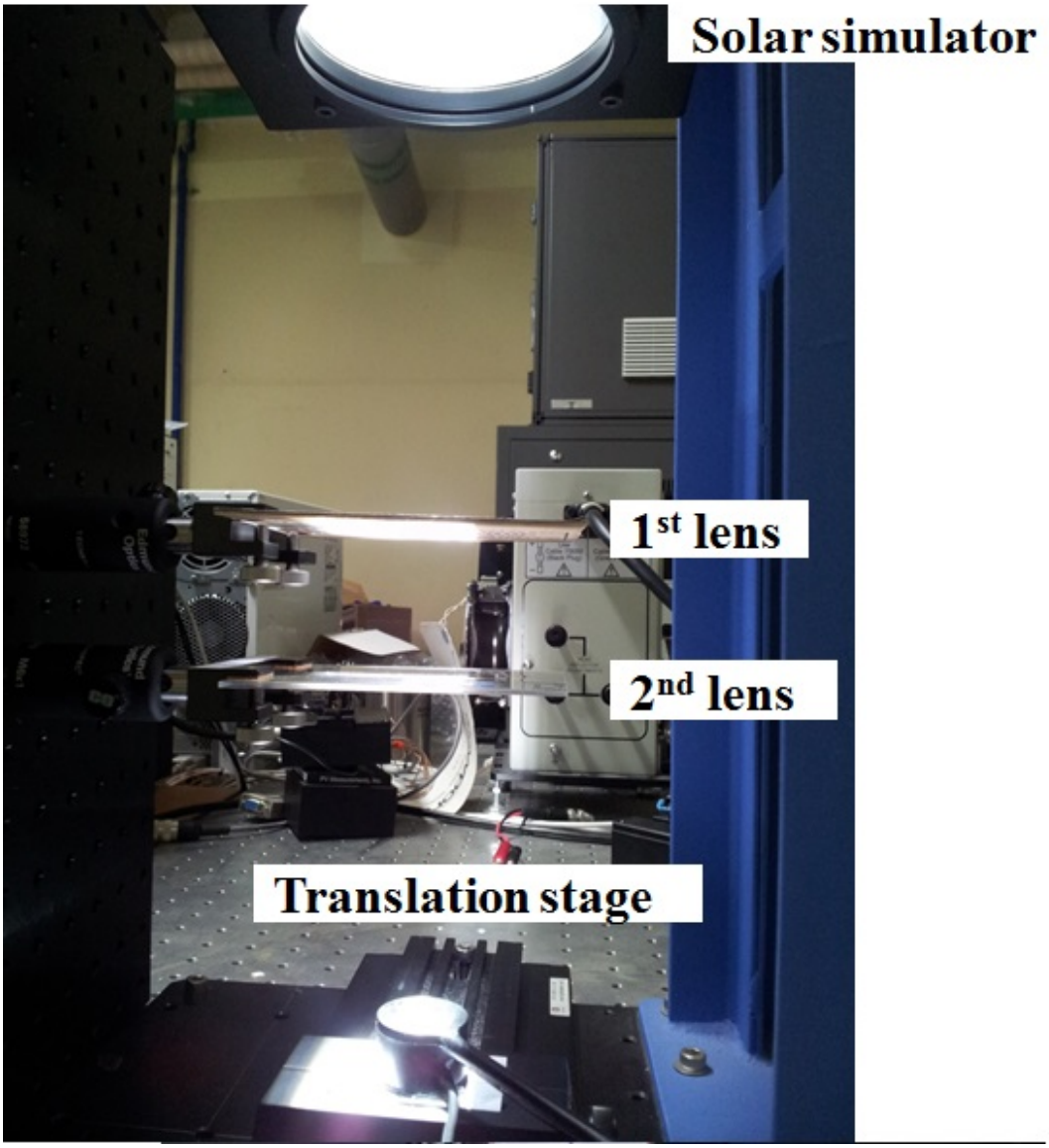

Figure 3.3 Process of experiment by using two convex lenses.

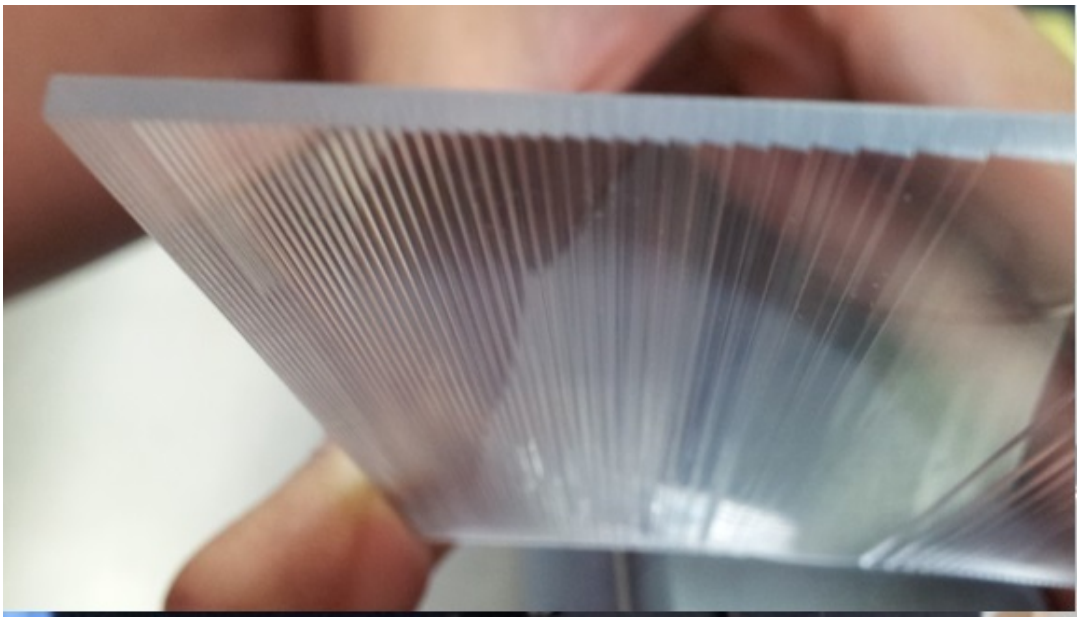

Figure 3.4 Shape of linear Fresnel convex lens.

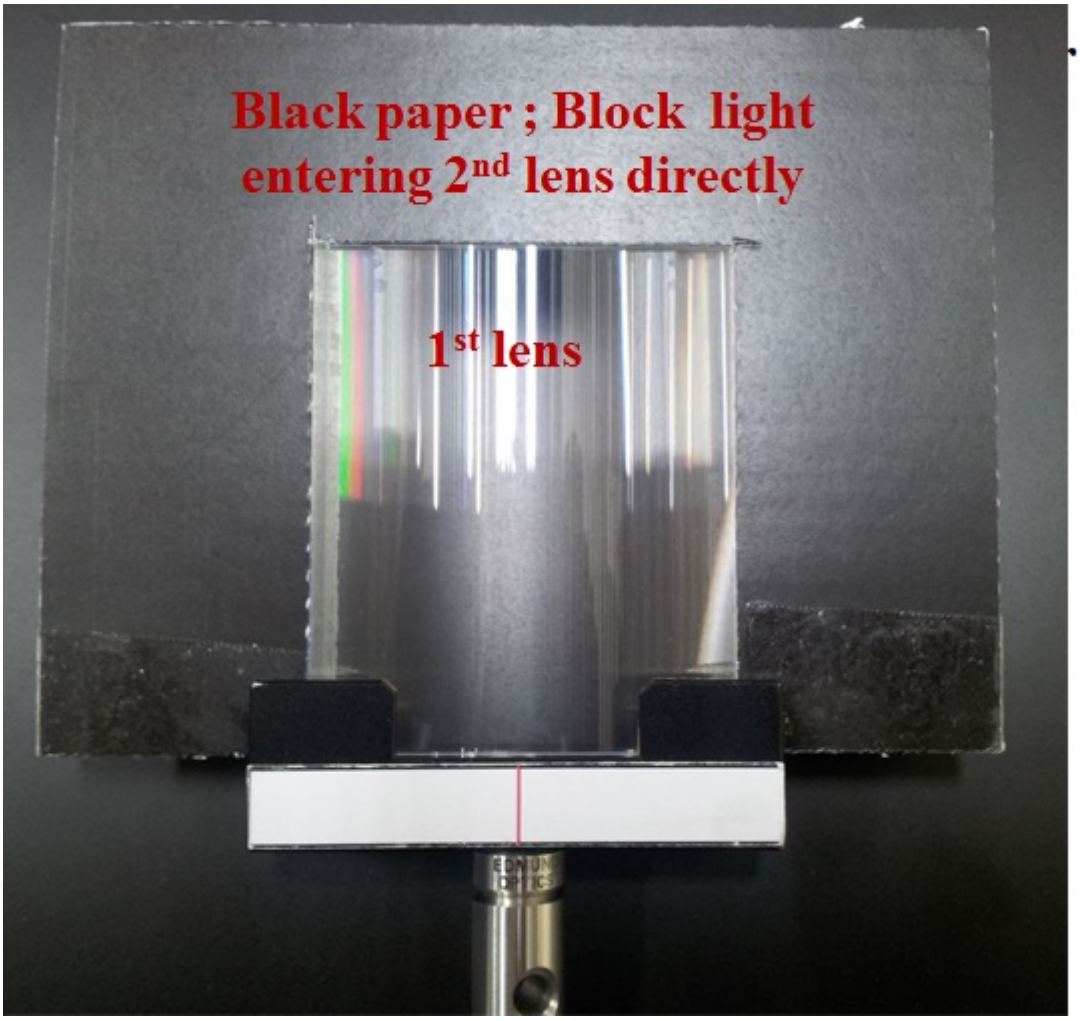

Figure 3.5 Attached black paper on sides of 1st lens.

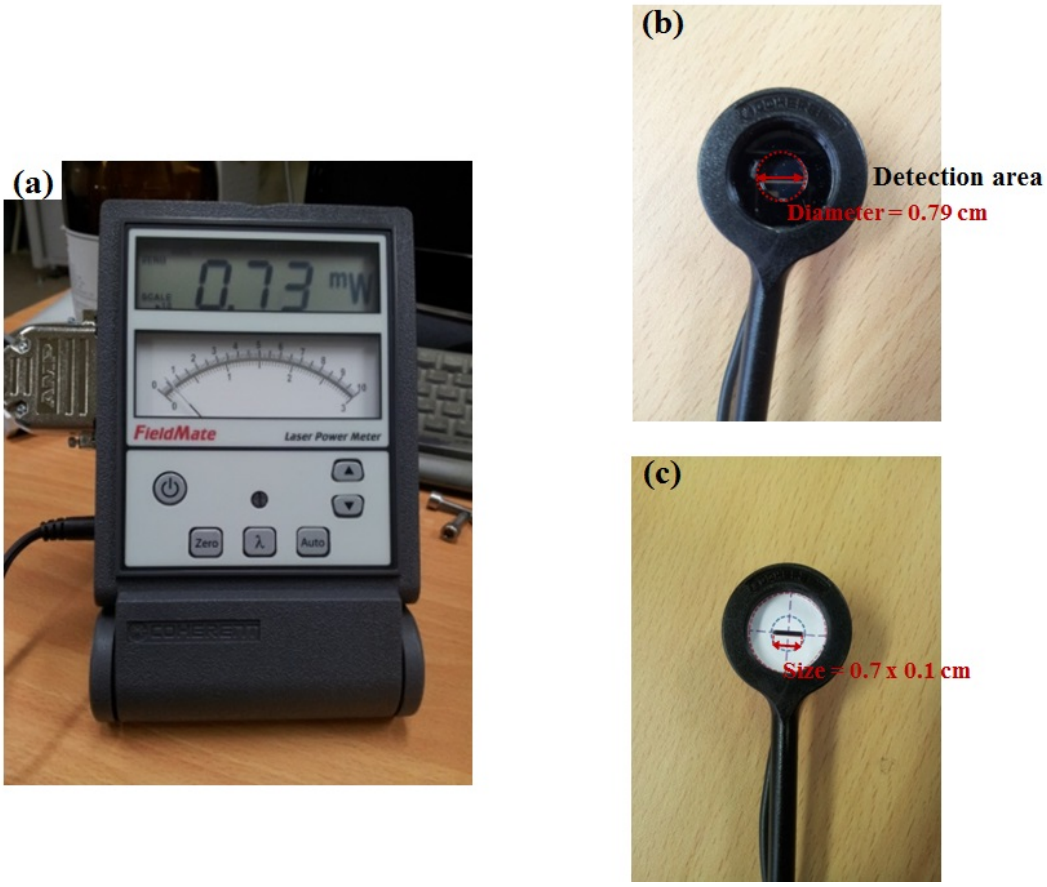

Figure 3.6 Powermeter (Model; OP-2 UV, Coherent): (a) monitor, (b) original detection area, and (c) modified detection area.

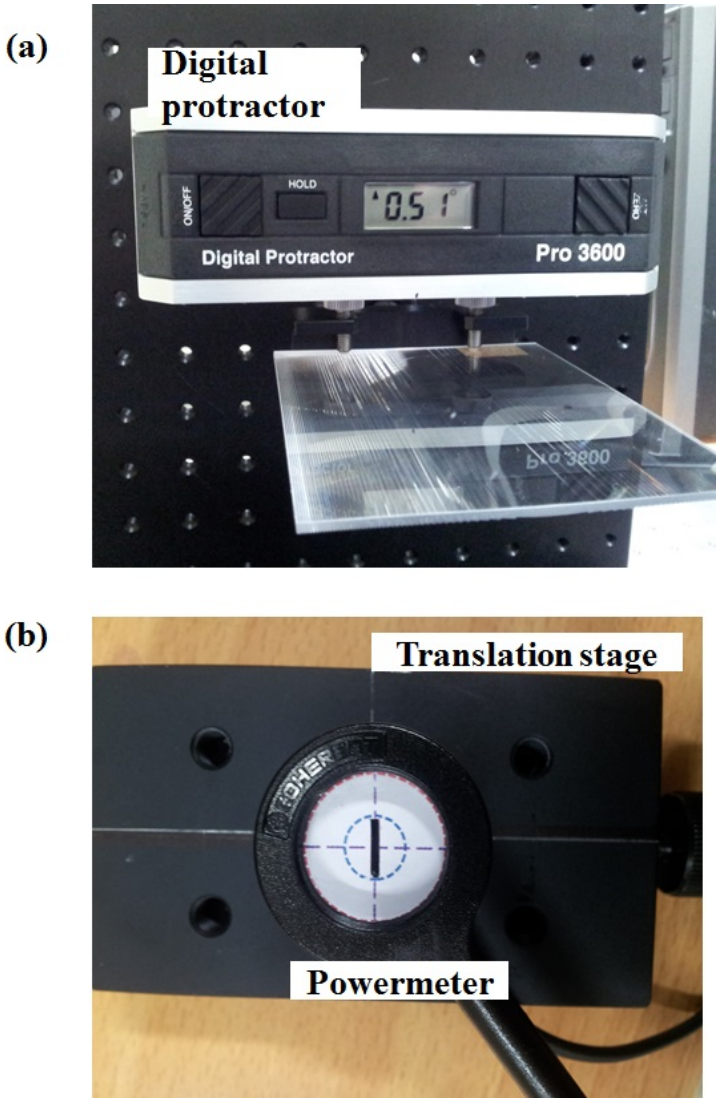

Figure 3.7 Method for alignment of optical device: (a) Alignment of installment angles by using digital protector, and (b) Alignment of center by hand.

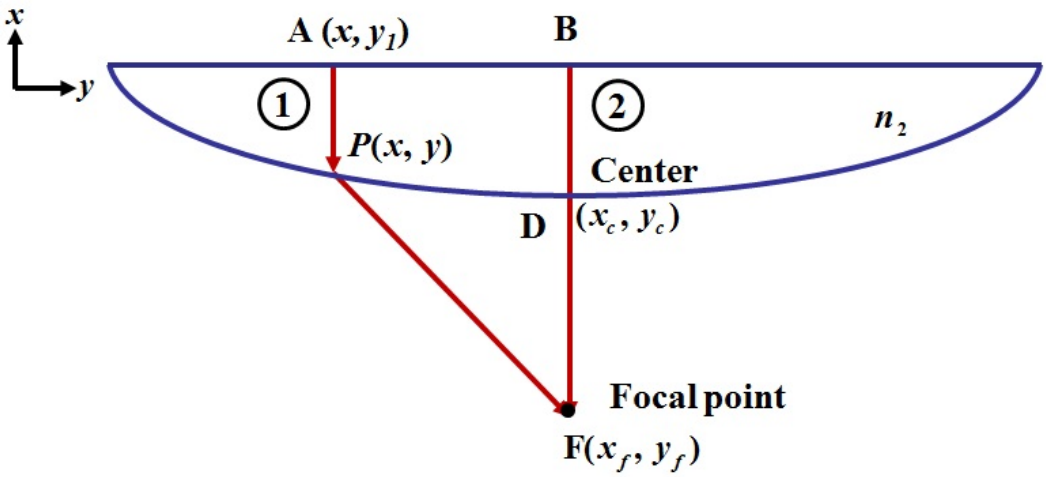

Figure 3.8　Trace of ashperical lens by applying Fermat`s principle.

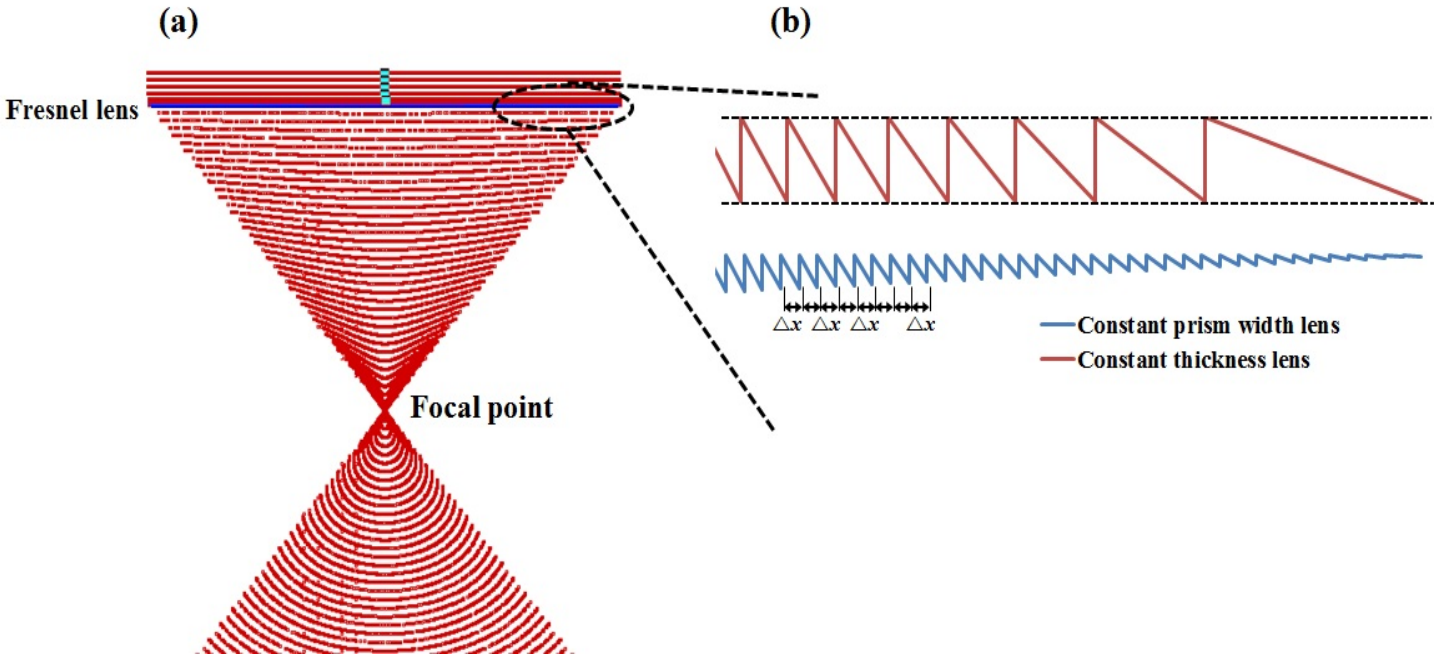

Figure 3.9 Kinds of Fresnel lens having the same focal length: (a) Light distribution after passing Fresnel lens, and (b) Configurations of different type of Fresnel lens.

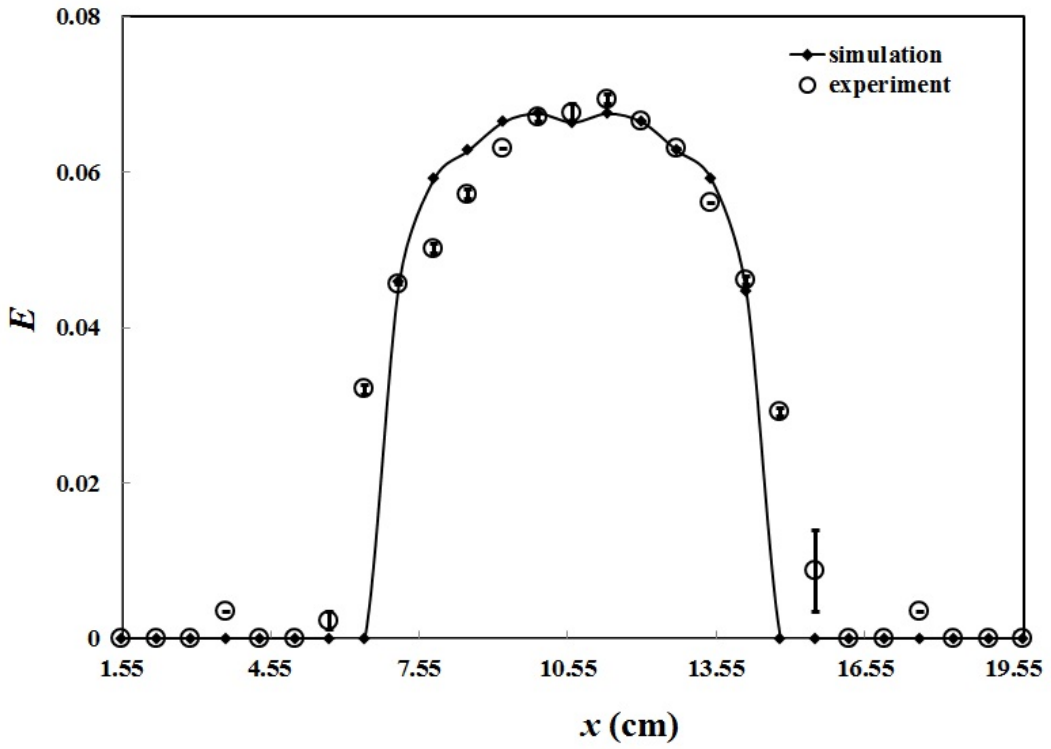

Figure 3.10 1-dimensional power distributions by passing two lenses in simulation and experiment

Chapter 4.

Optimization of static concentrator

4.1 Three lenses system

4.1.1 Introduction

Figure 4.1 shows concentration of rays passing designed 2nd lens based on non-imaging optics. Many rays concentrated onto a PV well. However, some ray in dot circles were deviated from a target region. These rays can be collected by other optical devices. Firstly, vertical or designed reflection such as equiangular spiral is one of the solutions to collect deviated rays. Reflector, on the other hand, has a fatal drawback when various ray`s angle enter to the reflector. Although collection performance of reflector is quite higher at particular incident angle that of reflector is rapidly dropped as incident angles change. Another optical device is lens that is designed lens by non-imaging optics. As mentioned earlier, designed lens has better concentration efficiency than reflector. Therefore, another lens, this is the 3rd lens' was designed in order to collect deviated rays passing 2nd lens and increase concentration ratio.

4.1.2 Methodology

The configuration of system with 2nd and 3rd lens can be seen in Figure 4.2. The

3rd lens was located between the 2nd lens and a PV. There were a lot of parameters in Figure 4.2. All parameters except $\theta_{prism,2nd}$, $\theta_{prism,3rd}$, $w_{prism,3rd}$, and $l_{3rd\ lens}$ were fixed, because the objective of 3rd lens design was collecting deviated rays passing 2nd lens. Thus, design parameters were $\theta_{prism,2nd}$, $\theta_{prism,3rd}$, $w_{prism,3rd}$, and $l_{3rd\ lens}$. Design parameters except $\theta_{prism,2nd}$ were directly related to the 3rd lens shape. Although $\theta_{prism,2nd}$ was not the component for the 3rd lens, $\theta_{prism,2nd}$ was set as design parameters. Since a role of 2nd lens was changed. The role of 2nd lens in chapter 2 was to concentrate dispersed lights passing by concave lens onto a PV. However, A role of 2nd lens was to change direction or magnitude of the refraction angles. In figure 4.3, if lights moved from right to left, sign of lights was designated by (-) in this study. The major role of 2nd lens in three lens system was to reversely change sign of refraction angle before light entered to 3rd lens. Therefore, 2nd lens helped effective design of 3rd lens by causing new ray distribution. The role of 3rd lens was to collect light onto a PV. It was the same as role of 2nd lens in previous chapter. The algorithm for setting width and angle of prisms basically was the similar to method for 2nd lens design in chapter 2. But the order of determining design parameters was somewhat changed. In earlier study for 2nd lens design, design parameters for 2nd lens were sequentially set by following this order; 1st step: set prism width of 2nd lens, 2nd step: set prism angles of 2nd lens

and the last: set location of 2nd lens. However, all design parameters was simultaneously determined by iterations, because ray distributions were continuously changed whenever prism angles in 2nd lens were changed in design process for three lenses system. Comparing the ray`s angle variance which was changed with ray distribution was critical procedure for non-imaging lens design. The small angle variance was required for effective lens design and better performance. In 3rd lens design procedure, rays distribution for setting 3rd lens shape such as width and angle was affected by variation of prism angle of 2nd lens. Therefore, iteration was surely necessary for lens design.

The algorithm of setting 3rd lens location was different from that of lens location in earlier chapter for 2nd lens design. Actually, 2nd lens location was set where concentration ratio is the maximum values between 1st lens and photovoltaic in previous chapter. However, 3rd lens adjoined 2nd lens in this process, because the closer 3rd lens was to 2nd lens, the smaller ray`s angle variance was. Figure 4.4 shows the path of light about different 3rd lens location. When the distance between 2nd lens and 3rd lens was bigger, angle distribution which was arranged by 2nd lens changed and angle variance became worse. The prism design for 3rd lens was performed in edge parts, because deviated lights existed in these parts.

4.1.3 Results and discussion

Figure 4.5(b) indicates the ray distribution about 3rd lens. In the figure, many

deviated lights after passing 2nd lens and 3rd lens was disappeared. 3rd lens surely helped concentrate deviated lights onto a PV. Prism angles in edge parts of 2nd lens became the smaller than angles of earlier designed lens, because the role of 2nd lens was to change direction of rays and sign of light`s angle instead of concentration. A dot circle in Figure 4.5(b) shows ray`s behaviors after passing 2nd lens in detail. In Figure 4.5(a), lights with large refraction angles concentrated toward a PV. However direction of many rays were changed as expected in Figure 4.5(b). Its angles seemed to be perpendicular.

The comparison of ray distribution between only 2nd lens system and 2nd lens with 3rd lens (three lenses) system along *x* direction at PV position can be seen as Figure 4.6. Lights of edge parts in only 2nd lens system can be disappeared and concentrated near center of PV. The collection ability of 3rd lens was confirmed by this phenomenon. However, concentration ratio of system with 3rd lens was rarely the same as that of system having only 2nd lens, because an amount of deviated lights in only 2nd lens system were small. Although system which consisted of 3 different lenses can concentrated more rays onto a PV, the increase of concentration ratio was little. Therefore 3rd lens could not guarantee the high concentration performance.

4.2 Parametric study for static concentrator

Some parameters in two lenses system were fixed by qualitative evaluation for

effective design of static concentrator, because fixed parameters such f_{1st}, w_{1st}, and l_{pv} didn`t manly affect system performance. The changes of theses fixed parameters may affect system performance. However, parameter study should be required to become robust system. Therefore estimation about variation of performance for some parameters which were fixed during 2nd lens design in chapter 2 were conducted by ray tracing method.

4.2.1 Prism width of 1st lens (w_{1st})

As mentioned before, prism width of 1st lens was 0.1 during considering 2nd lens design. This value was arbitrary set for reducing calculation time for simulation and simple design. The variation of prism width in 1st lens could suggest the different performance of system because different angle distribution (angle variance) of rays was caused by different prism width of 1st lens. Analysis about variation of prism width in 1st lens was conducted. The three cases of different sizes were simulated and each result was compared. The shape of 2nd lens such as prism width, prism angle and location was fixed during analysis. Figure 4.7 demonstrates the results about variation of prism width in 1st lens. Change of prism width in 1st lens barely affects system performance.

4.2.2 Focal length of 1st lens (f_{1st})

When 2nd lens was designed earlier in present study, the minimum focal length at which all incident lights didn`t cause total internal reflection considered as losses was set. The value was 1.9. The focal length of 1st lens need not be changed. Shorter focal length caused the losses by total internal reflection. Thus, shorter focal length was not mentioned any more. In case of longer focal length, since position of PV was directly related to focal length of 1st lens. The whole system was elongated by increasing focal length of 1st lens. The big system may be a barrier for installing it at houses and small buildings and manufacture-wise. Therefore, the focal length of 1st lens was maintained.

4.2.3 Location of PV (l_{PV})

As mention previous section, position of PV was the same as focal length of 1st lens. Therefore, location of PV was not changed.

4.2.4 Refractive index (n)

In previous work for 2nd lens design, typical refractive index was used. The value was 1.5 that is reference value of plastic glass. In other words, refraction in simulation was simply considered by a typical value. However, in real situation refractive index is generally a function of wavelength. Variation of refractive index about various wavelengths must be considered, because real sunlight consists of

continuing infinite wavelengths. The refractive index of PMMA was used in order to analyze concentration ratio about change of refractive index, because PMMA is typical material of plastic lens. The characteristics of PMMA are good resistant to sunlight, thermally stable and high transmittance. Relation between refractive index of PMMA and wavelength is expressed by

$$n^2 = 2.3996 - 0.0831\lambda^2 - \frac{0.1920}{\lambda^2} + \frac{0.0872}{\lambda^4} - \frac{0.0166}{\lambda^6} + \frac{0.0012}{\lambda^8}$$

where, λ is wavelength.

Three different refractive index which match bule, yellow and red wavelengths (blue; n=1.497, yellow; n=1.491, red; n=1.448) were used in simulation, because performance change about other wavelengths may exist within results about between maximum and minimum. Figure 4.8 indicates concentration ratio about variation of refractive index by wavelength. In conclusion, variation of refractive index by wavelength barely affected system performance, because variation difference of refractive index by wavelength was small. ($\triangle n$ = 0.049)

4.3 Diffusive radiation effect

4.3.1 Introduction

The global radiation consists of direct radiation and diffusive radiation. (Figure 4.9) Direct radiation means sunlight directly reaches the earth's surface and diffusive radiation is that solar rays enter the surface of receiver after having been scattered by molecules or small particles like water droplet and dusts in the atmosphere. Jo, Dok-ki et al (2009) measured yearly diffusive radiation in Korea. Korea`s climate includes much diffusive radiation, especially its value are higher than direct radiation in summer. Until now, static concentrator was designed by only direct radiation in present study. Validating performance of novel concentrator about diffusive radiation should be conducted for application. Therefore, simulation for evaluating system performance about diffusive radiation was carried out.

4.3.2 Methodology

Diffusive radiation means randomly scattering sunlight by molecules in sky. In simulation, applying perfect scattering phenomenon which randomly occurs by molecules having various sizes is extremely difficult work. Thus, isotropic sky was assumed in simulation. In other words, sunlight is hemispherically and uniformly scattered from sky**.** (Figure 4.10) Concentration ratio of designed system in earlier chapter was calculated by changing incident angles (range; -90° ~ 90°) in order to describe diffusive radiation in isotropy sky.

4.3.2 Result and discussion

Figure 4.11 illustrates the variation of collection efficiency about various diffusive angles. Concentration ratio remarkably increased by decreasing diffusive angles. The yearly average concentration ratio was about1.7. Even, this value was higher than concentration ratio of previous some models in direct radiation. Therefore, concentration ability of 2nd lens which are designed by non-imaging optics was remained in diffusive radiation.

4.4 Summary

In this chapter, optimization process is introduced. Three lenses system is suggested. Its objective is to collected deviated rays and improve concentration ratio. The algorithm for design and role of each are changed. All design parameters are computationally calculated by applying iteration. However, procure of design is conducted simultaneously rather than sequentially. As a result, 3rd lens can collect rays onto PV, however the ability collection of 3rd lens isn`t outstanding.

Parameter study is conducted to be robust system. Some design values are fixed during 2nd lens design, because it doesn't manly affect system performance. Variation of performance about parameter changes is estimated. As a result, variations of w_{1st} and n barely affected system performance.

In Korea, diffusive radiation is significant, because Korea`s climate includes much diffusive radiation. Variation of performance about diffusive radiation is evaluated. In simulation, isotropic sky is assured because it is so difficult to apply real scattering effect. As a result, average *CR* is about 1.7. Therefore concentration ability of system is maintained

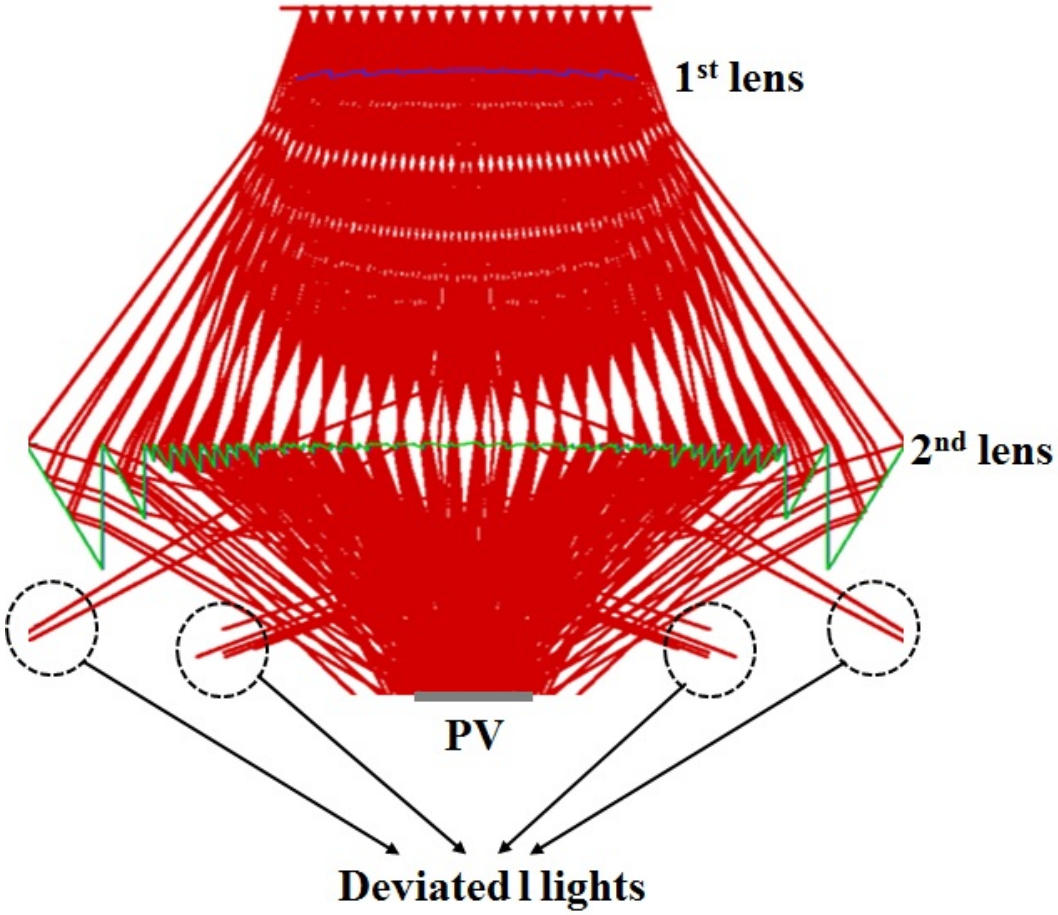

Figure 4.1 Deviated lights in designed SCPV (two lenses in chapter 2) system

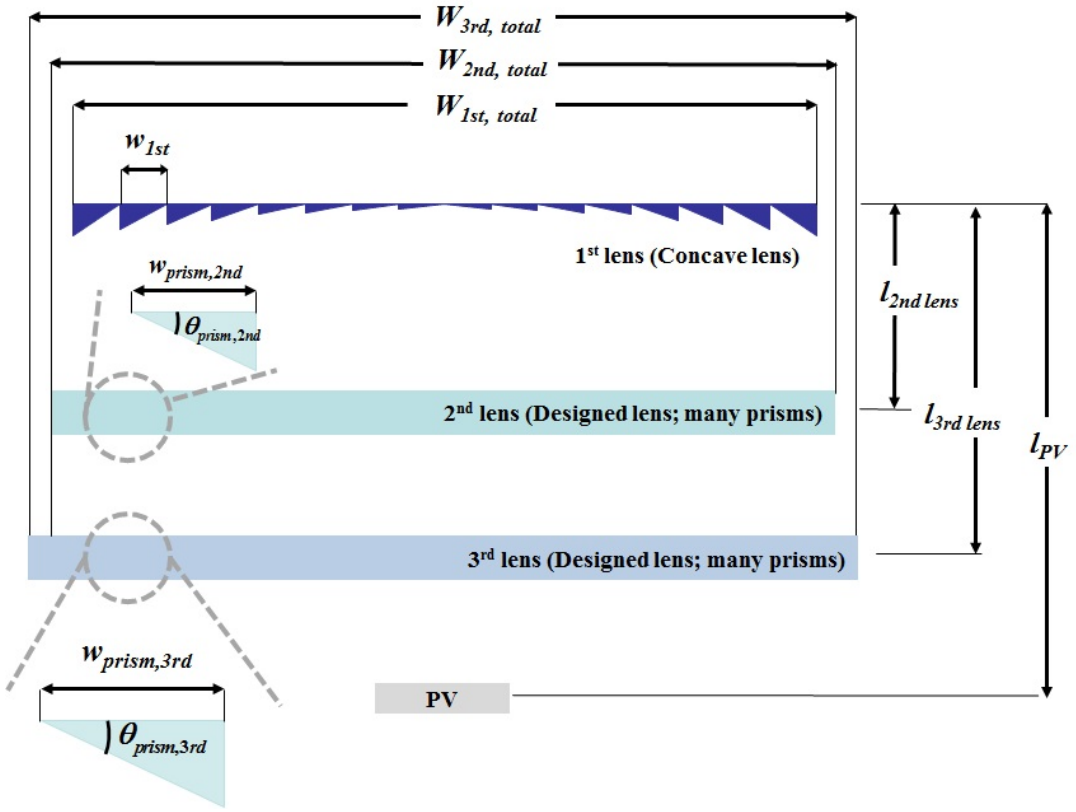

Figure 4.2 Configuration of three lenses system (3rd lens system)

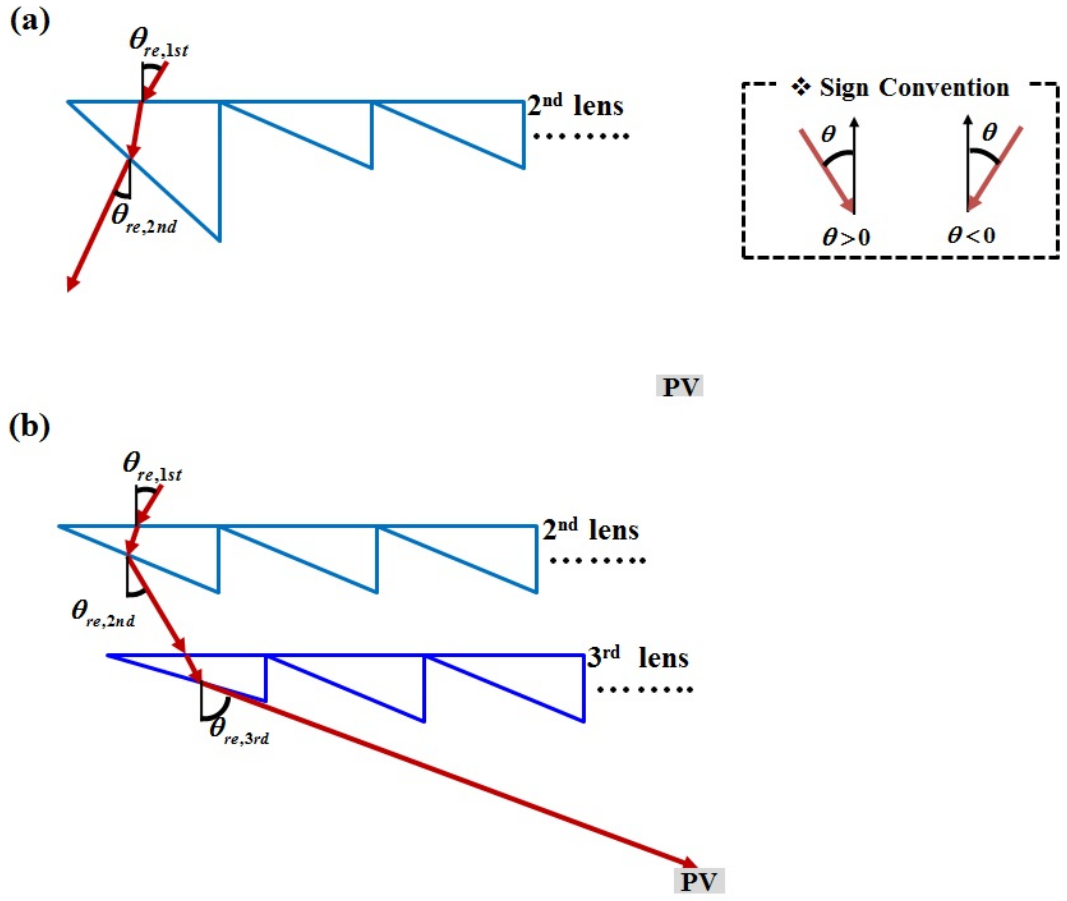

Figure 4.3 Concept of system having 3rd lens and roles of 2nd lens and 3rd lens: (a) Deviated rays after passing 2nd lens in designed SCPV, and (b) Possible path of rays in 3rd lens system.

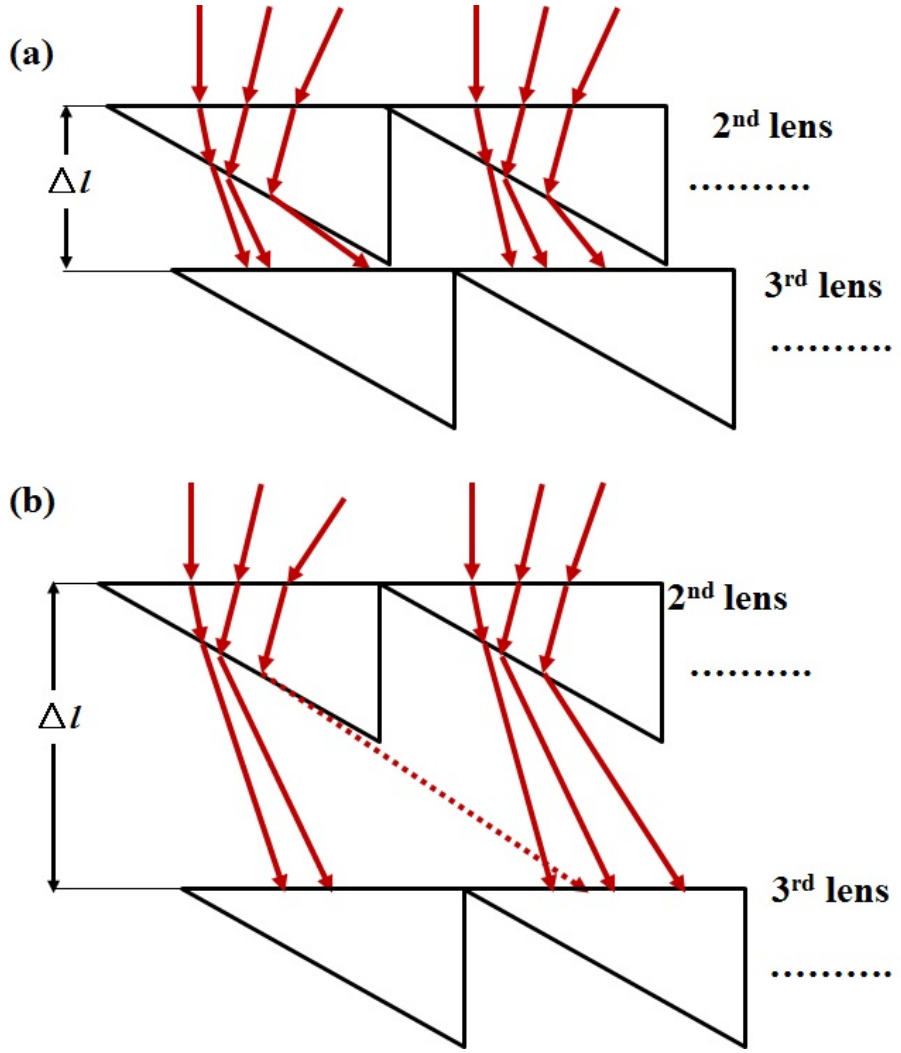

Figure 4.4 The path of light about different 3rd lens: (a) Good example for 3rd lens location, and (b) Bad example for 3rd lens location; angle variance become worse

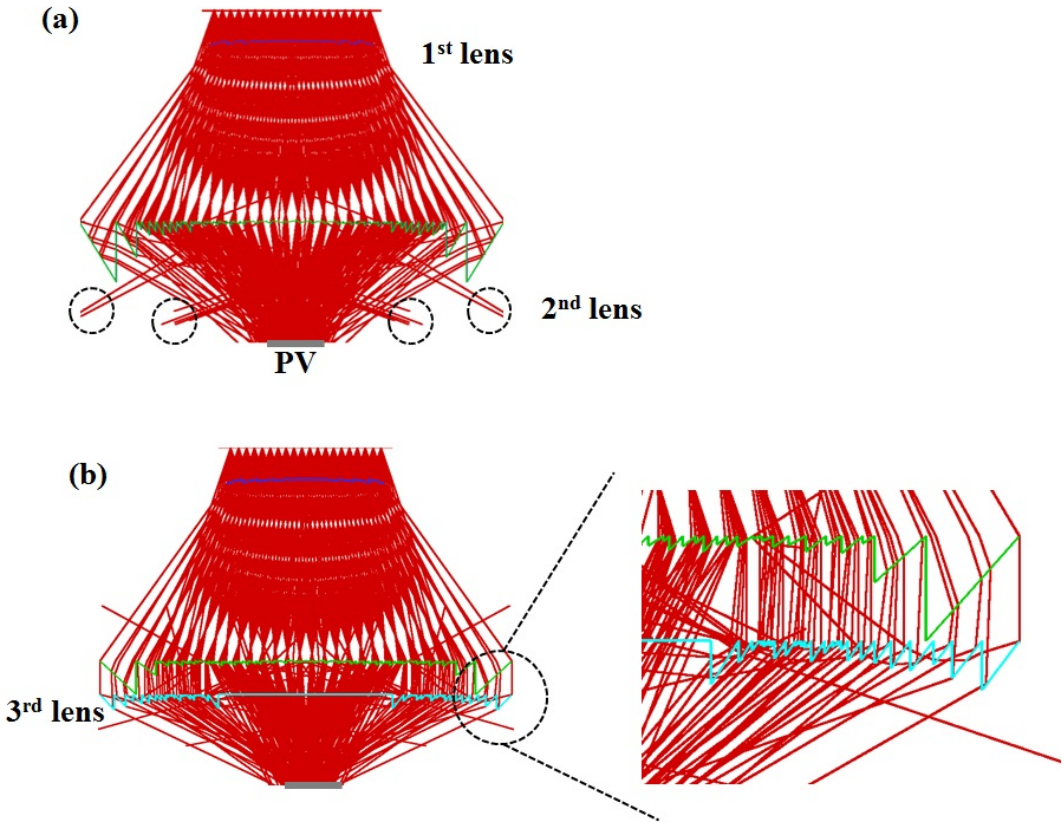

Figure 4.5 Comparison of ray's distribution after passing lenses: (a) Ray`s distribution passing only 2nd lens, (b) Many vertical lights generating by 2nd lens enters to 3rd lens.

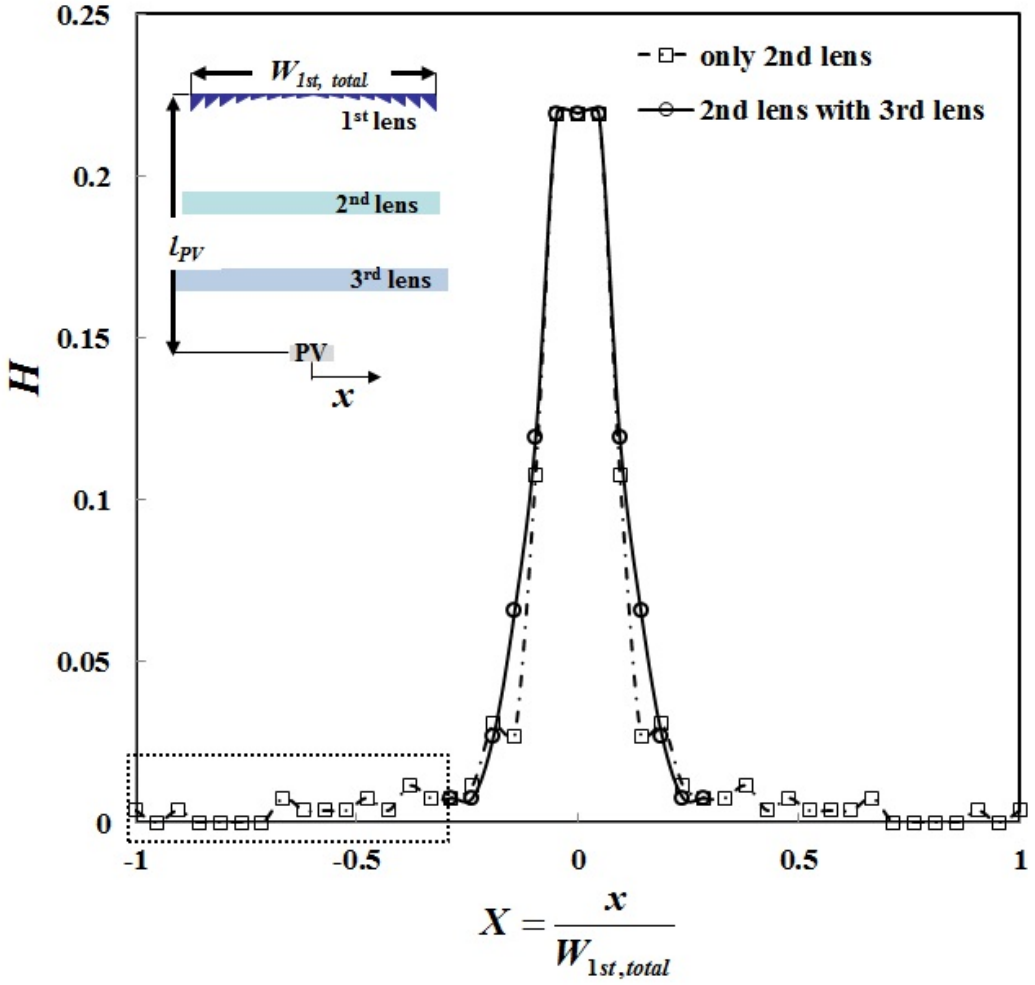

Figure 4.6 Comparison of ray distribution between only 2nd lens system and 2nd lens with 3rd lens (three lenses) system along *x* direction at PV position

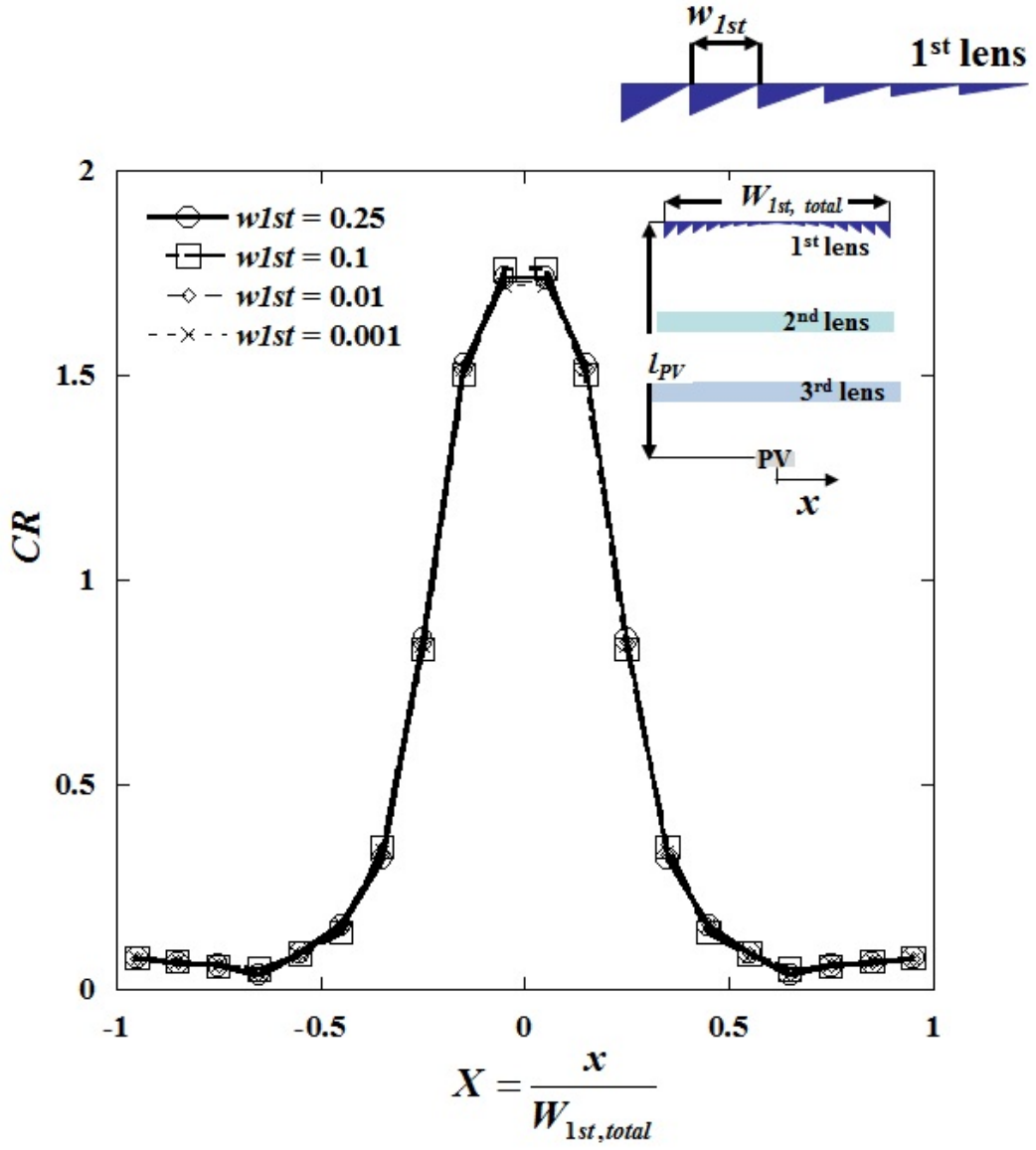

Figure 4.7 Concentration ratio about variance of prism width of 1st lens

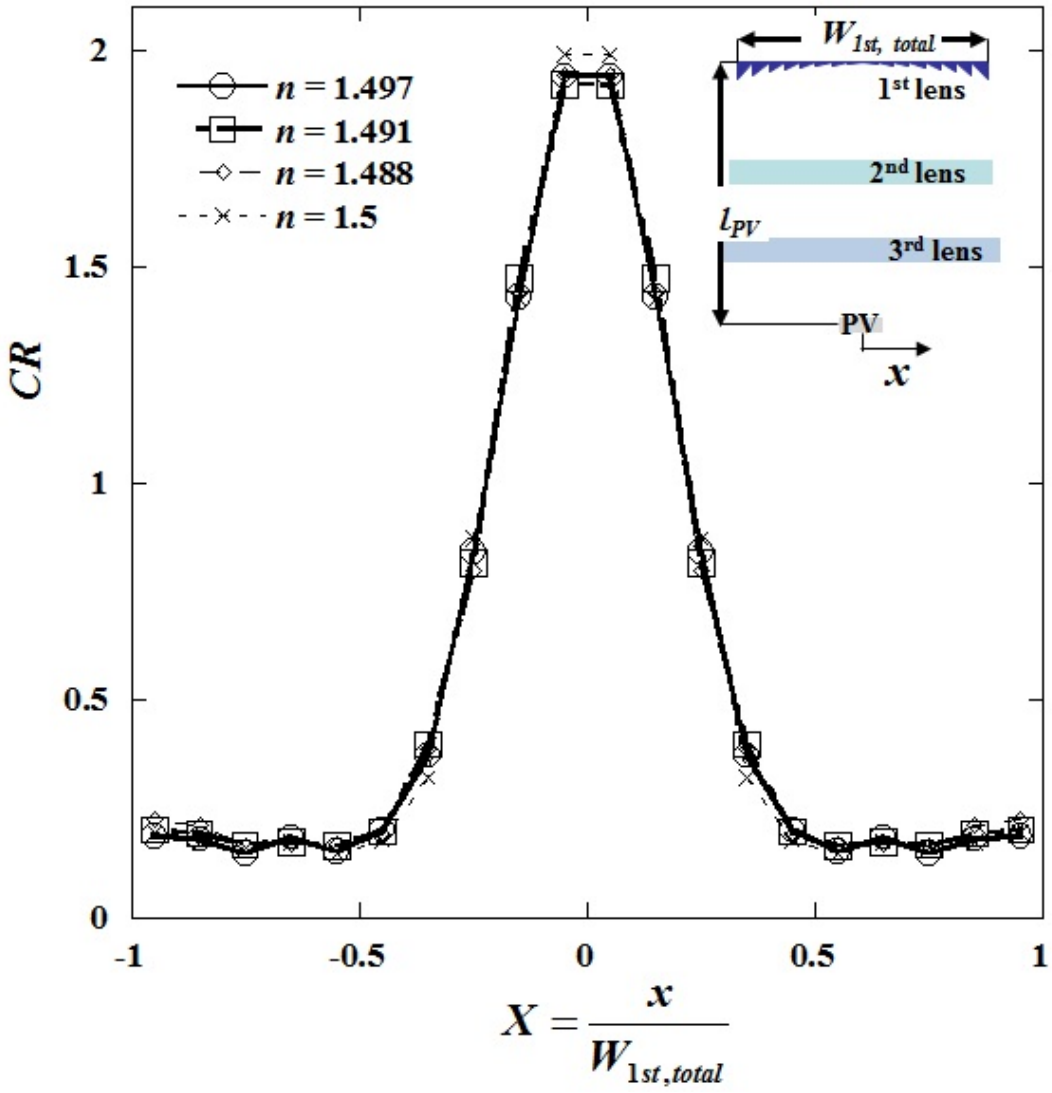

Figure 4.8 Result about variance of *n* by wavelength

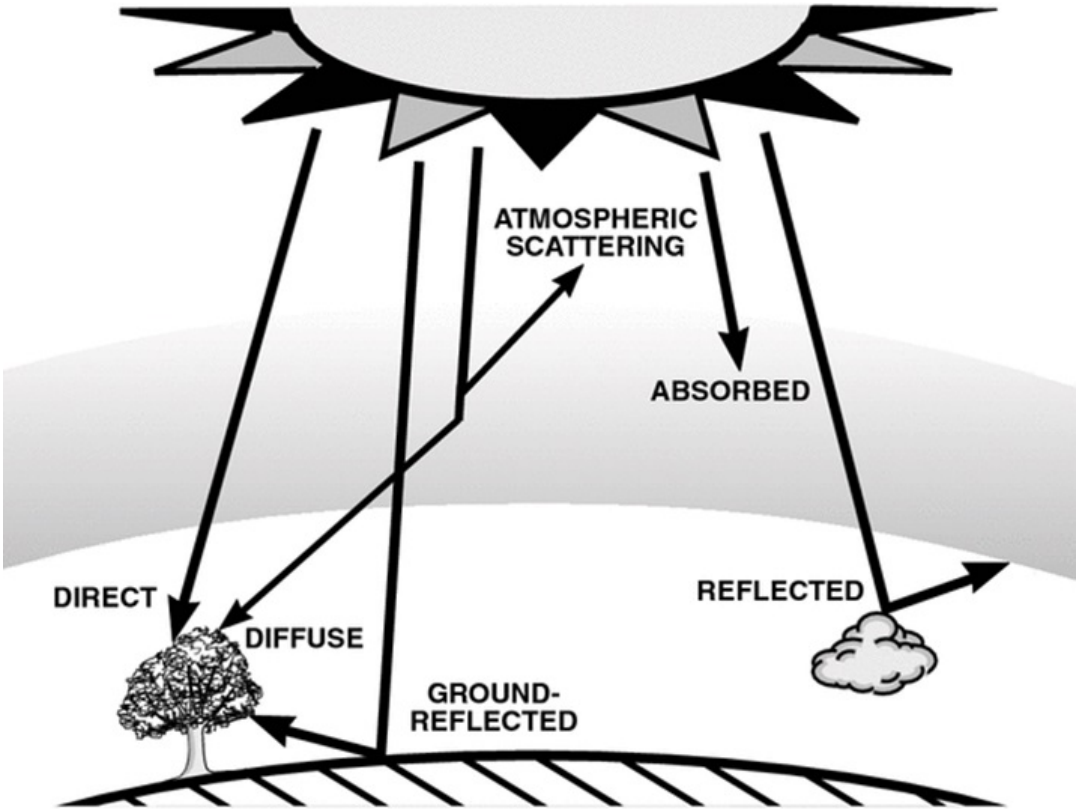

Figure 4.9 The schematic of solar radiation.

Table 4.1 Diffusive radiation in Korea during a year. (Jo, Duk ki et al. 2009)

	Spring	Summer	Fall	Winter	Average
Diffuse radiation (%) $\left[\frac{\text{Diffuse radiation}}{\text{Global radiation}} X100\right]$	43.890	55.088	41.642	43.433	46.013

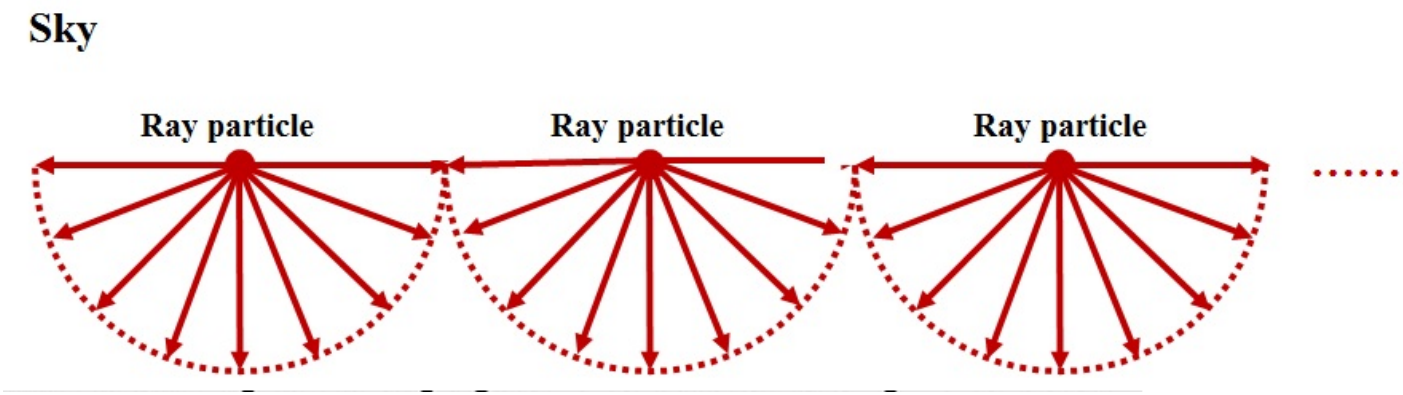

Figure 4.10 Schematic of isotropic sky modeling in simulation

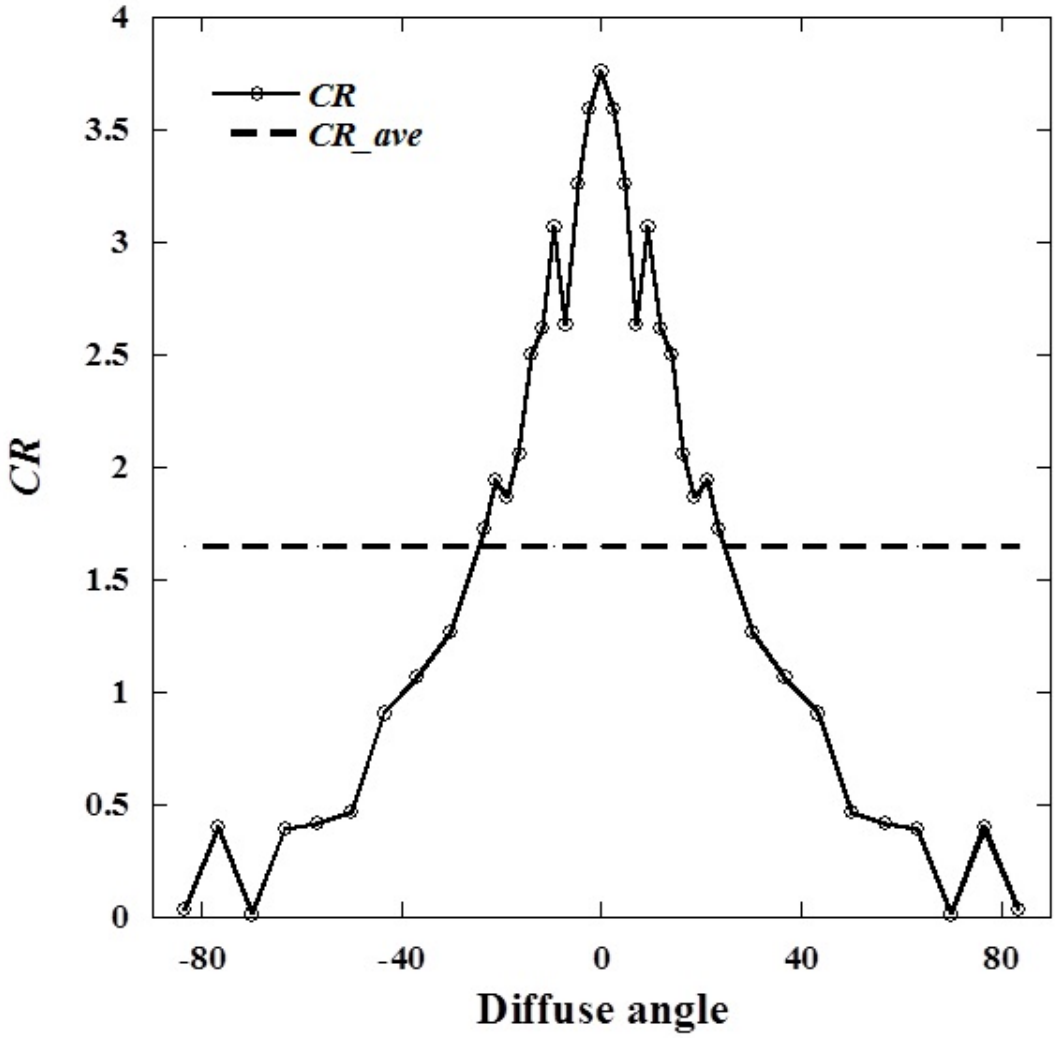

Figure 4.11 Concentration ratio of SCPV about various diffuse angles

Chapter 5.

Practical model systems

5.1 Array system

5.1.1 Introduction and methodology

In previous section, static concentrated PV system was composed of two lenses which were concave lens and designed lens based on non-imaging optics. And performance of designed static concentrator was estimated and was compared with models in earlier study. As a result, higher concentration effect of 2^{nd} lens was verified by higher concentration ratio than previous models. This useful static concentrator should develop for application in real.

In the general PV and CPV system, when systems are installed in real, small-sized modules are combined. In other words, connecting small-sized modules is more practical than bulky single system because bulky single system has the limitation about cost-effectiveness and installment-wise. The manufacturing price of small lens is quite cheaper than that of large lens. And weight of system generally increases with size, so big system may be obstacle by application for house due to heavy system. Therefore, combining small–sized modules which consists concave and designed lens in previous chapter 2 was considered for

application. This connecting small-sized system was called array system in present study. Figure 5.1(b) indicates configuration of arrays system. Performance of array system was evaluated by applying periodic condition. Because small-sized system was periodically and continuously installed in array system, periodic condition was suitable for estimation of array system.

5.1.21 Result and discussion

Figure 5.2 shows the concentration ration of array system. The yearly average *CR* of arrays system indicated 2.33. This value was 29.5 % higher than bulky single system which was shown in chapter 2. And its value was within about 10% of the thermodynamic limit of CPC. (Table 5.1) Especially concentration ratio in summer and winter solstices remarkably improved. At these seasons, incident angles become higher. These inclined initial rays having large incident angles easily were deviated by passing edge parts of 2^{nd} lens. Figure 5.1(b) shows that deviated rays from target region in bulky system entered to PV in adjacent system. Concentration ratio in summer and winter solstices could be improved by this phenomenon. Therefore array system could help collect sunlight having large incident angle than perpendicular sunlight. As a result, array system can overcome the designed drawback of SCPV which is to become the lowest *CR* below '1' in summer and winter.

In previous chapter, single static concentrator performance by changing seasons

was shown. When it is installed, the static concentrator can be used in various settings other as well as array system than that of the stand-alone type considered before. Bulky single system can be installed with vertical side mirrors to increase its concentration performance. In fact, both array system and bulk single system with vertical mirror imply the same boundary condition in ray-tracing method. That is, at the location of the vertical wall, or that of the boundary with neighboring concentrators, the ray is reflected perfectly. Its performance was the consistent with collection efficiency of array system. Since ray distribution was symmetric. This means that concentration effect of coming rays after hitting reflector from left sides to right sides is the same as its entering rays from right another system to left sides by passing transparent materials. (Figure 5.3)

5.2 Semi-SCPV system

5.2.1 Introduction and methodology

In this study, novel concentrator for SCPV system was designed. Its performance was higher than previous studies whose concentrators were based on reflection. Static concentrator in this thesis could produce more energy following power demand about seasons. Since when light perpendicularly entered a system, quite higher concentration ratio of designed 2^{nd} lens than 2.51 which corresponds with ideal value at 23.5° acceptance angle was ensured.

However, in previous results of 2nd lens, when sunlight having the maximum inclined angle entered a system, performance was terribly dropped. At this time, the merit of novel concentrator disappeared. In this research, the semi-SCPV systems were suggested to complement this limitation of novel static concentrator. The meaning of semi-SCPV system is that passively changing installment angles of static concentrator for facing the a few times a year without dynamic tacking system. In other words, while this system had and hold 2nd lens as static concentrator, it simultaneously moved by following particular sun altitudes.

Thus, two different benefits could be achieved. First benefit was that total concentration ratio of semi-SCPV system was increased than those of static concentrator. And another benefit was to effective concentrate onto a PV for the peak of power consumption during years. Lastly, as minor advantage is that performance of system become reliable by periodic cleaning dust on lens surface. In present study, two models for semi-SCPV which can move its installed location just twice a year were considered. The 1st model as semi-SCPV is shown in figure 5.4(a) and (b). At the middle of between vernal and summer, position of SCPV changes to receive sunlight perpendicularly and after 6 month, position of SCPV change. At this time sunlight normally enter the system. Thus, in 1st model, acceptance angle for this model became 11.75° which was an half of acceptance angle of SCPV. Therefore, higher CR was expected by reduction of acceptance angle.

Figure 5.4(c) and (d) demonstrates configuration other semi-SCPV. Since purpose of 2nd was to maximize concentration ratio for peak seasons .Unlike the 1st model, acceptance angle was the same as SCPV but location of system changed in order to receive perpendicularly sunlight at summer and winter solstice in 2nd model. In summer and winter solstice, power consumption rapidly increases due to heating and cooling. Therefore, this model for semi-SCPV could produce effective energy following peak wattage during years.

For 1st model of semi-SCPV, 2nd lens for semi-SCPV must be designed again, because rays distribution after passing 1st lens was changed by reduction of incident angle. The algorithm about 2nd lens design just utilized for 1st model of semi-SCPV. 2nd lens shape of SCPV was maintained in 2nd model of semi-SCPV, because range of incident angle was changed.

5.2.2 Result and discussion

Semi-SCPV system was considered in order to increase yearly average concentration ratio and overcome novel static concentration`s limitation which is to have lower value than '1' at summer and winter solstice. Algorithm for 2nd lens location in previous section, 2nd lens was put location at which *CR* was the maximum. Algorithm for setting 2nd lens location of semi-SCPV is the same as that of SCPV system. Figure 5.5 shows results of 2nd lens location for the 1st model of semi-SCPV system with SCPV. In semi-SCPV system, 2nd lens was put a

location which distance ratio is 0.737. 2nd lens location of semi-SCPV system is farther from a PV than that of SCPV. And Table 5.2 shows the information of 2nd lens for 1st model of semi-SCPV. The position and shape of non-imaging lens in 2nd model for semi-SCPV were the same as original SCPV which was introduced in previous section.

Figure 5.6 indicates concentration ratio of semi-SCPV. In result of 1st model, the yearly average *CR* is 3.31 which was almost 2 times as high as previous static concentrator. Especially the maximum *CR* was 5.925 and the minimum value was 1.765 in seasonal *CR* distribution. 1st model of semi-SCPV achieved higher *CR* as expected. As another merit of the 1st model of semi-SCPV system, this system can produce suitable wattage about requiring power by season. As can be seen Table 5.3 *CR* was periodically varied by season. In SCPV case, the period was an half of year. On the other hand, the periodic of 1st model for semi SCPV was quarter. Period of variation concentration ratio reduced to half. Therefore, more of energy can be collected by semi-SCPV during whole season.

Concentration ratio distribution of 2nd model for Semi-SCPV system reversely changed that of SCPV, because 2nd model didn`t conduct new design and just change installment angles of SCPV for effective concentration. Thus, yearly average concentration ratio, the maximum *CR* and minimum *CR* in 2nd model of semi-SCPV system were the same SCPV. However, in 2nd model of semi-SCPV system, peak value of concentration ratio was shifted to the summer and winter

solstices as planned. Therefore, 2nd model of Semi-SCPV system can flexibly concentrate quite more lights at summer and winter which is the peak power demand.

5.3 Summary

In this chapter, two practical model systems are introduced in application. Frist practical model system is array system which is composed by connecting small-sized system. It is more profitable than bulky single system in cost-effectiveness and installment-wise, because bulky system spend more cost for manufacturing big-sized lens. Its performance is simulation by applying periodic condition. As a result, yearly average concentration ratio remarkably increases, because many deviated rays in single system are collected onto PV in adjacent system. This phenomenon contributes to improve *CR*. The yearly average CR is 2.33. This value is 29.5% higher than yearly average *CR* of single system. And its value was within about 10% of the thermodynamic limit of CPC.

The second practical model system is semi-SCPV. The meaning of semi-SCPV system is that passively changing installment angles of static concentrator for facing the a few times a year without dynamic tacking system. In present study, two models for bi-yearly semi-SCPV. The purpose of 1st model is to maximize average concentration ratio and major objective of 2nd model is maximize concentration ratio for peak power demand. In result of 1st model, yearly average *CR* is 3.31 and

maximum *CR* was 5.925 and the minimum value was even 1.765. And periodic of variance with seasons reduces, thus more energy provides during each season. In 2nd model of semi-SCPV, yearly average, maximum and minimum *CR* are consistent with SCPV system. However, peak value of *CR* is shifted to the summer and winter solstices as planned. Therefore semi-SCPV achieves effective concentration during peak periodic of power demand.

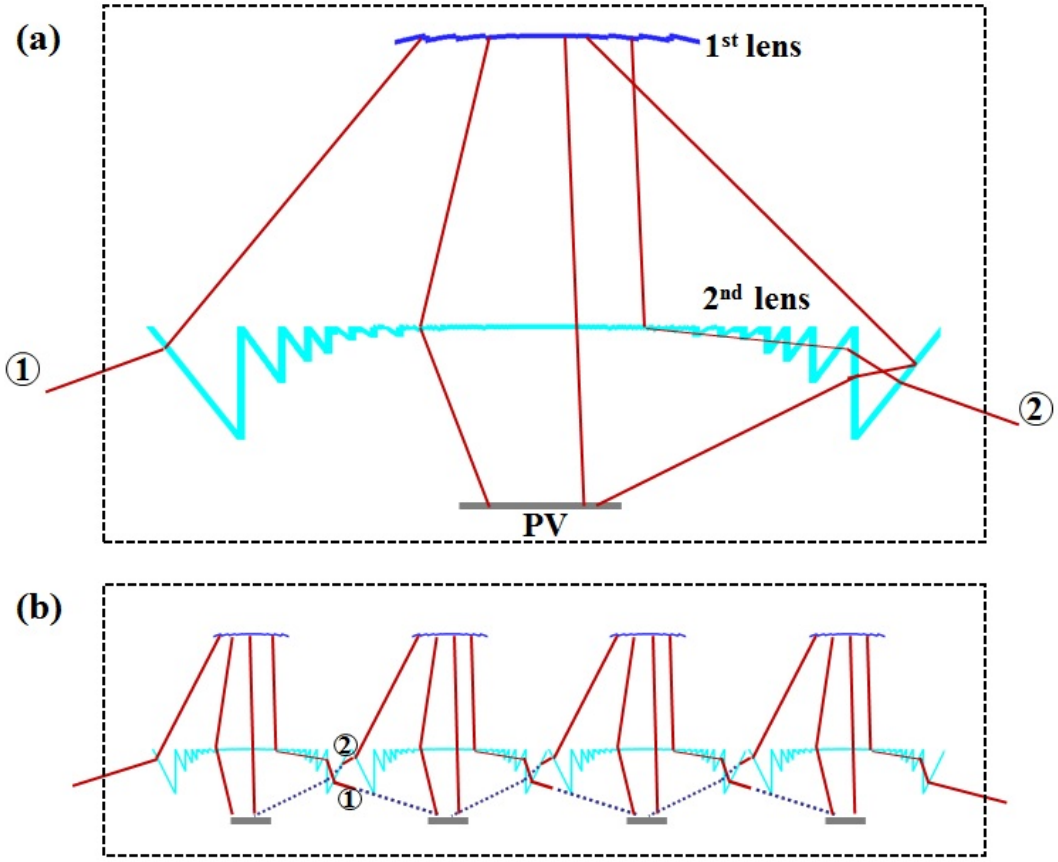

Figure 5.1 Configuration of bulky single system and array system in equivalent area of system: (a) Schematic of bulky single system, and (b) Combining small-sized systems for array system.

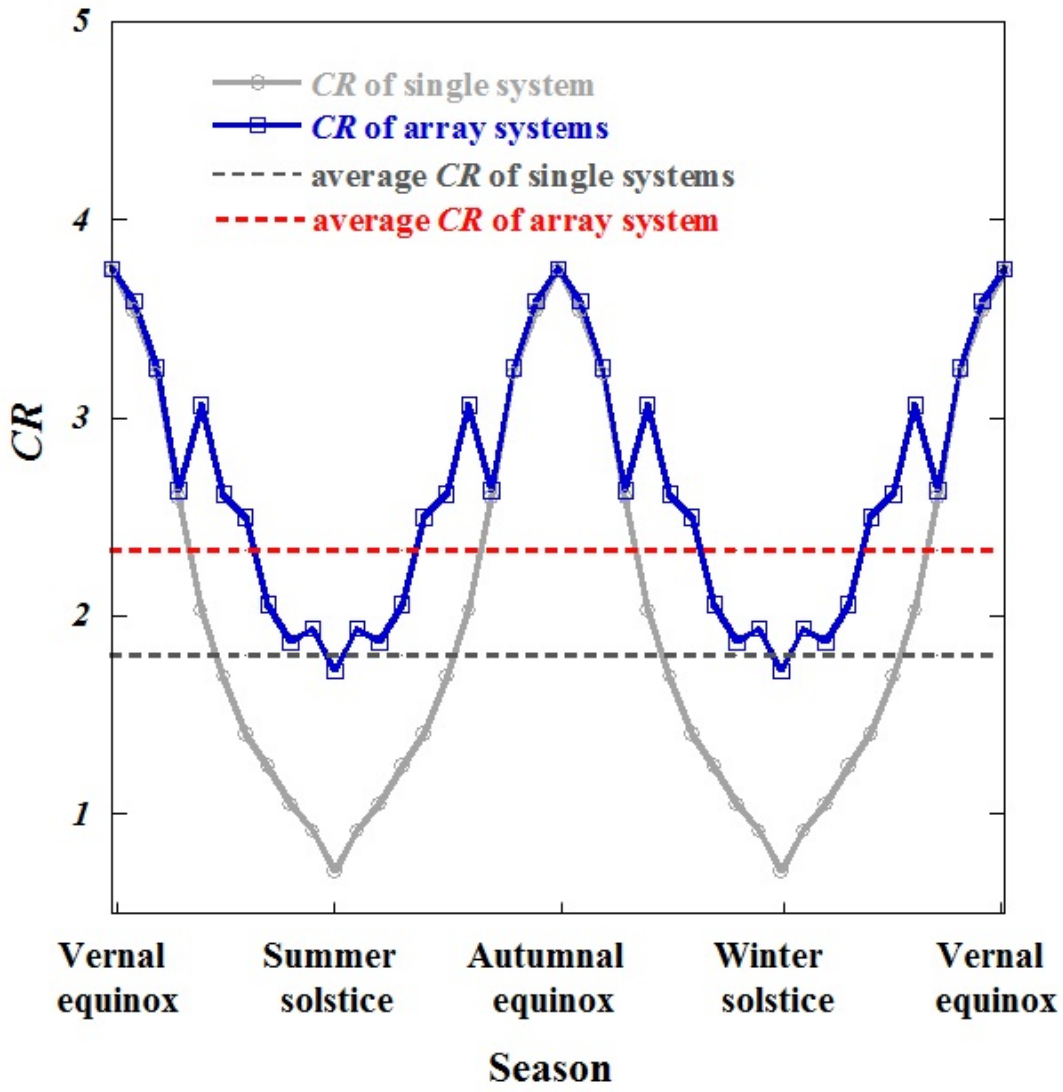

Figure 5.2 Performance of bulk singe system and array system.

Table 5.1 Comparison of system performance in previous study results: (a) S. Bowden et al. (1993), (b) K. Yoshioka et al. (1994), (c) K.J. Weber et al. (2001) (d) K.J. Weber et al. (2006)

Schematic	Mechanism	CR
CPC 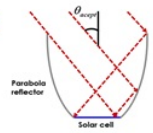	Non-imaging -Reflective mirror	2.51
(a) 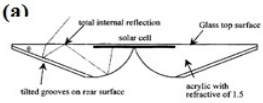	Total internal reflection	~ 1.8
(b) 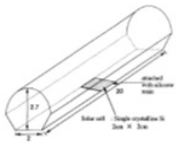	Reflection & Refraction	~1.6
(c) 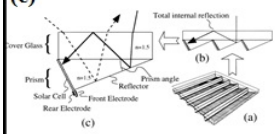	Total internal reflection	~1.8
(d) 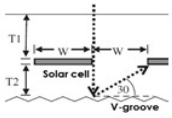	Reflection (V-groove)	~1.6
SCPV 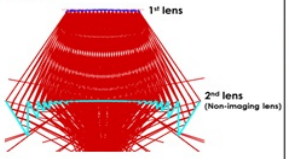	Non-imaging – Designed Lens (refraction)	1.82
Array system 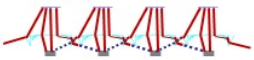	Connecting small-sized system with non-imaging lens	2.33

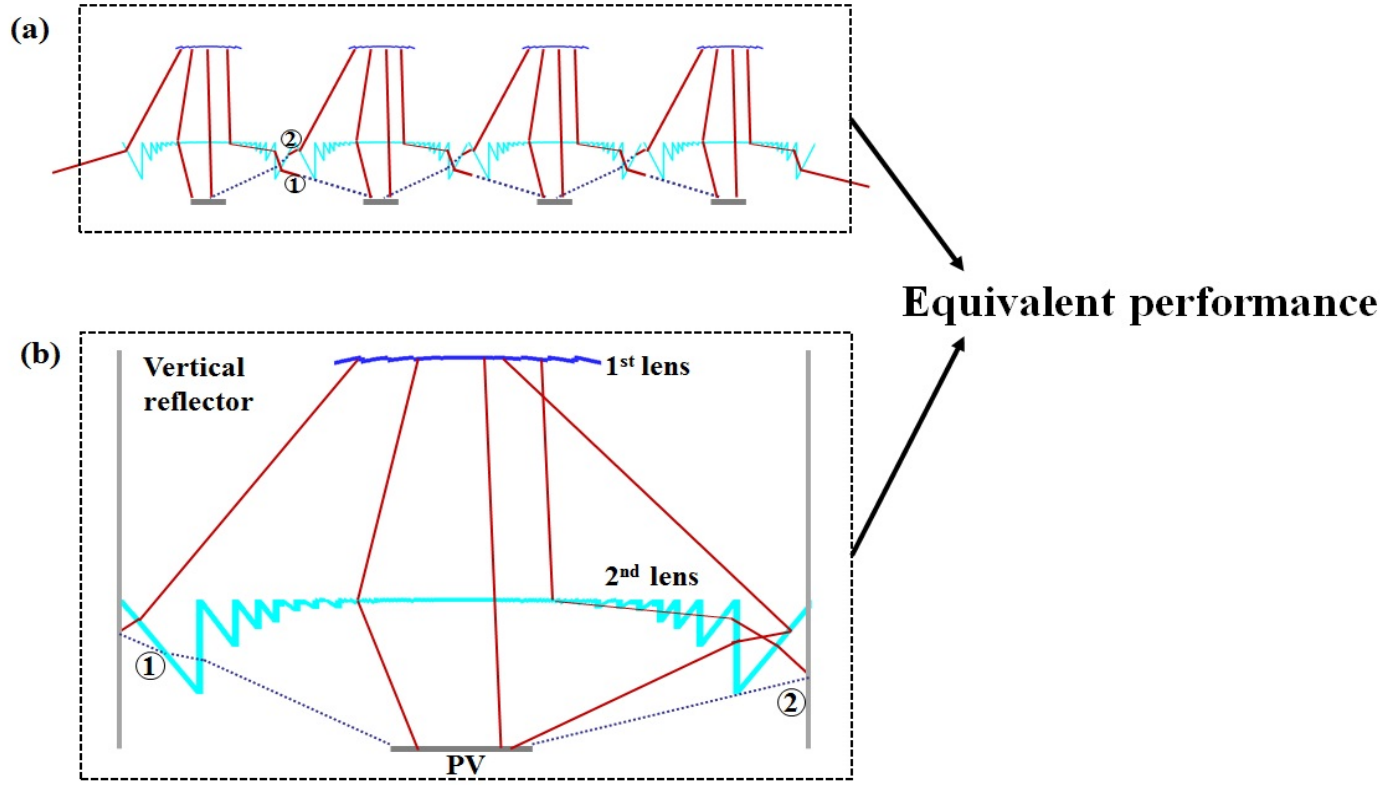

Figure 5.3 Bulky single systems with vertical reflector. : (a) Ray distribution in array system and (b) Path of deviated rays in Bulky single systems with vertical reflector

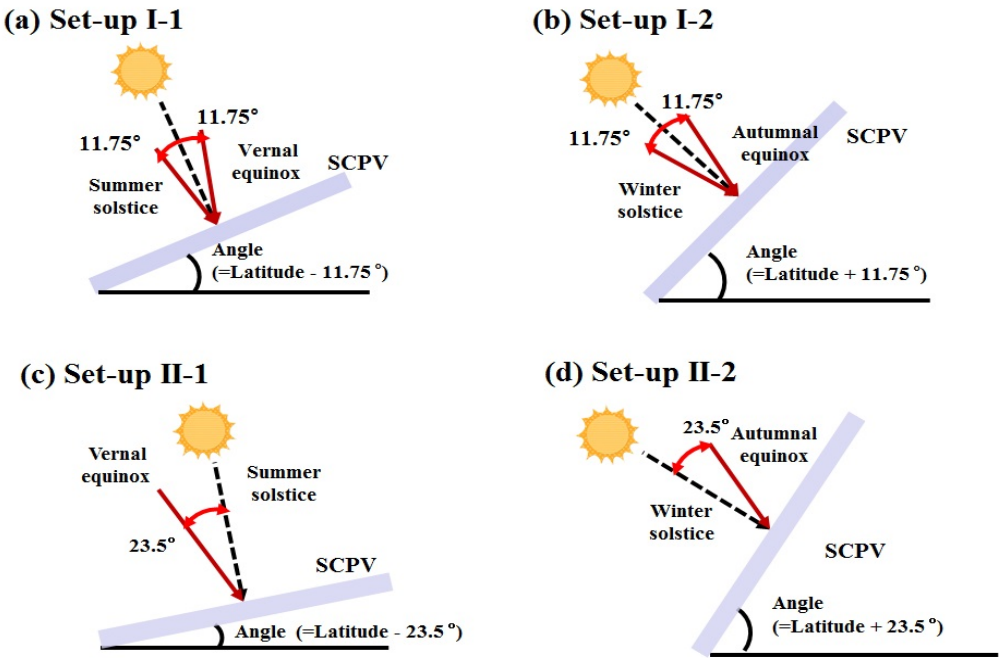

Figure 5.4 Configuration of installment angles and ways for semi-SCPV: (a) 1st model during between vernal equinox and summer solstices, (b) 1st model during between autumnal equinox and winter solstices, (c) 2nd model during between vernal equinox and summer solstices, and (d) 2nd model during between autumnal equinox and winter solstices

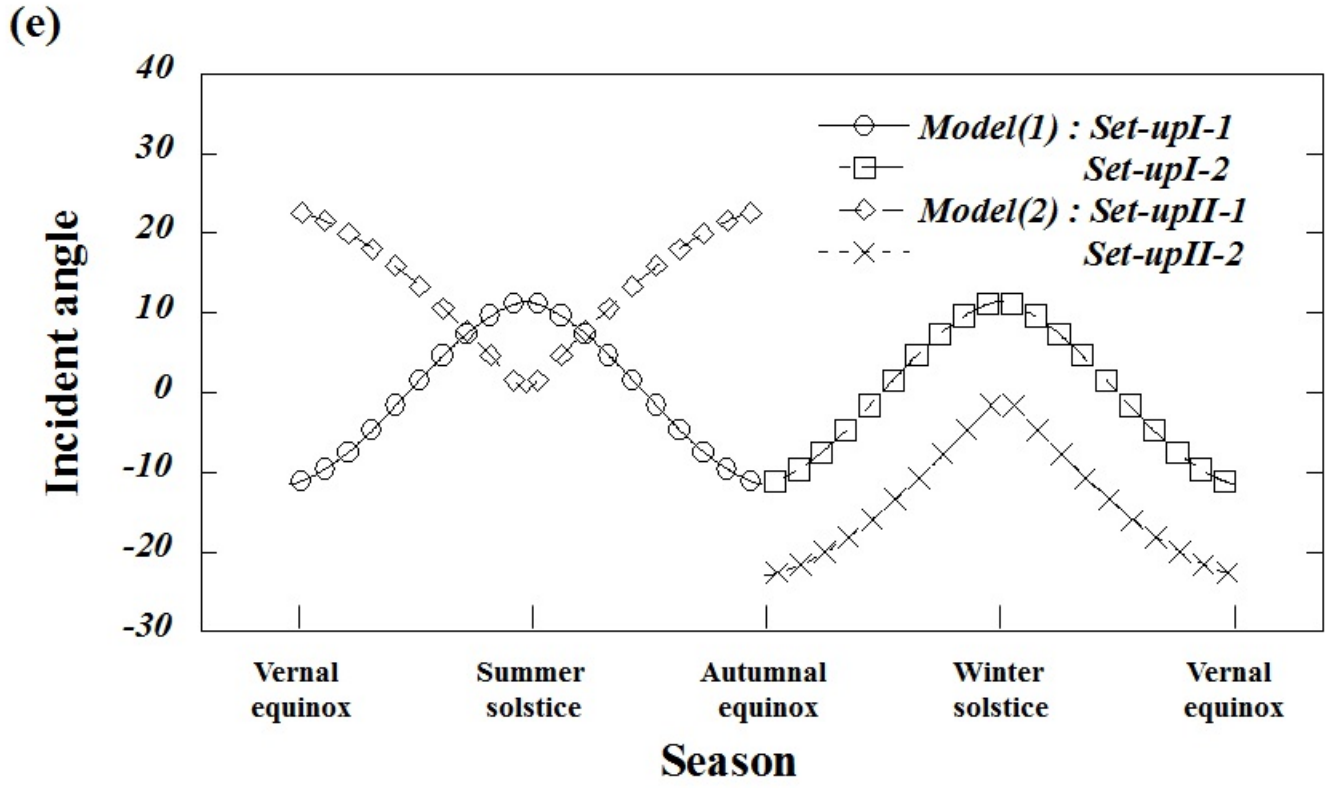

Figure 5.4 Configuration of installment angles and ways for semi-SCPV: (e) Installment angle for semi-SCPV during a year

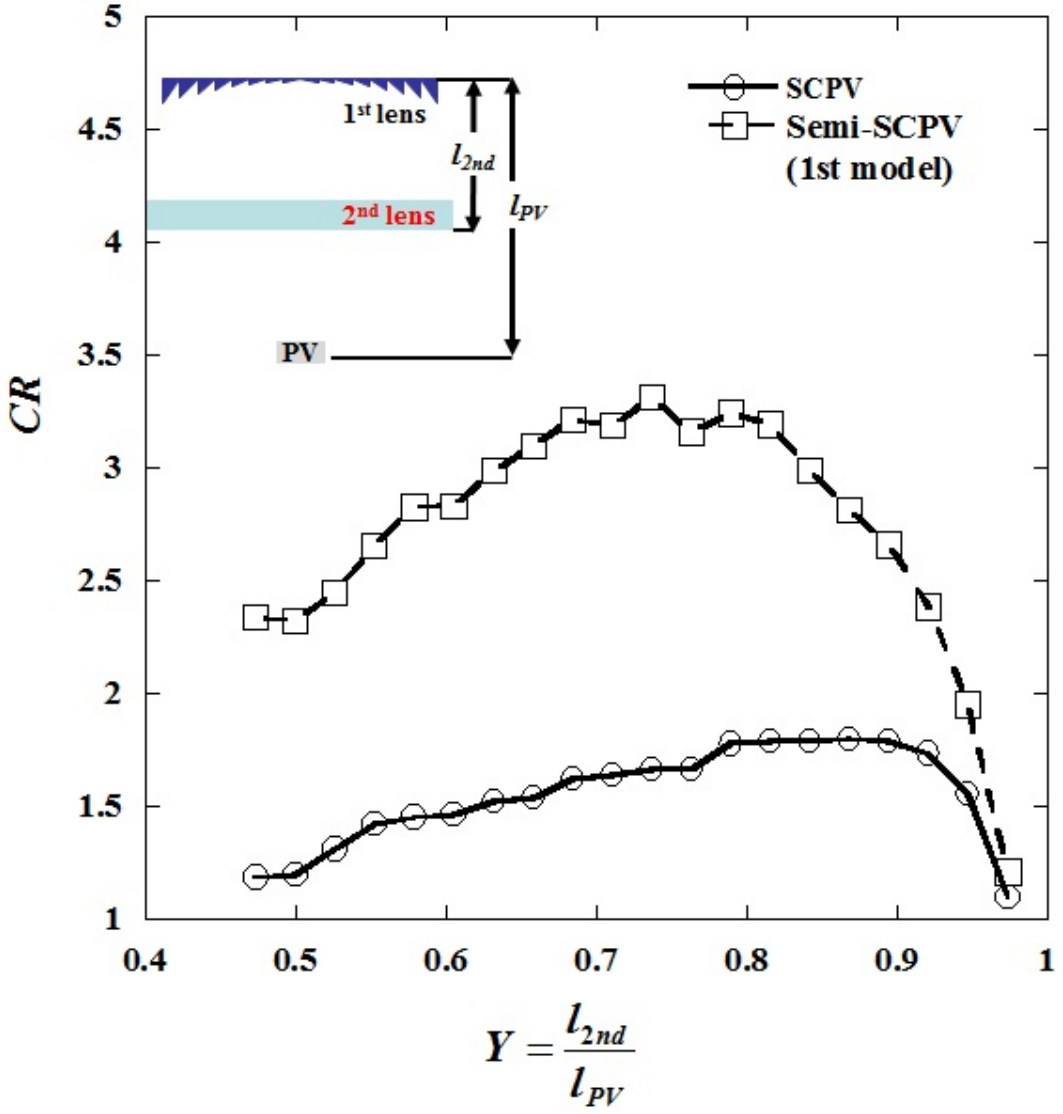

Figure 5.5 Comparison of 2nd lens location between SCPV and semi-SCPV system

Table 5.2 Comparison of 2nd lens information between SCPV and semi-SCPV

Parameter	2nd lens (SCPV)	2nd lens (Semi-SCPV)
The number of prism	4094	2979
Width of prism (w_{2nd})	0.0005 ~ 0.1015	0.0000289 ~ 0.1213
Prism angle (θ_{prism})	0.17° ~ 71.62°	0.1 ~ 64.16
Location (Y)	0.868	0.7367

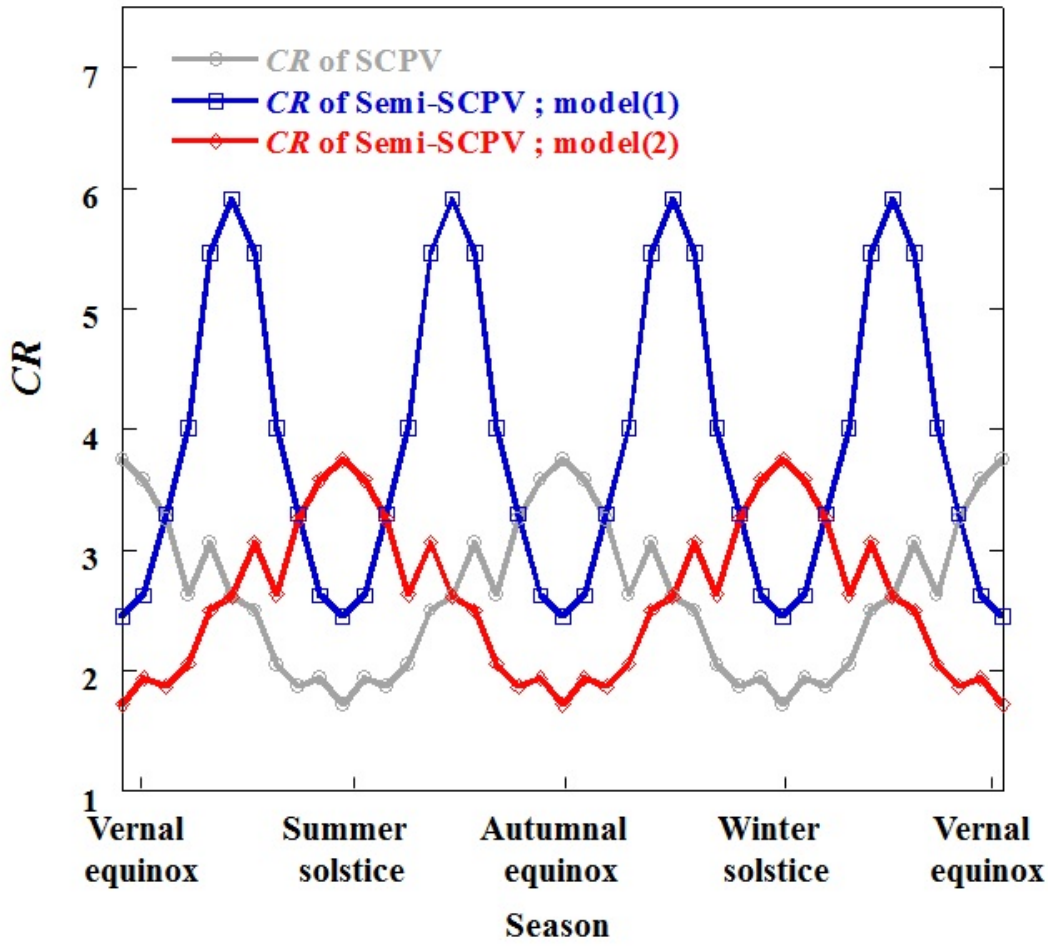

Figure 5.6　Yearly concentrator ratio of SCPV vs semi-SCPV.

Table 5.3 Concentration performance of SCPV and semi-SCPV

system	Semi-SCPV (Model(1))	Semi-SCPV (Model(2))	SCPV
Average *CR*	3.6	2.33	2.33
Max *CR*	5.92	3.76	3.76
Min *CR*	2.45	1.72	1.72
Period of *CR*	Quarter	Half	Half

Chapter 6.

Summary and Conclusion

In present study, the major objective is to develop and cheaper static concentrator for higher *CR* and more flexible concentration for seasonal variation and to present an optical design for small & medium–range concentrator for the usage in house and remote areas. Proposing a design optimization procedure using the non-imaging lens as the primary method of concentration is minor objective.

To achieve objective, two lenses system is considered where role of each lens is different; a role of 1^{st} lens is to reduce variance in ray angles and 2^{nd} lens is convex lens and help to direct rays into a designated position. Ray tracing method which is in-house code utilized for optic design. In simulation, simultaneous analysis method is applied and converged value is used for initial condition. And typical transmittance is applied, because variance of transmittance about incident angles is quite small. Major design parameter is determined by estimating importance about performance. Design parameters are computationally calculated. As a result, designed lens based on non-imaging help many light concentrate onto a PV. It is composed by a lot of prism having different size. Concentration ratio varies seasonally. Then maximum concentration ratio is far higher than average concentration ratio and yearly average concentration ratio (1.82) is higher than

most of the previous studies. Therefore this system has potential for effective concentration for peak power demand.

In this present, experiment is conducted. The objective of experiment is to validate simulation method. Simple system which consists of two linear convex Fresnel lenses having different sizes is set for experiment. Power distribution is measured and compared with simulation results. Based on comparison of both results, reliability of simulation method is verified because the error (MAPE) is less than 5%.

Optimization process is performed. Three lenses system is suggested. Its objective is to collected deviated rays and improve concentration ratio. The algorithm for design and role of each are changed. All design parameters are computationally calculated by applying iteration. However, procure of design is conducted simultaneously rather than sequentially. As a result, 3rd lens can collect rays onto PV, however the ability collection of 3rd lens isn`t outstanding. Parameter study is conducted to be robust system. Some design values are fixed during 2nd lens design, because it doesn't manly affect system performance. Variation of performance about parameter changes is estimated. As a result, variations of w_{1st} and n barely affected system performance. In Korea, diffusive radiation is significant, because Korea`s climate includes much diffusive radiation. Variation of performance about diffusive radiation is evaluated. In simulation, isotropic sky is assured because it is so difficult to apply real scattering effect. As a result, average

CR is about 1.7. Therefore concentration ability of system is maintained

Two practical model systems are introduced in application. Frist practical model system is array system which is composed by connecting small-sized system. It is more profitable than bulky single system in cost-effectiveness and installment-wise, because bulky system spend more cost for manufacturing big-sized lens. Its performance is simulation by applying periodic condition. As a result, yearly average concentration ratio remarkably increases, because many deviated rays in single system are collected onto PV in adjacent system. This phenomenon contributes to improve *CR*. The yearly average CR is 2.33. This value is 29.5% higher than yearly average *CR* of single system. And its value was within about 10% of the thermodynamic limit of CPC. The second practical model system is semi-SCPV. The meaning of semi-SCPV system is that passively changing installment angles of static concentrator for facing the a few times a year without dynamic tacking system. In present study, two models for bi-yearly semi-SCPV. The purpose of 1st model is to maximize average concentration ratio and major objective of 2nd model is maximize concentration ratio for peak power demand. In result of 1st model, yearly average *CR* is 3.31 and maximum *CR* was 5.925 and the minimum value was even 1.765. And periodic of variance with seasons reduces, thus more energy provides during each season. In 2nd model of semi-SCPV, yearly average, maximum and minimum *CR* are consistent with SCPV system. However, peak value of *CR* is shifted to the summer and winter solstices as planned.

Therefore semi-SCPV achieves effective concentration during peak periodic of power demand.

References

Vikrant A. Chaudhari, 2009, “From 1 Sun to 10 Suns c-Si Cells by Optimizing Metal Grid, Metal Resistance, and Junction Dept”, Hindawi Publishing Corporation International Journal of Photoenergy, Volume 2009, pp. 11

Akiba Segal, Michael Epstein, Amnon Yogev, 2004, “Hybrid concentrated photovoltaic and thermal power conversion at different spectral bands”, Solar Energy 76 pp. 591-601

E. Lorenzo and A. Luque, 1982, “Comparison of Fresnel lenses and parabolic mirrors as solar energy concentrators”, Applied Optics, Vol. 21, Issue 10, pp. 1851--1853

K.K. Chong, F.L. Siaw, C.W. Wong, G.S. Wong, 2009, “Design and construction of non-imaging planar concentrator for concentrator photovoltaic system”, Renewable Energy 34, pp. 1364–1370

Kenji Araki, Hisafumi Uozumi, 2005, “Development of a new 550× concentrator module with 3J cells-performance and reliability”, IEEE, pp. 631-634

Kenji Araki1, Hisafumi Uozumi1, Toshio Egami, Masao Hiramatsu, Yoshinori Miyazaki, Yoshishige Kemmoku, Atsushi Akisawa, N. J. Ekins-Daukes, H. S. Lee and Masafumi Yamaguchi, 2005, “Development of Concentrator Modules with Dome-shaped Fresnel Lenses and Triple-junction Concentrator Cells”, Issue

Progress in Photovoltaics: Volume 13, Issue 6, pp. 513–527

Joe S. Coventry, 2005, “Performance of a concentrating photovoltaic/thermal solar collector”, Solar Energy 78 , pp. 211–222

Abraham Kribus, Daniel Kaftori, 2006, “A miniature concentrating photovoltaic and thermal system”, Energy Conversion and Management 47, pp 3582–3590

B. Robles-Ocampo, 2007, “Photovoltaic/thermal solar hybrid system with bifacial PV module and transparent plane collector”, Solar Energy Materials & Photovoltaic (PV)s 91, pp 1966–1971

J.I Rosell, 2005, “Design and simulation of a low concentrating photovoltaic / thermal system”, Energy Conversion and Manegment 46, pp 3034–3046

Mueller-Steinhagen, Hans, “Concentrating solar thermal power”

Carlo Renno, Fabio Petito, 2013, “Design and modeling of a concentrating photovoltaic thermal (CPV/T) system for a domestic application”, Energy and Buildings Volume 62, pp 392–402

Garboushian V et al., 1994, “A Novel High Concentration PV Technology for Cost Competitive Utility Bulk Power Generation”, Presented at First World Conference on Photovoltaic Energy Conversion (Hawaii), pp 1060 – 1063

.

Cuevas A, Luque A, Eguren J, Alamo J, 1982, “50 Per cent more output power

from an albedo-collecting flat panel using bifacial solar cells" Solar energy volume 29, pp 419–420

Brunotte M, Goetzberger A, Blieske U, 1996, "Two-stage concentrator permitting concentration factors up to 300x with one-axis tracking", Solar energy volume 56, pp 285–300

Tilford C, Sinton R.A, Swanson R.M, Crane R.A, Verlinden, P, 1993, "Development of a 10 kW Reflective Dish PV System", Proc. IEEE Photovoltaic Specialists Conference, pp 1222–1227

VD Rumyantsev, M Hein, VM Andreev, AW Bett, 2000, "Concentrator Array Based on Ga As Cells and Fresnel Lens Concentrators", Presented at Sixteenth European Photovoltaic Solar Energy Conference (Glasgow, UK, 2000)

Blakers A, Smeltnik J, 1998, "The ANU PV/Trough Concentrator System", Presented at Proc. Second World Conference on Photovoltaic Solar Energy Conversion (Vienna, Austria)

O'Neill M, Danal A,1994, "Fourth-Generation Concentrator Systems: form the Lab to the Factory to the Field", Presented at Proc. First World Conference on Photovoltaic Energy Conversion (Hawaii)

21. Blieske U et al., 1994, "Optimization of GaAs Photovoltaic (PV)s for Application in Concentrator Modules", Presented at Proc. Twelth European Photovoltaic Solar Enegy Conference (Amsterdam,)

JB Lasich, A Cleeve, N Kaila, 1994, “Close-Packed Cell Arrays for Dish Concentrators”, Presented at First World Conference on Photovoltaic Energy Conversion (Hawaii)

CL Tilford, RA Sinton, RM Swanson, 1993, “Development of a 10 kW Reflective Dish PV System”, Proc. IEEE Photovoltaic Specialists Conference, pp 1222–1227

Juan C. Min˜ano, Juan C. Gonza´ lez, 1995, “A high-gain, compact, nonimaging concentrator: RXI” , Applied Optics, Vol. 34, pp. 7850-7856

J.C. Godlez, “Flat high concentration devices”, First WCPEC, pp 1123 - 1126

S. Bowden, S.R. Wenham, P. Coffey, 1993, “High efficiency photovoltaic roof tile with static concentrator” , IEEE, pp 1068-1072

S.R. Wenham, 1997, “Low cost photovoltaic roof tile”, Solar Energy Materials and Solar Cells Volume 47, pp 325–337

K.J. Weber, V. Everett, P.N.K.Deenapanray, 2006, “Modeling of static concentrator modules incorporating lambertian or v-groove rear reflectors” Solar Energy Materials & Photovoltaic Volume90, pp 1741-1749

Ortabasi U, 1997, “Performance of a 2X Cusp Concentrator PV Module Using Bifacial Photovoltaic (PV)s”, Proc. 26th IEEE Photovoltaic Specialists Conference (Anaheim, CA), pp 1177-1181

Goetzberger A, 1998, “Static Concentration Systems with Enhance Light Concentration”, 20th IEEE Photovoltaic Specialists Conference (Las Vegas)

Antonio luque, Steven Hegedus, 2003, “Handbook of photovoltaic science and engineering”, John Wiley

Ralf Leutz, Akio suzuki, 2001, “Nonimaging Fresnel lenses. (Design and performance of solar concentrators)” Springer

Julio Chaves, 2007, “Introduction to non-imaging optics”, CRC press

Duffie, John A., Beckman, William A, 2007, “Solar Engineering of Thermal Processes”, John Wiley 36.

K. Yoshioka, K. Endoh, M. Kobayashi, 1994 “Design and properties of a refractive static concentrator module”, Solar Energy Materials and Solar Cells 34, pp 125–131

고정식 태양 집광기의 굴절을 기반으로 한 광학 설계

서울대학교 대학원
기계항공공학부
하 성 문

요 약

본 연구에서는 경제적이고 높은 집광율을 갖는 고정식 집광형 태양전지를 위해 여러 개의 프리즘으로 구성된 비이미지 렌즈의 광학설계를 고찰하였고, 설계방법의 신뢰성을 검증하기 위해 실험을 수행하였다. 실용화를 고려하여 여러 개의 작은 시스템이 배열된 시스템에 대한 성능 평가를 수행하였다. 또한 높은 연간 집광율을 얻고, 계절별 전력 수요에 탄력적인 대응하기 위해서 시스템의 설치 각도를 변경하는 두 가지 세미-고정식 집광 태양전지도 고안 하였다.

효율적인 집광을 위해서 두 개의 렌즈가 사용하였다. 첫 번째 렌즈는 상용화 된 오목렌즈이며, 이 렌즈의 주 역할은 두 번째 렌즈의 효과적인 집광을 위해 빛을 퍼트려 주는 것이다. 두 번째 렌즈는 본 연구의 주목적인 비 이미지 렌즈로서 여러 개의 서로 다른 크기를 갖는 프리즘으로 구성되어 있다. 이 프리즘들은 입사각의 분산 값에 의해 크기가 결정되고, 입사 빛들이 굴절 또는 내부 전반사로 인해 태양전지로 집광되었다. 광학 설계의 도구로 인-하우스 코드인 광 추적 방법을 활용하였다. 또한, 저렴하고 쉽게 구할 수 있는 두 개의 렌즈를 이용해 실험을 수행 하였으며, 이 실험으로 본 연구의 설계 방법의 신뢰성을 검증하였다. 설계된 비이미지 렌즈는 서로 다른 입사각을 갖는

빛들을 부분적으로 프리즘으로 제어하여 효과적으로 집광 하였다. 연간 집광율은 기존 보고된 고정 집광장치보다 향상되었고, 춘•추분에는 최대 집광율을 가졌다.

설계된 집광장치의 실용화를 고려하여, 연속적으로 여러 개의 작은 집광장치가 연결된 시스템의 집광 효율을 periodic condition을 적용하여 검토하였다. 하나의 독립된 시스템에서 필요한 큰 렌즈를 가공하기 위해 많은 비용과 힘든 제조 공정을 거쳐야 하며, 시스템의 크기가 크면 설치에 제약으로 실용화에 어려움이 발생한다. 따라서 하나의 독립된 큰 시스템의 면적과 동일하게 여러 작은 시스템의 연속적으로 결합한 어레이 시스템을 제시하였다. 어레이 시스템은 경제적인 시스템 비용과 공정의 단순성을 보장 할 뿐만 아니라, 높은 집광 효율이 제공 하였다. 그 이유는 큰 독립된 시스템에서 양측 면으로 빠져나가는 빛들이 어레이 시스템에서는 이웃한 다른 시스템으로 들어가게 되어 보다 많은 빛을 집광 할 수 있기 때문이다.

실용화를 대비하여 고안된 또 다른 시스템은 세미-고정식 집광형 태양전지이다. 세미-고정식 집광형 태양전지는 고정 집광기를 동적 기구가 아닌 기계적으로 일 년에 몇 차례 태양 빛이 수직으로 들어오게끔 바꿔주는 것이다. 두 가지 다른 목적으로 세미-고정식 집광형 태양전지를 제시하였다. 첫 번째 목적으로는 연간 집광 효율을 향상시키기 위함으로 춘분과 하지의 정중앙인 시점에 태양 빛이 집광기에 수직으로 들어오게끔 집광기 설치 각도를 조절하며, 약 6개월이 지나서, 즉 추분과 동지의 정중앙인 날에 시스템의 설치 위치를 바꿔지는 주는 것이다. 이 때 태양 빛은 시스템에 수직으로 입사한다.

따라서 연간 집광 효율은 크게 상승하였고, 계절에 따라 변화되는 집광율의 주기도 줄어들어 계절별로 보다 많은 집광이 이루는 것을 관찰하였다. 세미-고정식 집광기의 두 번째 목적은 냉난방으로 인하여 높은 전력 부하가 걸리는 여름과 겨울에 대비해 하자와 동지에 최고의 집광 효율을 가질수 있도록 집광장치의 설치 각도를 바꿔주는 것이다. 이 세미-고정식 집광형 태양지의 연간 집광 효율은 고정식 집광형 태양전지와 동일하나, 겨울과 여름에 최대 집광율을 제공하므로서 최대 전력 수요 계절에 탄력적인 집광을 제시하였다

주요어 : 고정식 집광형 태양전지, 비이미지 광학, 집광효율, 광추적 방법, 어레이 시스템, 세미-고정식 집광형 태양전지

학 번 : 2007-20867